Università degli studi di Parma

DOTTORATO DI RICERCA IN

PROGETTAZIONE E SINTESI DI COMPOSTI BIOLOGICAMENTE ATTIVI

XXIII ciclo (2008-2010)

Synthesis of Cysteine-Reactive Compounds as Drugs or Pharmacological Tools

Relatori

Prof. Marco Mor

Correlatore:

Dott.ssa Caterina Carmi

Coordinatore

Prof. Gabriele Costantino

Candidato

Dott. Stefano Vezzosi

To my wife Anna and my little Chiara.

Aknowldgements

I would like to thank Professor Marco Mor who made this work possible and gave me the opportunity to deal with this interesting topic. Furthermore, a big thanks goes to Dr. Caterina Carmi for her time, patience and her pro-active availability.

I would further like to thank all my colleagues for their efforts to make the lab work funnier, with a particular mention to Dr. Elisa Dallaturca and Dr. Pier Cesare Capponi for their collaboration during the accomplishment of this PhD work.

Last but not least, I would like to thank all people that have supported my work providing to me materials and reagents.

Abstract

L'impiego di molecole reattive nei processi di drug discovey è spesso scoraggiato a causa della loro potenziale tossicità od instabilità metabolica. Infatti, se non adeguatamente indirizzata verso il bersaglio desiderato, la loro reattività nei confronti di bersagli biologici alternativi o rispetto a nucleofili biologici come il glutatione (GSH) potrebbe tradursi in effetti tossici indesiderati. D'altra parte, composti reattivi in grado di legare selettivamente i loro recettori con interazioni covalenti potrebbero essere utili per il trattamento di molte malattie clinicamente rilevanti, nonché per lo sviluppo di nuovi strumenti per l'indagine biologica o farmacologica. All'interno di questa classe di sostanze, i composti in grado di legare covalentemente i gruppi tiolici cisteinici rappresentano una delle classi più promettenti per lo sviluppo di composti farmacologicamente sfruttabili. La reattività specifica di questi composti nei confronti dei gruppi sulfidrilici fornisce loro la capacità di legare selettivamente i residui cisteinici esposti dal bersaglio designato limitando, nel contempo, la loro interazione con altri nucleofili presenti nell'ambiente biologico. Considerando che la cisteina è scarsamente espressa nella struttura primaria di molte proteine rispetto ad altri aminoacidi strutturali, solo un limitato sottoinsieme di bersagli biologici dovrebbe presentare residui cisteinici esposti al solvente disponibili ad essere legati da questa classe di composti. Inoltre, dal momento che è raro rilevare proteine non correlate che condividano uno stesso pattern di esposizione di residui cisteinici dopo il processo di folding, il microambiente esistente intorno ai residui cisteinici esposti può essere sfruttato per sviluppare composti covalenti ad alta specificità, in grado di discriminare target biologici differenti fra le proteine esprimenti residui cisteinici accessibili. In questo modo, i composti sviluppati potrebbero essere utilizzati come "tagging agents" ad alta specificità nel contesto della sperimentazione biologica ma anche, successivamente ad un

incremento della loro stabilità metabolica e/o della loro specificità di azione ottenuto attraverso opportune ottimizzazioni strutturali, come farmaci. Farmaci cisteino-reattivi già in commercio quali la Fosfomicina (Monouril ®), l'Omeprazolo (Antra ®) ed il Disulfiran (Antabuse ®), così come molti altri composti in fase di sperimentazione, rappresentano ottimi esempi di come composti in grado di legare covalentemente residui cisteina possano essere sfruttati a livello farmacologico. Durante lo svolgimento di questo progetto di Dottorato di Ricerca sono stati progettati e sintetizzati nuovi inibitori covalenti ad attività cysteine-trap per il dominio **T**yrosin **K**inasico dell'**E**pidermal **G**rowth **F**actor **R**eceptor (**EGFR-TK**) e per l'enzima **M**ono**A**cyl**G**lyceorol **L**ypase (**MAGL**). Entrambi questi enzimi presentano residui di cisteina esposti al solvente adatti ad essere legati da composti ad attività cystene-trap opportunamente progettati. L'interazione covalente di questi composti con i loro relativi bersagli porta alla formazione di complessi farmaco-enzima sufficientemente stabili da produrre un binding irreversibile, o per lo meno di lunga durata, dei residui cisteinici bersaglio e quindi in grado di assicurare un'elevata occupazione recettoriale. Il binding covalente di EGFR-TK risulta essere utile per il trattamento di forme di cancro in cui l'espressione di una forma mutata di EGFR (T790M) è in grado di conferire farmaco-resistenza nei confronti dei convenzionali inibitori non covalenti di EGFR. In questi casi, il legame covalente con il residuo cisteinico Cys773 presente all'interno del sito attivo di EGFR-TK comporta un'incrementata affinità di legame per il target, garantisce un'elevato livello di occupazione recettoriale e consente di superare il fenomeno della farmaco-resistenza. L'aumento di affinità indotto dall'instaurarsi dell'interazione covalente fra questi composti ed un dato bersaglio biologico può anche essere considerata come un buon punto di partenza per la messa a punto di studi SAR finalizzati all'ottimizzazione strutturale dei composti considerati. In questo senso, infatti, la

manipolazione strutturale di composti ad attività covalente può essere effettuata con un diminuito rischio di perdere affinità per il bersaglio designato. Questo concetto è stato applicato alla progettazione di nuovi inibitori cysteine-trap per MAGL. In questo caso, i composti sintetizzati sono stati progettati per presentare livelli elevati di diversità strutturale al fine di ottimizzare il loro fitting recettoriale.

Tutti i composti sintetizzati nell'ambito di questio progetto di Dottorato presentano una porzione cisteino-reattiva (warhead) di struttura variabile legata a diversi motivi strutturali non reattivi (driver groups) progettati per modulare il receptor fitting.

L'inibizione di EGFR-TK mediante composti ad attività cysteine-trap è stata portata a termine utilizzando composti caratterizzati da un driver group di tipo 6-amino-4-(3-bromoanilino)chinazolinico collegato ad una piccola collezione di warheads, selezionate in modo da possedere un ampio spettro di meccanismi di interazione covalente. Per i composti sintetizzati è stata valutata la capacità di inibire il processo autofosforillativo di attivazione di EGFR come anche di inibire la proliferazione di popolazioni cellulari tumorali overesprimenti EGFR. Inoltre, al fine di valutare il loro potenziale terapeutico nei riguardi di tumori resistenti ai convenzionali inibitori non covalenti di EGFR, è stata indagata la loro efficacia nell'inibire la proliferazione cellulare in cellule tumorali esprimenti EGFR T790M.

L'inibizione di MAGL mediante composti ad attività cysteine-trap cisteina è stata ottenuta variando sia le warheads sia i driver groups caratterizzanti i composti utilizzati. Dal momento che per tale scopo si sono utilizzate solamente tre tipologie di warhead eterocicliche, la variabilità dei gruppi cisteino-reattivi in questo studio SAR può essere considerata modesta. Al contrario, al fine di esplorare l'intorno farmacoforico dei residui cisteinici bersaglio, la porzione driver è stata oggetto di una più ampia manipolazione strutturale.

L’elevata potenza inibitoria fornita dai composti sintetizzati relativamente a EGFR-TK e MAGL è incoraggiante e dimostra come composti ad attività cysteine-trap possano essere efficacemente utilizzati nell’ambito dei processi di drug discovery. Inoltre, i bassi profili di citotossicità rilevati unitamente all'efficacia dimostrata di alcuni inibitori di EGFR-TK nell’inibire la proliferazione cellulare su linee tumorali resistenti mostra come tipi di warhead differenti possano essere impiegate per lo sviluppo di nuovi inibitori irreversibili di EGFR capaci di superare la farmaco-resistenza indotta dell’espressione di EGFR T790M con un migliorato rapporto di efficacia/tossicità.

Abstract

The use of reactive molecules in drug discovery is often discouraged because of their potential toxicity or metabolic instability. Indeed, if not properly driven to the desired target, their reactivity toward biological nucleophiles like glutathione (GSH) or unwanted biological target could result in unfavourable toxicological outcomes. On the other hand, reactive agents able to selectively bind their receptors with covalent interactions could be beneficial for the treatment of many clinically relevant diseases as well as for the development of new tools for biological or pharmacological investigation.

Among covalent reactive compounds, cysteine trapping compounds are one of the most pharmacologically exploitable classes of substances able to bind their target by establishing a covalent interaction. Their specific reactivity toward thiols provides them the ability to selectively bind cysteine exposing target without covalently interacting with other nucleophiles presents in the biological environment. Considering that cysteine has a low expression level in proteins with respect of other structural aminoacids, only a limited subset of biological targets should present solvent exposed cysteine suitable to be bound by cysteine trapping agents. Moreover, since it is uncommon to find unrelated folded proteins with a similar cysteine exposure pattern, the microenvironment around cysteine residues can be exploited to develop specific cysteine trapping agents able to discriminate different targets among cysteine exposing proteins.

In this way, cysteine trapping agents could be used as specific labelling agents in biological investigations or, once their metabolic stability and target specificity are increased by proper structural optimizations, as drugs.

Commercial cysteine reactive drugs like fosfomycin (Monouril ®), omeprazole (Antra ®) or disulfiram (Antabuse ®), as well as many other

drug candidates, are good examples of the pharmacological exploitability of this kind of covalent modifier.

New specific cysteine reactive covalent inhibitors for **E**pidermal **G**rowth **F**actor **R**eceptor **T**yrosine **K**inase domain (**EGFR-TK**) and for **M**ono**A**cyl**G**lyceorol **L**ypase enzyme (**MAGL**) were designed and synthesized during this accomplishment of this PhD project. Both of these enzymes present solvent exposed cysteine residues suitable for binding with properly designed thiol reactive compounds. The resulting covalently strengthened drug-enzyme complexes are often stable enough to provide long-lasting or irreversible binding of the targeted cysteine and to assure high receptor occupancy. The irreversible binding of EGFR-TK is beneficial for the treatment of cancer in which the expression of a mutated form of EGFR (T790M) induces drug resistance toward conventional non-covalent drugs. In this case, the covalent binding of Cys773 on EGFR-TK provides an increased binding affinity for the target, assures high level of EGFR-TK occupancy and overcomes the drug resistance. The increased target affinity provided by the covalent binding mode can also represents a good starting point to set-up SAR studies focused on the structural optimization of selected ligands. Indeed, the structural manipulation of a covalent binder can be carried out with a decreased risk of binding affinity loss. This concept was applied to the design of new cysteine trapper MAGL inhibitors. In this case, the synthesized compounds were designed to present high structural diversity levels in order to optimize their receptor fitting.

All synthesized compounds within this PhD project present a variable cysteine reactive portion (warhead) linked to different non-reactive structural motives (driver group) designed to modulate the receptor fitting. EGFR-TK cysteine targeting was achieved using a well-known 6-amino-4-(3-bromoanilino)quinazoline driver group linked to a small panel of warheads based on a wide spectrum of cysteine trapping

mechanisms. In this case, the ability of the synthesized compounds to inhibit the auto-phosphorylative EGFR activation process as well as to inhibit the proliferation of EGFR overexpressing cells was evaluated. Moreover, their effectiveness to hamper the proliferation of cells expressing EGFR T790M was evaluated too, in order to evaluate their therapeutic potential on drug resistant tumour cells.

MAGL cysteine targeting was achieved varying both warheads as well as driver portions. Because only three kinds of heterocyclic cysteine reactive portions were used as warhead portions, the warhead diversity was maintained low in this SAR study. On the other hand, a wider structural manipulation of the driver portion was carried out to explore the pharmacophoric space around the targeted cysteine.

The high inhibition potency achieved by synthesized compounds on EGFR-TK and MAGL is encouraging and shows how much cysteine trapping agents could be useful in drug discovery processes. Moreover, the low cytotoxicity profiles and the effectiveness of some synthesized EGFR-TK inhibitors to hamper the proliferation of cell harbouring T790M EGFR shows that different kinds of cysteine reactive warheads could be used to develop new EGFR irreversible inhibitors able to overcome the drug resistance in tumours with enhanced efficacy/toxicity ratio.

Table of Contents

Chapter 1

Cysteine modifiers in drug discovery

1.1 Introduction

Pharmaceutical industry usually disregards or filters out screening hits containing potentially reactive functionalities, in favour of compounds that modulate protein functions through non-covalent interactions. Indeed, the potentially non-discriminant covalent interactions of these reactive substances with biological nucleophiles like glutathione (GSH) or with unwanted biological target (off-target proteins, DNA, etc.) could result in early or delayed unfavourable toxicological outcomes.[1] In addition, even when screened covalent drug candidates display attractive toxicological profiles in preclinical models, their reactivity could represent a possible triggering element for idiosyncratic reactions. Because of the eventual occurrence of these detrimental effects, development of drugs containing reactive functionalities is often discouraged in pharmaceutical companies, even when the reactivity of the designed compounds is modest and/or limited to the desired biochemical target.

On the opposite, there are instances where controlled covalent modification of target has proven to be exploitable for the development of drugs, pharmacological tools or biomarkers for biological assays. Many commercially available drugs were recognized as covalent modifiers in hindsight, exerting their pharmacological functions on enzymes, receptors or structural proteins by covalent modification of their target.[2] All of these compounds present a molecular structure in which a chemically reactive fragment "warhead" is able to establish covalent interactions, reversible or not, with one or more nucleophilic residues exposed on the surface or into an inner cavity of the target. Their target selectivity depends on their structure as well as on their warheads reactivity. While the former is important for drug-target recognition and for proper warhead positioning, the latter is

fundamental to ensure an effective covalent binding to the target without reacting with off-target nucleophiles. The covalent binding of one of these drugs to the desired biological target usually, but not exclusively, provides a prolonged non-competitive and irreversible target inactivation at low micromolar or nanomolar concentration range.

Among covalent modifiers, compounds able to selectively bind the thiol portion of cysteine residues on proteins without reacting with other nucleophiles are attracting the interest of scientific community. Indeed, if compared to other nucleophile-reactive compounds (such as serine or tyrosine-reactive molecules), the cysteine-oriented reactivity of this kind of compounds could furnish an additional source of selectivity that is beyond the fitting optimization provided by proper structural modulation. This is because cysteine residues in a primary protein structure are usually less abundant than the number of other structural amino acids.[3] In this way, the positions of cysteines on folded protein structure can be used as a specific binding point for cysteine-trapping covalent modifiers and the microenvironment around cysteine residues could be exploited to develop specific cysteine trapping agents able to discriminate different targets among cysteine exposing proteins. This concept has been applied to the development of drugs such as cysteine-protease inhibitors (e.g. cathepsin and caspase inhibitors), tyrosine kinase inhibitors (e.g. EGFR inhibitors) and lipase inhibitors (MAGL cysteine trap inhibitors) but also to the development of pharmacological tools to localize, study and validate cysteine exposing targets.

1.1.1 Covalent drug-target interaction: an orthogonal approach to design pharmacological tools or drugs

Covalent modifier can orthosterically [4] as well as allosterically, [5] modulate the biological activity of their targets through a typical kinetic sequence. In the early stages of drug-target complex formation, a given covalent modifier competes with endogenous ligands or substrates to reach its binding site. Once reached the target, a covalent bound is formed within the drug-target complex, which is thus stabilized. This stabilization hampers the binding of other ligands or substrates to the target and switches the kinetic of interaction from competitive to non-competitive. This switching process takes some time to be completed and this can explain why the inhibition of enzyme and receptor by covalent modifier is usually time-dependent. Considering this double-staged binding behavior, non-covalent interactions provided by structural features of a given covalent modifier play a fundamental role during the target-ligand competitive recognition. The covalent reactivity of these compounds becomes determinant only once the warhead is properly positioned in the targeted binding site. In this way, covalent and non-covalent interactions concur to define both binding affinity and reversibility of covalent modifiers. Notably, the contribution of warhead reactivity to the observed target occupancy increases as the non-covalent structural contribution decreases. Thus, a low reactive covalent binder requires a highly optimized structure to deliver its covalent reactivity on the desired target.

Often, the additional binding energy provided by the formation of covalent bounds between a covalent modifier and its biological target is enough to decrease the number of non-covalent interactions usually needed to achieve the desired pharmacological potency. Thus, very often the operational binding affinity, as much as the observed

biological activity, of a covalent modifier for a biological target results higher than those shown by their non-covalent counterparts. While this could be useful to assure high binding affinity also to structurally unoptimized ligands, the same covalent reactivity could be responsible for target selectivity lacking and/or metabolic instability of these compounds. Thus, the potential indiscriminate reactivity of warheads carried by these molecules could result in early or delayed unfavourable toxicological outcomes.[1] These would be due to immunological responses, genetic or epigenetic changes of expressed proteins or long-term inhibition of key biological targets involved in housekeeping functions (e.g. enzymes involved in protein synthesis). Despite these problems, the use of covalent modifiers for QSAR set-up could be beneficial, at least in preliminary stages of drug design studies. Indeed, the high basal biological effectiveness possessed by these compounds could represent a good starting point for further structural optimization. In this way, an improved biological potency as well as target selectivity could be easily achieved, minimizing the occurrence of off-target toxicity. Furthermore, once the nature of targeted residues is defined, a proper warhead reactivity modulation can further improve the selectivity of designed compounds, driving the covalent reactivity only toward target that expose the same kind of residues (see Chapter 1.2).

Most of covalent modifiers react with their targets inhibiting them. Nevertheless, it is reported that some covalent binder are able to covalently activate their targets. For instance, isothiocyanate AM841 (**40**, scheme 1) was reported to be able to covalently activate GPCR cannabinoid receptor type 1 (CB_1) stabilizing the active form of this receptor by Cys355 targeting.[6]

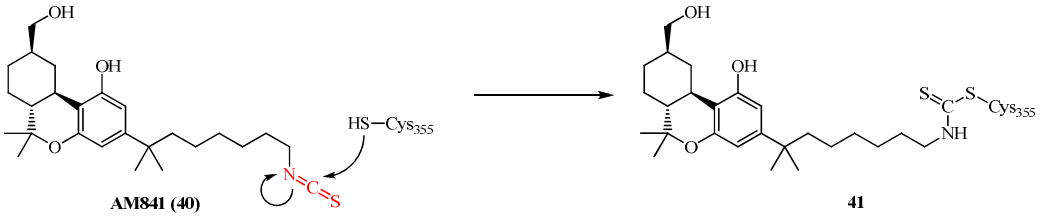

Scheme 1.1. Covalent binding of AM841 to CB_1 receptor. Isothiocyanate warhead colored in red.

Since the largest part of the binding energy of a covalent modifier is generated by the covalent bond formation event, the extent of the obtained pharmacological effect can range from reversible to irreversible, depending on the stability of covalent strengthened drug-target complex.

In case of a covalent irreversible interaction, the provided long-lasting target inhibition or activation can be directly exploited to develop highly effective pharmacological or biological tools. On the other hand, an irreversible target inhibition could be clinically useful too, because it possesses some advantages with respect to the reversible one. For instance, an irreversible modifier doesn't need prolonged circulating blood levels to achieve a desired biological effect. Once the target is deactivated by covalent bond formation, the biological effect should persist even after the drug leaves the bloodstream.[7] Moreover, irreversible covalent modulation should be considered the first choice strategy to achieve an effective treatment of diseases such as cancer or aggressive infections, which require high target occupancy to be treated.[2]

1.1.2 From reactants to drugs

As previously described, the warhead reactivity could be responsible for poor toxicological or pharmacokinetic profiles because of off-target toxicity or extensive metabolic degradation respectively. Moreover, it is reported that some warheads, normally focused to react only with a tight spectrum of nucleophile species, can be metabolically over-activated, increasing their reactivity and becoming able to indiscriminately react with an enlarged collection of nucleophiles. An example of this behavior can be provided by the comparison of reactivity of halogenated and non-halogenated derivatives of isothiazol-3(*2H*)-one. Non-halogenated isothiazol-3(*2H*)-one based warheads have been recognized as very specific cysteine-trapping moieties because of their ability to selectively react with strong nucleophile like thiols without undergoing any relevant addition of weaker nucleophiles carrying hydroxyl- or amino- functionalities. [8] Non-halogenated 2-methylisothiazoli*N*-3(*2H*)-one (**42**, Scheme 1.2) reacts with aqueous solution of *N*-acetylcysteine, a model nucleophile designed to mime biological thiols like glutathione, preferentially undergoing a ring opening reaction triggered by the attach of the nucleophile species on sulfenamidic sulfur atom.

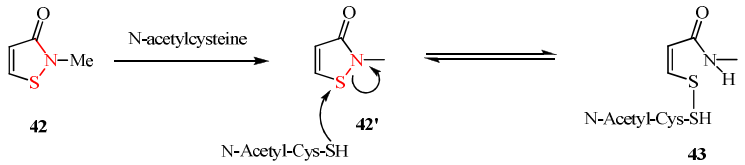

Scheme 1.2. Reactivity of non halogenated isothiazol-3(2H)-one toward thiols. Warhead portion colored in red.

On the other hand, halogenated derivatives like 5-chloro-2-methylisothiazolin-3(2H)-one **44** are more reactive in the same reaction

conditions. They react with *N*-acetylcysteine producing open chain product like **46**, **48** and **49** (Scheme 1.3).

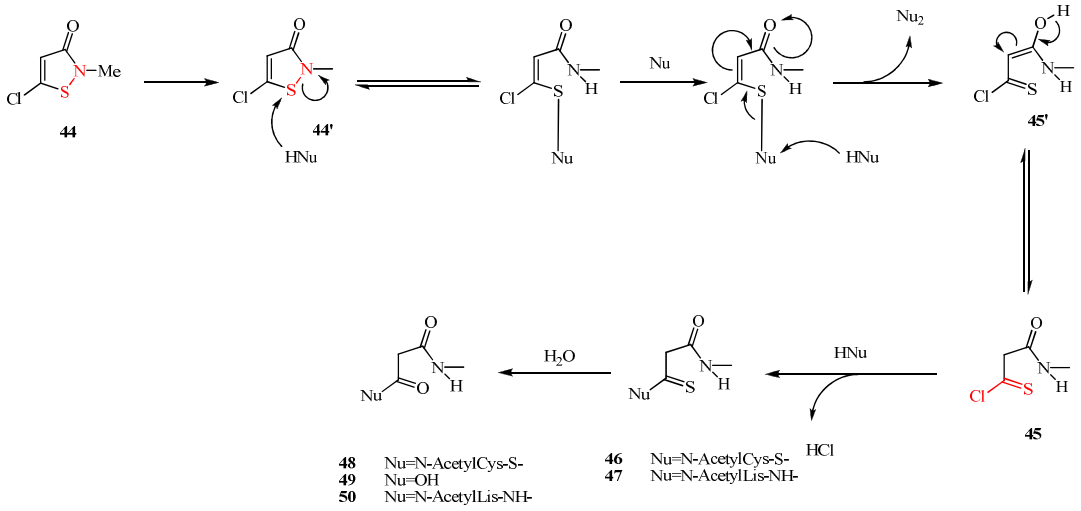

Scheme 1.3. Reaction pathway *N*-Methyl 5-chloroisothiazol-3(2*H*)-one 1 once exposed to nucleophiles (Nu) like *N*-acetyllysine, H_2O and *N*-acetylcysteine. **46**, **48** and **49** represent the general main products observed in this study.

These product are formed by a two-step mechanism in which 5-chloroisothiazol-3(2*H*)-one **44** can initially undergo a simple addition of thiol to the sulfur atom forming a mixed disulfide. Subsequently, this disulfide undergoes a second nuclephilic attack resulting in the cleavage of the disulfidic bond and forming a very reactive thioacyl chloride intermediate **45**.[8,9] The latter is too reactive to exert any kind of specific reactivity and so can freely react with *N*-acetylcysteine or H_2O to produce the observed open chain products **46** and **48** or **49** respectively. The different reactivity of 5-chloroisothiazol-3(2*H*)-one **44** toward *N*-acetyllysine in absence or in presence of *N*-acetylcysteine also support the proposed double stage mechanism. Indeed, while in absence of *N*-acetylcysteine 5-chloroisothiazol-3(2*H*)-one **44** doesn't react with *N*-acetyllysine, in presence of *N*-acetilcysteine only *N*-acetyllisyl derivative **47** and **50** were detected. These finding confirm the

role of thiols to enhance the reactivity of chlorinated isothiazol-3(*2H*)-one inducing the formation of unselective thioacyl chloride intermediate **45**.[8]

Since both non-halogenated isothiazol-3(*2H*)-one and benzo[d]isothiazol-3(*2H*)-ones derivatives can quickly react with biological thiols like glutathione, it was proposed that intracellular glutathione could neutralize the biocide effect of these sulfenamides in living cells whereas, on the contrary, it could over-activate 5-chloroisothiazol-3(*2H*)-one **44** enhancing its toxicity.[10,11]

The "double facet" chemical and biological behaviour described for isothiazol-3(*2H*)-one related warheads represents a good example of how small modifications of warhead structure could result in big reactivity changes. This wide range of reactivity modulation gives a great opportunity to calibrate the chemical reactivity of covalent modifiers for the desired biological target, in order to achieve selectivity and good metabolic stability. In theory, the best toxicological and pharmacokinetic profile achievable by a covalent modifier is matched by compounds carrying low reactive warheads which show poor reactivity toward solution of nucleophiles under physiological conditions but, after appropriate positioning on target binding site, becomes able to selectively react with the desired nucleophile residue. Thus, even if there are examples of blockbuster drugs containing very active warheads like activated esters (aspirin **50**, figure 1.1) and epoxides (fosfomycin **51**, figure 1.1), the majority of successful drugs contains functionalities in which the reactivity is attenuated to achieve targeted modulation.

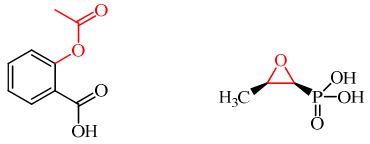

Acetylsalicylic, 50
Aspirine (R)

Fosfomycin, 51
Monouril (R)

Figure 1.1. Highly reactive blockbuster drugs. Warhead portions colored in red.

Despite the warhead reactivity modulation could represent a good way to develop covalent binder able to deliver the desired therapeutic effect with good safety profiles, very often a proper structural optimization is also required to reach these goals. Indeed, as discussed in the previous chapter, an improved receptor fitting is useful to enhance the ligand-target recognition, limiting off-target risks and, especially in presence of low reactive warhead, to increase the receptor occupancy. The structural optimization can involve the whole molecular structure of a covalent modifier but, usually, it is focused on a specific non-reactive "driver portion" linked to the "warhead" by a neutral "linker portion". The modular structural scheme here described is very common among pharmaceutically-oriented covalent binders and it is thought to allow a free manipulation of structural determinants without accidentally modifying the warhead reactivity. Also length or shape changes of the "linker portion" can assist in the structural improvement process. It should be designed to bring the reactive portion of the covalent binder close and with a proper orientation to the targeted nucleophile residue, favouring the establishment of covalent bonds. Finally, driver groups as well as linker portions can be decorated with different substituents not only to enhance the pharmacodynamic profile but also to improve ADME parameters. For instance, introduction of hydrophilic substituents on these compounds represents a common strategy to increase their solubility and to modulate their distribution and/or elimination.

An example of well-balanced reactivity and recognition is represented by β-lactam antibiotics like penicillins and cephalosporins. They possess a highly optimized structure able to mime the acyl-D-alanyl-D-alanine terminal portion of the endogenous substrate of bacterial DD-transpeptidase enzyme.[12] "Driver group" and the "warhead" portions are largely overlapping in these compounds so that structural

manipulation of the former can impact on the reactivity of the latter (Figure 1.2)

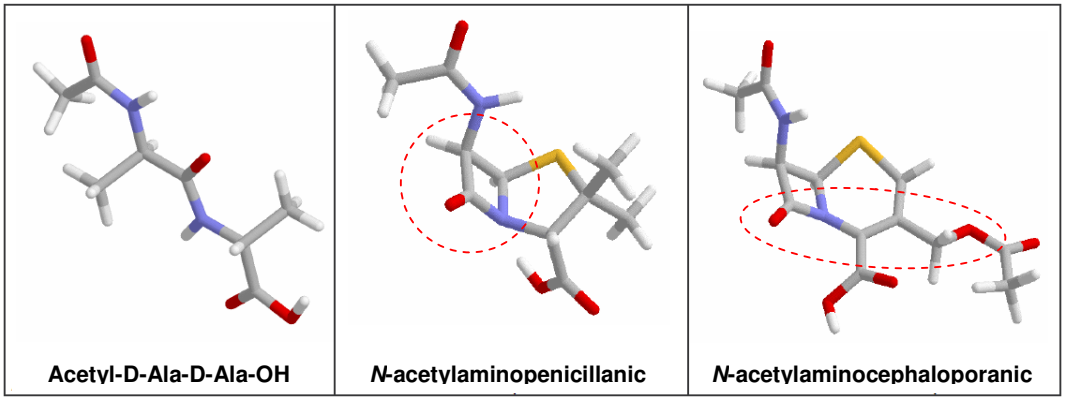

Figure 1.2. The structure of a D-alanyl-D-alanine dipeptide model is compared with *N*-acetylaminopenicillanic and *N*-acetylaminocephalosporanic acids scaffolds, used as penicilline and cephalosporine backbone models respectively. The role of acetyl group on D-ala-D-ala model is to mime the peptidic bond that join the D-ala-D-ala dipeptide to the remaining structure of growing peptidoglycan within cell wall. Warhead portions (circled in red) are recognizable within the driver group structural motif.

Once competitively bounded to the DD-transpeptidase active site, the carbonyl portion of β-lactam warhead present in these antibiotics starts to undergo nucleophilic attack of the catalytic serine of the enzyme. This attack, followed by subsequent β-lactam ring opening and amide nitrogen displacement, results in the formation of a catalytically inactive and hydrolytically stable form of acyl-DD-transpeptidase (scheme 1.4)

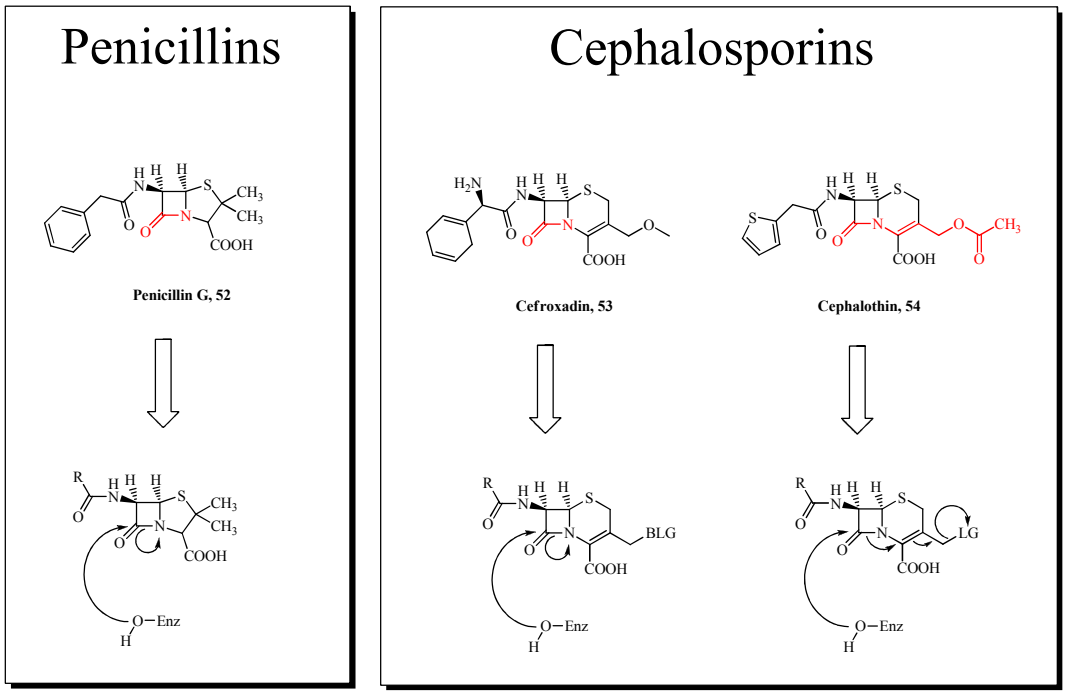

Scheme 1.4. Acylation mechanisms of penicillin and cephalosporin derivatives. It has been proposed that cephalosporines and penicillins can share or not the same serine acylation mechanism dependently to the presence of a good or a bad leaving group (LG or BLG respectively) in vinilogous position to the β-lactam nitrogen atom.[13]

The irreversible inhibition of DD-transpeptidase activity leads to the blockade of bacterial cell wall biosynthesis and provide to these antibiotic agents with a very effective bactericidal action. Notably, the D-alanyl-D-alanine fragment mimicry provided by these compounds limits the intrinsic reactivity of the β-lactam warhead only to the desired target and drastically decreasing their off-target toxicity.

An alternative strategy to focus the warhead reactivity of a given covalent modifier on the desired target without using highly optimized driver portion is to limit its action within a specific biological compartment only. The easiest way to achieve this goal is to perform a pharmacokinetic parameter modulation. For instance, the reactivity of some covalent modifiers could be limited only to a specific biological district by simply changing their solubility or their trans-mucosal uptake. A

good application of the described strategy has been reported for β-lactone THL (Tetrahydrolipstatin, Orlistat ®, **55**, Figure 1.4), a human Pancreatic Lipase (hPL) covalent irreversible inhibitor.

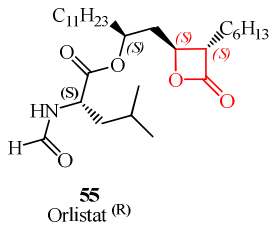

Figure 1.4. Structure of Orlistat **55**, a hPL irreversible inhibitor drug.

In this case, the poor intestinal uptake of THL helps to keep the acylating potential of THL within the intestinal lumen so excluding the occurrence of any systemic toxicity. In this way, the reactivity of THL β-lactone warhead has been pharmacokinetically driven toward the catalytically active serine of hPL without requesting any structural optimization.

Otherwise, a more complex approach to compartmentalize the action of covalent binders is to design them to act as pro-drugs or as mechanism-based inhibitors. In this way, their masked warhead will be unveiled only near or inside the desired target respectively and so dramatically decreasing their unspecific toxicity. A good example of covalent reactive pro-drugs is represented by H+/K+ ATPase inhibitors like Omeprazole (Antra ®, **18**, Scheme 1.6). The latter possesses a good trans-membrane uptake and no recognizable warheads can be found within its structure. After administration, it can freely reach the bloodstream without delivering its reactivity until it reaches gastric oxyntic cells. At this stage, omeprazole is exposed to pH value below 4 and its structure starts to undergo a complex rearrangement that leads to the formation of highly reactive compounds **58** and **59** (Scheme 1.6).

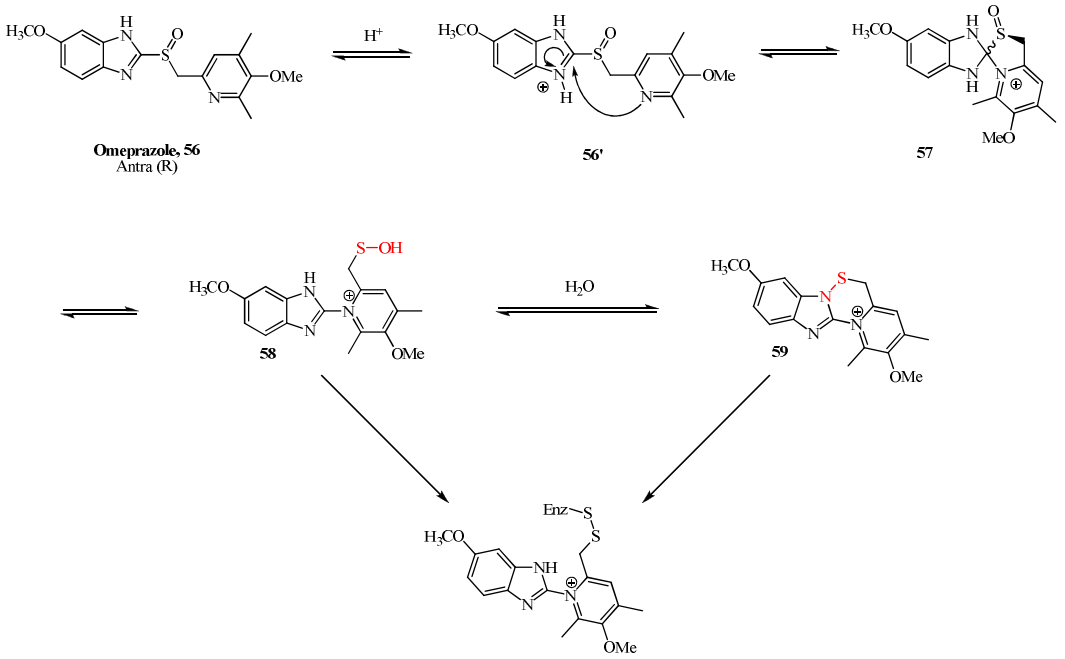

Scheme 1.6. Omeprazole acidic assisted rearrangement. The formation of two kind of cysteine trapping intermediates (warheads colored in red), a sulfenic acid **58** or a cyclic sulfenamide **59** respectively, has been proposed.[36]

Immediately after, these unstable intermediates quickly react with one or more cysteine residue on H+/K+ ATPase, inhibiting its catalytic activity. Since, omeprazole efficiently undergoes this kind of rearrangement only at pH<4, the covalent inhibitory effect of this drug is highly compartmentalized within oxyntic cells. This target-localized formation of reactive intermediates reduces the systemic exposure to this drug and decreases the occurrence of potential off-target toxicity.

Finally, vigabatrin (Sabril ®, **60**, scheme 1.7) represents a good example of mechanism-based covalent modifier. vigabatrin can be orally administered providing a specific covalent and irreversible inhibition of human GABA aminotransferase, a key enzyme involved in GABA catabolism. In animal models, vigabatrin has been recognized to protect against convulsion seizures inducing raised brain GABA levels in CNS. The anticonvulsant potential of this drug has been quickly

pharmacologically exploited for the short-term treatment of epilepsy in human. It has been proposed that vigabatrin **60**, once reversibly and non-covalently bound into the enzyme active site, inhibits GABA aminotransferase by irreversible alkylation of Lys258 residue, normally involved to the binding of cofactor pyridoxal phosphate (PLP).[14] As previously described, the warhead responsible of the covalent GABA aminotransferase inhibition is not directly embedded into vigabatrin structure but is formed thanks to the normal transaminase activity of its target enzyme. Indeed, it is postulated that vigabatrin can form an imminium adduct **61** with PLP cofactor. The tautomerization of imminium compound **61** lead to an activated enamine species **62** able to covalently and irreversibly bind Lys258 by a Mannich addition-based mechanism (scheme 1.7).

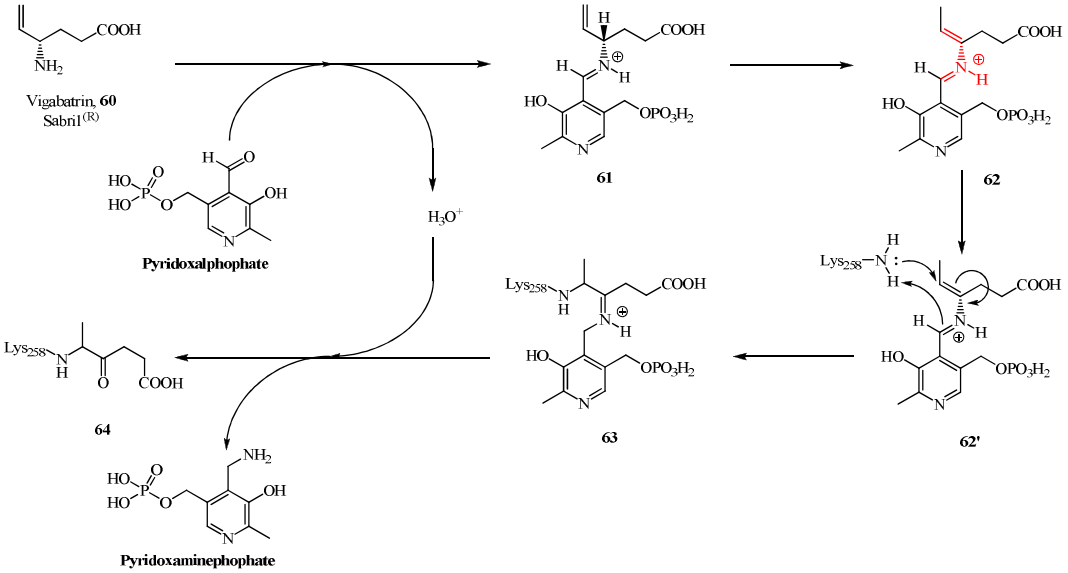

Scheme 1.7. Mechanism-based activation of vigabatrin **60** and subsequent GABA aminotransferase covalent inhibition. The alkylation of Lys258 by activated enamine warhead (colored in red, compound **62**) irreversibly inhibit the target.

In this way, this mechanism-based activation provides to vigabatrin **60** a very high specificity for the desired target and greatly limits the occurrence of off-target toxicity.

1.2 Cysteine reactive compounds

As reported in the previous chapter, a proper warhead reactivity modulation can enhance the specificity of designed covalent drug candidates for a given target. The same concept can be expanded designing warheads able to selectively bind a subset of nucleophiles in chemical reaction models as well as in biological environments. Indeed, following the **HSAB** (**H**ard and **S**oft **L**ewis **A**cids and **B**ases) theory, electrophile warhead centres could be tailored to have "hard" or "soft" properties in order to direct their reactivity mainly toward "hard" or "soft" nucleophiles, respectively. Hard nucleophiles usually have high charge-density so that are well represented by small charged or highly polarized species. Their charge-directed interactions with electrophiles species don't strictly require a well overlapping of nucleophile orbitals with the electrophile's accepting ones because charge attraction are enough to drive their nucleophilic attack.

On the opposite, soft nucleophiles reactivity is based on orbitals overlapping rather than on charge-directed interactions. Usually, they aren't particularly polarized and present large available orbitals for the nucleophilic interaction with the electrophilic partner.[15,16] From a biological point of view, it is reported that thiol residues of cysteines or glutathione and the oxygen of DNA bases are recognizable as the softest and the hardest biological nucleophiles respectively. Amino groups of lysine or histidine as well as hydroxyl group of serine or threonine are considered hard enough to occupy an intermediate position between thiols and oxygen atoms of DNA nucleotides.[17] On the base of these assumptions, a proper tuning of hard/soft reactivity could drive the warhead of a given covalent modifier to selectively react with soft nucleophiles like thiols, limiting side reactions with harder nucleophiles like amine- or hydroxyl- based species.

In this way, the achieved nucleophyle-based selectivity could provide additional selectivity to the designed covalent modifiers, help them to discriminate the desired thiol exposing target from undesired ones.
Considering that cysteines are coded only with a frequency of 2.26% on mammalian proteome,[3] is very improbable that different proteins would share the same cysteines distribution pattern. This finding represents a formidable source of diversity that can be exploited by researcher to design very specific covalent modifiers able, after proper structural optimization and warhead reactivity tuning, to discriminate similar cysteine exposing protein that only differs for their cysteine exposition pattern. This opportunity makes cysteine trapping the most promising pharmaceutically exploitable class of covalent binders because of their theoretical ability to reach the highest target selectivity among them.

Moreover, cysteine-trapping compounds should present a more favorable toxicological profile than other unspecific covalent modifiers. For instance, they should not able to directly produce stable covalent DNA modifications. On the other hand, their thiol-oriented reactivity could be responsible of their increased sensitivity toward glutathione mediated bioinactivation. Apart the impact that this detoxication mechanism could have on their pharmacokinetic profiles, the resulting reduced levels of glutathione induced by these compounds could be responsible of intracellular oxidoreductive equilibrium impairment and histological toxicity. Despite this, cysteine-trapping compounds are the most represented class among covalent reactive compounds currently evaluated as drug candidates or that have already reached the market.[2] Beyond their pharmaceutical exploitability, cysteine trapping compounds are also widely used as biological tool to study and/or validate clinically important biological targets. For instance, highly potent and specific cysteine-trapper are employed as **A**ctivity-**B**ased **P**robes (**ABP**)[18,19] or **AF**finity-**B**ased **P**robes (**AFBP**) to label a subset of

related cysteine exposing proteins across proteome. While the labeling potential of ABP is directed toward catalytically active cysteine residues, AFBP are designed to react less specifically with all kind of solvent exposed thiol residues. Cysteine reactive ABP and AFBP are usually designed to contain easily recognizable tag portions (e.g. fluorescent, radioactive or biotinylated functionalities) in order to improve the purification and the identification of labeled proteins.[19]

Development of cysteine-protease inhibitors has shown that many warheads with different chemical reactivity are able to selectively react with specific catalytic or non-catalytic cysteine residues in cysteine-protease active sites. Despite this, a specific cysteine trapping activity has been verified only for few of considered warhead classes. For instance, β-lactone based warheads has been claimed to irreversibly inhibit Hepatitis Virus A 3C cysteine protease (HVA 3C) by Cys172 covalent targeting[4] but, in the same time, this warhead has been reported to be responsible of the irreversible acylation of the catalytic serine of hPL.[20] In this way, only a limited kind of chemical entities can be considered to possess a true cysteine-specific reactivity.[2, 21] These cysteine-specific warheads can be classified on the base of their reaction mechanisms. So they can be grouped as (1) nucleophile substitution reaction based, (2) addition reaction based and (3) addition-elimination reaction based warheads.

1.2.1 Nucleophile substitution reaction-based cysteine reactive compounds: activated α-methylketones

α-methyketones having an appropriate leaving group attached to their α-methylene portion are able to alkylate cysteine targeted residue by nucleophylic substitution (Figure 1.5).

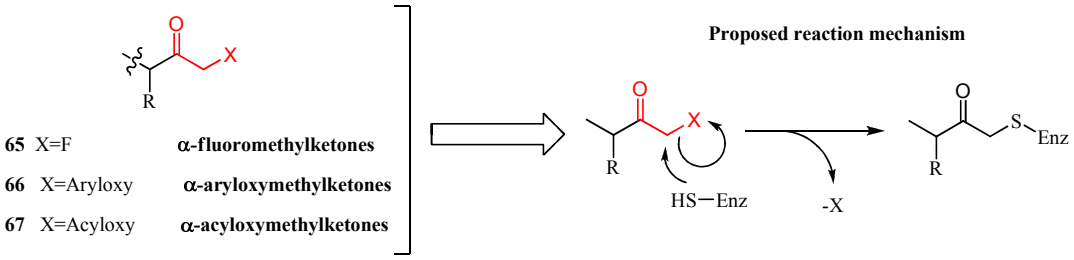

Figure 1.5. Structure and reaction mechanism of activated α-methylketone. Warhead portions are colored in red.

All activated α-methylketones here reported are widely used as labeling agents in biological investigation and many of them can be readily bought because of their commercial availability. α-fluoro-,[22] α-diazo-,[23] and α-acyloxy- methylketones[4] (**65**, **66** and **67** respectively, Figure 1.5) have been proved to be stable in model reactions carried out exposing them to thiols like glutathione and 1,4-dithio-*DL*-threitol (DTT).

This chemical behavior suggests that they should possess low warhead reactivity able to prevent the alkylation of unwanted targets or to hamper their glutathione-dependent biological deactivation. All reported α-methyketones have been joined to different kind of peptidic or peptidomimetic driver groups in order to develop potent and irreversible cysteine protease inhibitors. Dependently on their driver group tailoring, α-fluoromethylketone based compounds **65** have been reported to inhibit a wide range of pharmacologically relevant cysteine proteases[4, 24, 25] like cathepsin B, calcipain and cruzain. Good pharmacokinetic profiles have been reported for many α-fluoromethylketones. They were proved to be orally available and to have high target specificity and to not induce mutagenicity. Despite their therapeutic potential against disease like rheumatoid arthritis, Malaria and Chagas' diseases, α-fluoromethylketones presents some toxicity problems related to their metabolic reprocessing. Indeed, their metabolic degradation releases the extremely toxic fluoroacetate anion

that, miming acetate units in cellular Krebb cycle, acts as metabolic poison in mammalians.[4]

α-aryloxy- and α-acyloxy- methylketones (**66** and **67** respectively) were reported to irreversibly react with target cysteines forming stable thioether derivatives. Despite this, different kinds of α-aryloxy- and α-acyloxy- methylketones were reported to inhibit the cysteine protease caspase-1 irreversibly or reversibly as well. α-acyloxymethylketones are been found quite effective to inhibit liver cathepsin B activity after *in vivo* administration in rat. α-aryloxy- and α-acyloxy- methylketone warheads can be also recognized within the structure of new EGFR irreversible inhibitors designed and synthesized during the accomplishment of this PhD project.

1.2.2 Nucleophile substitution reaction-based cysteine reactive compounds: disulfides and sulfenamides

Disulfide bond forming warheads like disulfides (**A** and **B**, Figure 1.6) and sulfenamides (**C** and **D**, Figure 1.6) represent good examples of "soft" electrophiles able to selectively react with "soft" nucleophiles like thiols. Disulfides and sulfenamides are one of the most frequently pharmacologically exploited kind of cysteine trapping warheads reported in literature. In term of reactivity, disulfides[26] and sulfenamides[27] are mainly characterized by the ability of sulfur atom to be attached by soft nucleophile species with subsequent neighboring heteroatom displacement as reported in figure 1.6.

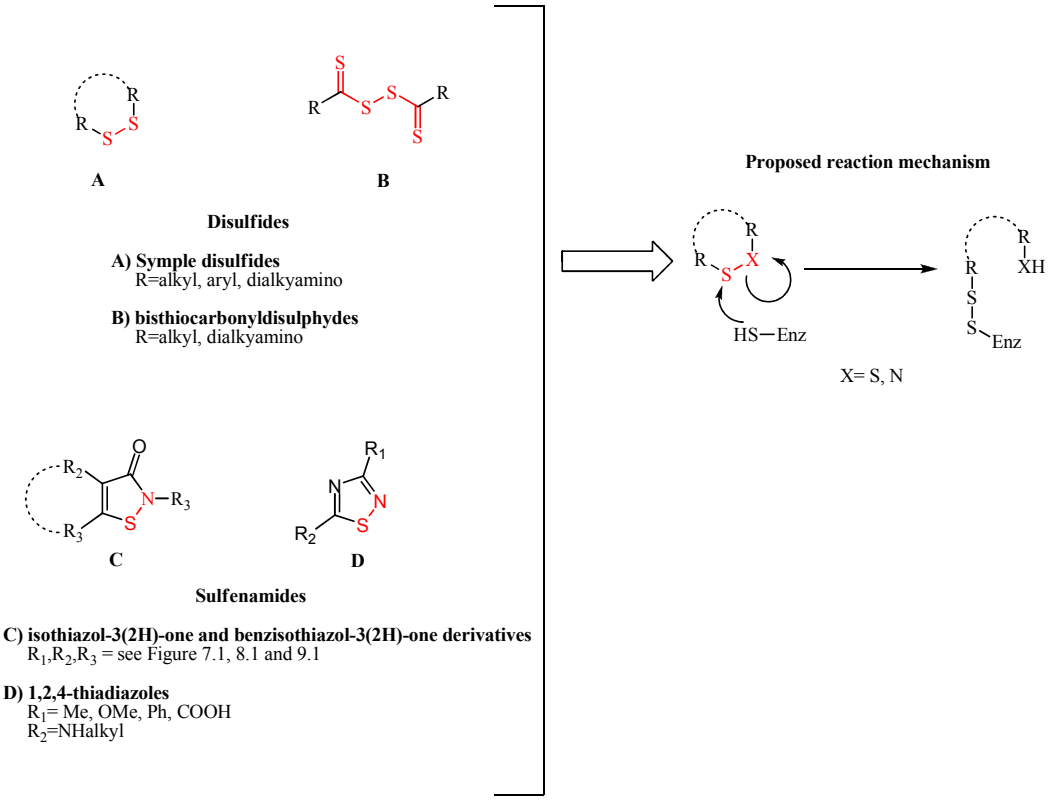

Figure 1.6. General structures and reaction mechanism of most relevant disulfides and sulfenamides warheads. The presence of dashed lines between two substituent "R" indicate that they can be part of an alicyclic or of an aromatic cyclic system as well. Warhead portions are colored in red.

Disulfides derivatives **A** and **B** were reported to inhibit alcohol dehydrogenase (ALDH),[28,29] Human Immunodeficiency Virus nucleocapsid zinc finger protein (HIV-1 NCp7),[30] Epidermal Growth Factor Receptor (EGFR)[31] and MonoAcylGlycerol apse (MAGL).[32,33]

HIV-1 NCp7 play a pivotal role for HIV life cycle and its mutation or modification is not tolerated. NCp7 select the viral RNA from cellular RNA for its dimerization and packaging, stimulate reverse transcription and protect the viral RNA from nucleases. It was reported that disulfides inhibits NCp7 by a covalent binding of one of three cysteine residues present within zinc-finger motives of the enzyme. The covalent modification destabilizes the Zn^{2+} ion coordination and triggers the

ejection of metal ion from the targeted zinc finger motif. The resulting unfolding of zinc fingers impairs the viral RNA recognition process and slow down viral replication. Despite this interesting finding about HIV-1 NCp7 inhibition, disulfides are more known as ALDH irreversible inhibitors. The commercially available drug disulfiram (Antabuse ®, **68**, Scheme 1.8) irreversibly inhibits human alcohol dehydrogenase (ALDH) *in vitro*[28] and *in vivo*[29] binding its catalytic residue Cys305.

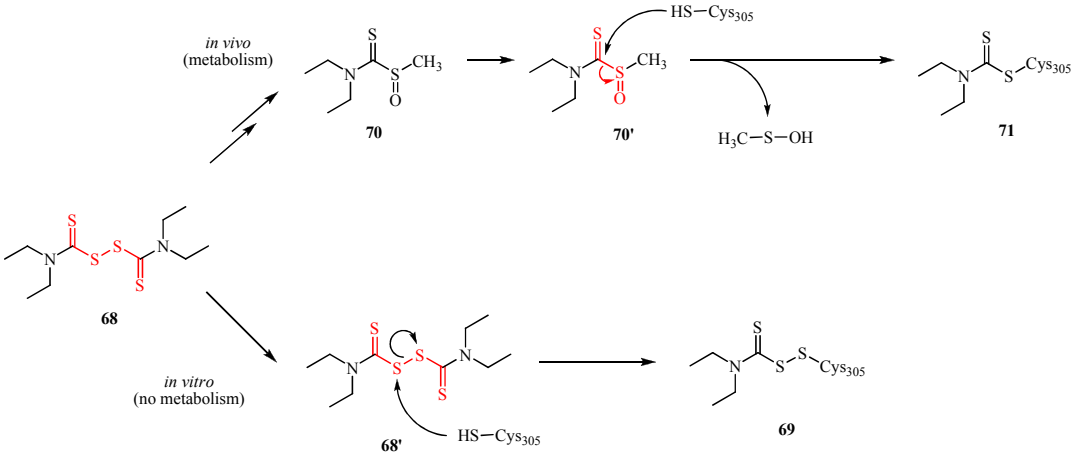

Scheme 1.8. Inhibitory mechanism of disulfiram **37** on human alcohol dehydrogenase.

While *in vitro* studies have suggested that the ALDH inhibition was accomplished by the formation of mixed disulfide **68**, a metabolic dependent activation of disulfiram has been observed in vivo. In this way, it is thought that Cys305 was irreversibly bound by the thiocarbamoylthioesther intermediate **71** rather than mixed disulfides adduct **69**.[29]

Despite no commercially available drugs are based on isothiazol-3(2*H*)-one (Figure 1.6, **C**) or 1,2,4-thiadiazole (Figure 1.6, **D**) warheads, these sulfonamide warheads have been reported to be present in a large amount of biologically active compounds. Even sharing a similar warhead structure, these compounds have shown an impressive versatility in term of biological target diversity range.

Dependence of observed biological activity to their reactivity toward thiols has been demonstrated only for few sulfenamide compounds like isothiazol-3(*2H*)-ones and 1,2,4-thiadiazoles (figure 1.7). Indeed, the formation of disulfide bridges between these warheads and their designed targets has been directly observed only for isothiazol-3(*2H*)-ones[34] and 1,2,4-thiadiazoles[35] derivatives by LC-MS analysis and X-ray diffraction respectively.

For instance, the inhibition P56^{lck} kinase by isothiazol-3(*2H*)-ones[34] has been confirmed by comparison of mass spectra of native P56^{lck} kinase with the isothiazol-3(*2H*)-one-labeled one. These spectra shows three different covalent modified cysteine residues and their positions have been elucidated by further LC-MS analysis on tryptic fragments of isothiazol-3(*2H*)-one-labeled P56^{lck} kinase.

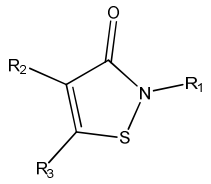

Isothiazol-3(*2H*)-ones

P56^{lck} Tyrosine Kinase inhibitors (anti-tumor compounds)
(R_1=aryl, heteroaryl; R_2R_3=H)

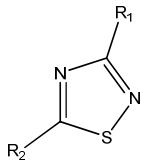

1,2,4-thiadiazoles

Papain inhibitors (Cysteine protease inhibitors)
R_1=alkyl
R_2= Peptydil

Figure 1.7. Sulfenamidic compound for which biological activity is proved to be dependent to their cysteine trapping reactivity.

On the hand, only indirect experimental evidences have been reported to support a possible correlation between the cysteine trapping activity of many others sulfenamide derivatives and their biological effects (Figure 1.8).[35,36, 37, 38,39, 40, 41]

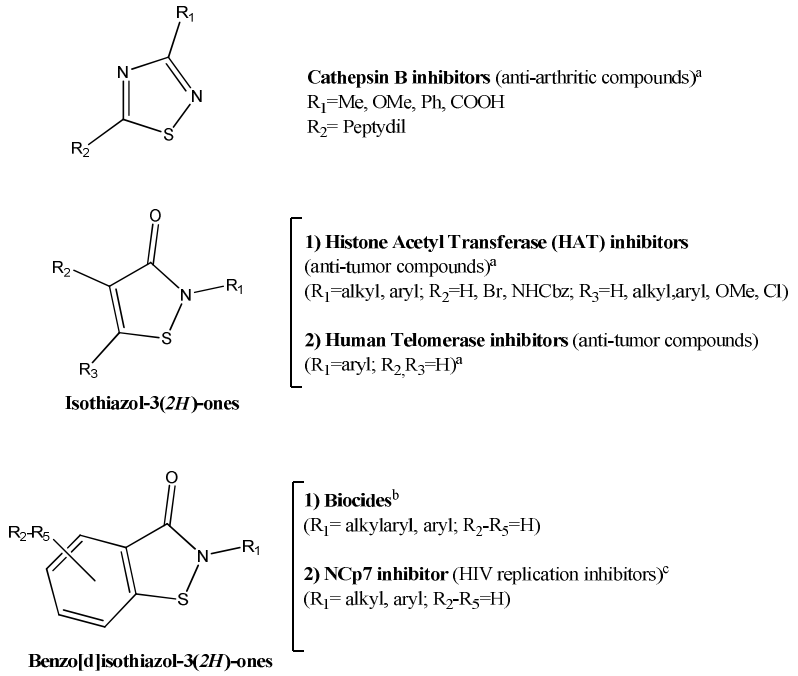

Figure 1.8. Sulfenamidic compounds for which biological activity is suspected to be dependent to their cysteine trapping reactivity. The experimental way used to verify the disulfidic nature of covalent target modification is specified by apex characters: [a] DTT addition, recovery of target biological activity; [b] L-cysteine addition, loss on biocide activity of tested compounds; [c] disulfide bond formation evaluation by zinc extrusion measurements, [d] DTT addition: loss of radioactivity from [H^3]-omeprazole-target adduct.

For instance, the formation of disulfide bridges between tested sulfenamide warhead and targeted cysteine residue has been often established observing the effects of disulfide reducing agents on the covalent modified target. Indeed, restoration of free cysteine residues usually leads to the target biological activity recovery[37a, 35, 38, 41] or to other measurable effects such as radioactivity loss when radio-labeled sulfenamides are used for target modification.[36] Unfortunately, these findings did not prove the occurrence of cysteine covalent modification but they only have provided indications about this occurrence. Finally, the thiol-trapping activity of some isothiazol-3(2*H*)one derivatives has been only postulated and not yet experimentally verified (Figure 1.9).[42,43,44]

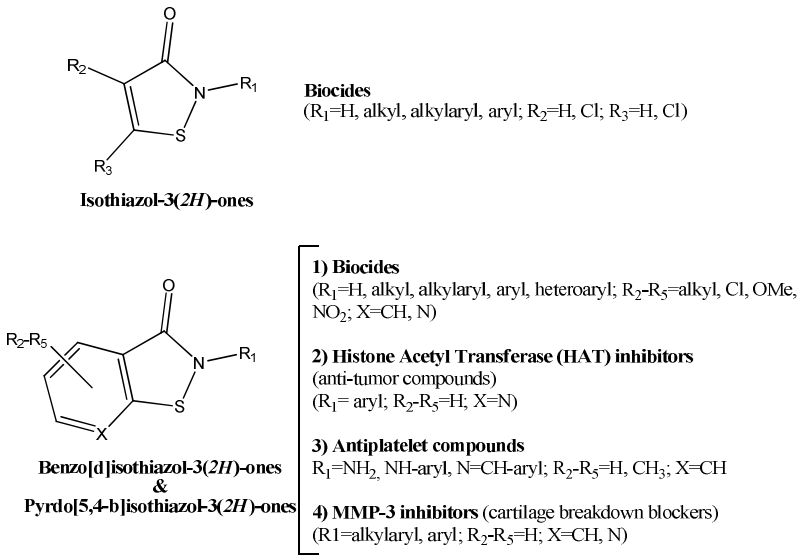

Figure 1.9. Sulfenamidic compounds for which biological activity is suspected to be dependent to their cysteine trapping reactivity.

Non-halogenated 2-methylisothiazol-3(2*H*)-one presents a very specific reactivity toward thiols and it has been found unreactive toward other nucleophiles like amines and alcohols in aqueous solution. Despite the presence of a potential Michael acceptor system, no Michael addition to the conjugated carbon-carbon double bond of isothiazol-3(2H)–one derivatives has been observed until now.[8] Since isothiazol-3(*2H*)-ones and benzo[d]isothiazol-3(*2H*)-ones derivatives have been reported as highly reactive toward thiols[9] and responsible to induce skin sensitization in exposed subjects,[8,45] one can be tempted to consider these warhead too reactive to be druggable. Otherwise, low *in vivo* toxicity and good bioavailability have been reported for some isothiazol-3(*2H*)-one derivatives.[40b, 42b] *N*-unsubstituted benzo[d]isothiazol-3(*2H*)-ones carrying different substituents on benzo fused ring have been *in vivo* orally administered in mice or rats to evaluate their antimicrobials potential. LD_{50} values for each of them have been collected (Table 1.1).

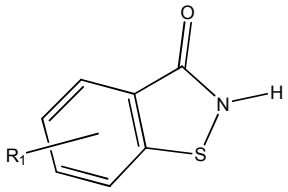

Benzo[d]isothiazol-3(*2H*)-ones

Compound	R_1	Form of preparation	Animal	LD_{50}
71	5-Cl	N/A	mouse	390 mg/Kg
72	6-CH_3	N/A	mouse	510 mg/Kg
73	6-Cl	Suspension (free base)	mouse	≈ 4600 mg/Kg
73	6-Cl	Suspension (free base)	rat	>4300 mg/Kg
73'	6-Cl	Sodium salt	mouse	1400 mg/Kg

Table 1.1. *In vivo* toxicity of benzo[d]isothiazol-3(*2H*)-one derivatives carrying different substituents on the aromatic portion.

Among tested compounds, 6-Chloro derivative **73** shows the lower LD_{50} value and its toxicity seems related to its solubility (the sodium salt derivative **73'** is more soluble and more toxic than suspended free base counterpart **73**). When orally administered in mice, 6-chlorobenzo[d]isothiazol-3(*2H*)-one **73** has been found able to inhibit the growth of a wide-spectra of microorganisms within the intestinal environment with no selection of any particular kind of them. Despite this, the bacteriostatic activity of 6-chlorobenzo[d]isothiazol-3(*2H*)-one **73**, probably due to its poor solubility, has been found restricted to the gastrointestinal lumen because it was unable to prevents systemic infections in mice induced by *E.coli* or *Str. Pyogenes* (with drug oral doses of 40 mg/Kg and 100 mg/Kg).

Despite 6-chlorobenzo[d]isothiazol-3(*2H*)-one **73** has shown a low acute toxicity, chronic administration of increased amounts of 6-

chlorobenzo[d]isothiazol-3(2*H*)-one **73** in rat has produced a significant but reversible increase in relative liver-weight. Notably, no histologically detectable changes have been found (table 1.2).

Oral dose	Relative liver-weight increased	Histological changes
60 mg/Kg	NO	NO
180 mg/Kg	YES	NO
540 mg/Kg	YES	NO

Table 1.2. *In vivo* chronic toxicity of 6-chlorobenzo[d]isothiazol-3(2*H*)-one at different oral doses.

In addition to these low toxicity levels, a very good pharmacokinetic profile has been reported for another *N*-alkyl benzo[d]isothiazol-3(2*H*)-ones like (2R,3S)-3-methyl-2-(3-oxobenzo[d]isothiazol-2(3H)-yl)pentanoic acid **74** (Table 1.3). This derivative has been *in vitro* found effective to inhibit the HIV proliferation in HIV infected Chick Embryonic Metastasis cells (EC_{50} from 1.9 to 6.7 μM dependently to the kind of considered HIV strain) with a good therapeutic indices (TC_{50}/EC_{50} > 12). The pharmacokinetic of **74** has been explored by *in vivo* (mice) sub-cutaneous and oral administrations (Table 3).

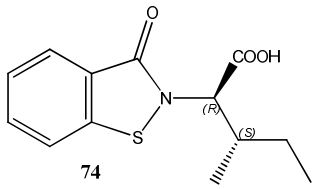

74

Adm. route	Dose (mg/Kg)	C_{max}[a] (µg/ml)	AUC[a] (µg*h/ml)	$T_{1/2}$ (h)	F %
SC	125	83	380	2.7	N/A
	200	108	645	4.6	N/A
PO	125	49	327	2.1	82
	200	83	661	4.6	100

Table 1.3. Pharmacokinetic data of *in vivo* (mice) administration of compound **45.**

[a] Plasmatic concentrations have been determined as free thiol equivalents by reduction of all samples with DTT.

The maximal reached concentration in plasma (C_{max}) and AUC were increased proportionally in tested dosing range. Compound **74** was reported well tolerated at the tested doses with a calculated half-life of 3.5 h and an oral bioavailability of 91%. Taken together, these findings provide a solid rational to consider isothiazol-3(*2H*)-one and benzo[d]isothiazol-3(*2H*)-ones as suitable warhead portions for the development of new highly selective and druggable cysteine trapping compounds.

Finally, 1,2,4-thiadiazoles have been reported to react with thiols with the same reaction mechanism suggested for isothiazol-3(*2H*)-one and benzo[d]isothiazol-3(*2H*)-ones warheads (Figure 1.6, **D**). Like previously reported sulfonamide warheads, 1,2,4-thiadiazoles have been reported to selectively react with soft nucleophiles like cysteine, without undergoing nucleophilic attack by other harder nucleophiles like amines or alcohols. Some 1,2,4-thiadiazole derivatives were reported be stable when exposed to reducing agents like DTT for hours and to inhibit

cysteine protease such as papain and cathepsin by covalent targeting of their catalytic cysteine residues [35]

The highly focused reactivity toward thiols shared by all reported sulfenamide warheads as well as the good pharmacokinetic and toxicological profiles characterizing some benzo[d]isothiazol-3(2*H*)-one based compounds could suggest a good druggability for these kind of warheads. In this way, they could be suitable for pharmacologic exploitation.

1.2.3 Addition reaction-based cysteine reactive compounds: simple addition reaction based warheads

This class includes strained three membered rings reactive moieties (**A**, **B**, **C**) as well as α-cyanomethyl derivatives (**D**) able to undergo addition reactions (Figure 1.10).

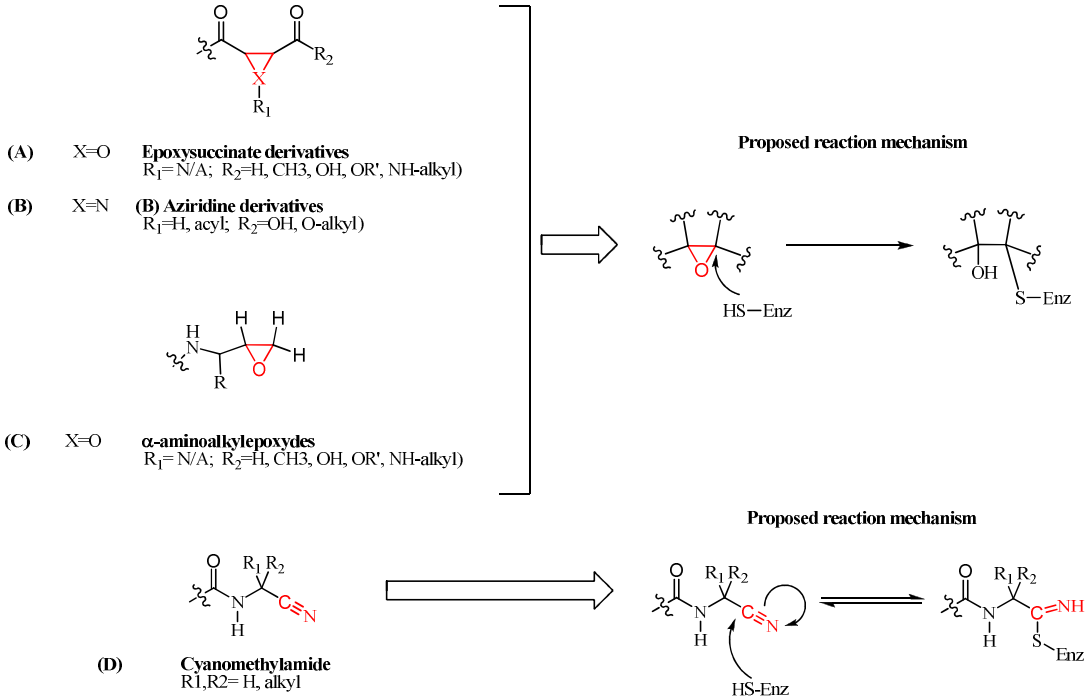

Figure 1.10. General structures and reaction mechanisms of most representative three membered ring and cyanomethylamide warheads. Warhead portions are colored in red.

Epoxysuccinates (**A**) and α-aminoalkylepoxydes (**C**) have been reported to be stable in presence of nucleophiles as thiols.[4] Moreover, aziridine derivatives (**B**) have been reported as stable in presence free thiols like cysteine and also in presence of species carrying free hydroxyl- or amino group like threonine or glutamate.[46] Among this collection of three membered ring warheads, epoxysuccinate warheads are the most studied and widely reported in literature. The first discovered epoxysuccinyl derivative with inhibitory activity toward cysteine protease was E-64 (**75**, Figure 1.11), a natural compound initially isolated from *Aspergillus japonicus*.

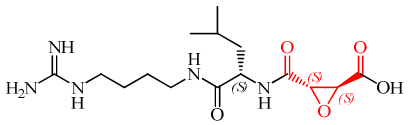

75, E-64

Figure 1.11. Structure of E-64 from *Aspergillus japonicus*. Warhead portion is colored in red.

E-64 was reported as highly potent irreversible covalent inhibitor of many cysteine proteases. It is reported that E-64 does not react with other kind of protease but was unable to selectively drive its reactivity toward a specific cysteine protease. In this way, E-64 inhibits a large number of cysteine proteases like papain, ficin, bromelain, chatepsin (subtypes B, H, F, K, L, O, S, V and X), calpain, cruzain and other proteases. For these reasons, since discovered, E-64 was used as unspecific ABP (Activity-Based Probe, see chapter 1.2) for biological investigation purposes. Many other derivativatives of E-64, all of them possessing a trans-configured epoxyde functionality, have been synthesized by modification of decorating groups neighboring the epoxyde warhead portion. They were used as AFBP (see also Chapter 1.2) to study the histochemical distribution and the biological functions of cysteine proteases.

Epoxysuccinates were found very effective *in vivo* as cysteine protease inhibitors because of their high potency, stability and permeability into cells and tissues. *In vivo* administration of epoxysuccinates has been found effective to decrease osteoblasts-dependent bone resorption and to induce cytoprotection in heart and brain ischemic animal models.[4]

Cyanomethylamides (**D**) were reported as cysteine protease inhibitors too. Since cyanomethylamide moiety can be easily recognized as warhead portion on both serine[47] and cysteine trapping compounds, cyanomethylamide warheads cannot be considered cysteine selective themselves. On the other hand, the high specificity and the excellent pharmacokinetic profile of cyanomethylamide armed compound like odanacatib (**76,** Scheme 1.9) make this warhead class worthwhile in term of druggability. Odanacatib has reported to covalently interact with an unspecified cysteine group on cathepsin K, inhibiting this enzyme by formation of a reversible thioimidate complex (Pinner reaction).

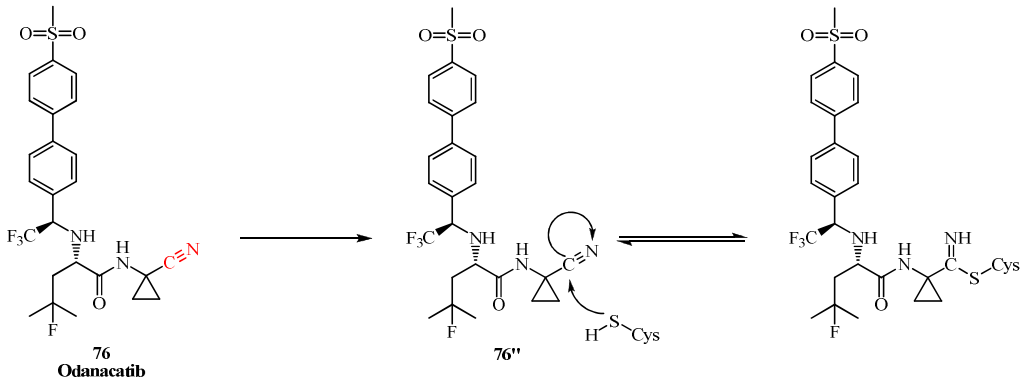

Scheme 1.9. Covalent binding mechanism of odanacatib toward cathepsin K by Pinner reaction. The equilibrium between thioimidate complex and the reaction mechanism intermediate **76''** make the covalent binding completely reversible. The odanacatib warhead portion is colored in red.

The inhibition of cathepsin K provided by odanactib could be useful to decrease the bone resorption rate in pathological conditions.[48]

Actually, odanactib represents one of the most clinically advanced drug candidate (phase III) for the treatment of post-menopausal osteoporosis.

1.2.4 Addition reaction-based cysteine reactive compounds: Michael addition reaction based warheads

As reported for disulfides and sulfenamides, α,β-unsaturated systems could represent good examples of "soft" electrophylic warheads able to selectively add "soft" nucleophiles (like thiols) to their conjugated carbon-carbon double bonds, undergoing Michael addition reaction. Both α,β-unsaturated carbonyls and α,β-unsaturated sulfones (**A'**, **A''** and **B** respectively, Figure 1.12) provide irreversible alkylation of targeted cysteines.

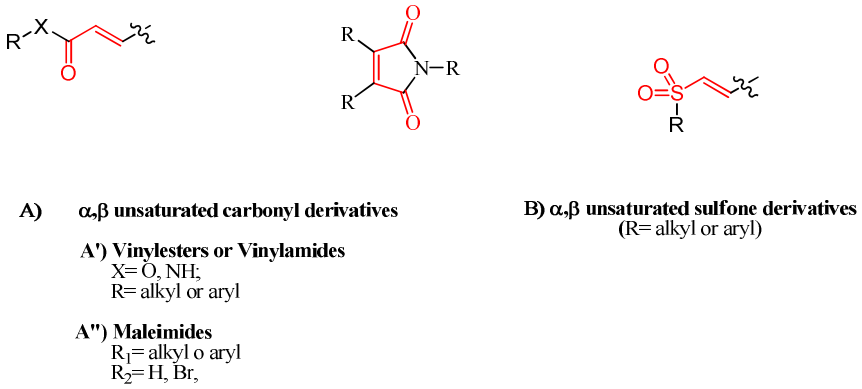

Figure 1.12. General structures of α,β-insaturated Michael acceptor warheads with specific reactivity toward cysteine residues.

Despite Michael acceptor systems are claimed to be highly selective for cysteine addition, not all of them are druggable enough to be embedded in molecules designed for therapeutic purposes. Among them, vinylsulphones (**B**) should represent the most druggable class because they were reported to be very stable toward glutathione exposure.[4] On the opposite, the highly activated Michael system present in maleimides (**A'**) quickly reacts with thiols suggesting an unfavorable

metabolic profiles for molecules carrying this warhead. On the other hand, the highly focused cysteine-trapping reactivity of maleimides allows their use as warhead portions in compounds designed to act as pharmacological or biological tools rather than as drugs.[49] The use of α,β-unsaturated carbonyl derivatives (**A**, figure 1.12) as cysteine protease inhibitors is very limited. Rhinovirus 3C protease (3CP) has been targeted by α,β-unsaturated carbonyl derivatives. This cysteine protease is essential for the rhinovirus life cycle because it is responsible of the cleavage of the virus polyproteins into structural and enzymatic proteins, crucial for virus replication. The most clinically advanced α,β-unsaturated carbonyl derivative for 3CP protease inhibition is rupintrivir **77** (phase II), a promising drug candidate for the treatment of "common cold" (Figure 1.13).

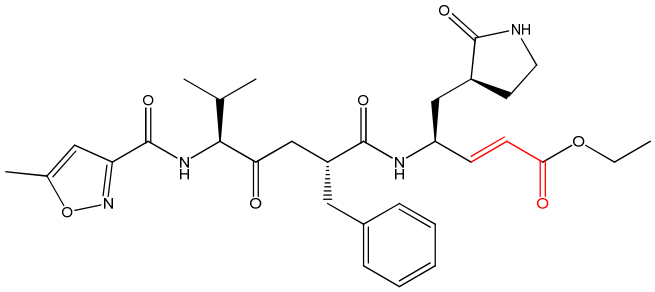

77
Rupintrivir (Phase II)

Figure 1.13. Structure of rupintrivir, the most clinically advanced irreversible peptidomimetic inhibitor of Rhinovirus 3CP. Warhead portion is colored in red.

Rupintrivir was reported to irreversibly inhibit Rhinovirus 3C protease by covalent binding of the catalytic cysteine residue in the active site of the enzyme, decreasing the severity of "common cold" in humans.[4] Unfortunately, the development of rupintrivir **77** is actually stopped because of lack of clinical efficacy in naturally occurred rhinovirus infections.[50]

α,β-unsaturated sulfones **B** were used as ABP or AFBP (see Chapter 1.2) for biological investigations as well as very successful cysteine

protease inhibitors. They are stable and unreactive toward nucleophiles outside the cysteine protease catalytic machinery. α,β-unsaturated sulfone warhead can be recognized within the molecular structure of promising bone resorption inhibitors as well as anti-trypanosome, anti-malarial and anti-protozoal agents. Outside of cysteine protease framework, both α,β-unsaturated carbonyl and α,β-unsaturated sulfones derivatives were reported to covalently bind and irreversibly inhibit pharmacologically important targets like EGFR (see Chapter 2).

1.2.5 Addition-elimination reaction based cysteine reactive compounds

Within this warhead class, only the alkylhydrazinecarboxylate warhead has been reported to selectively react with thiols rather than other kind of nucleophiles (Figure 1.14)

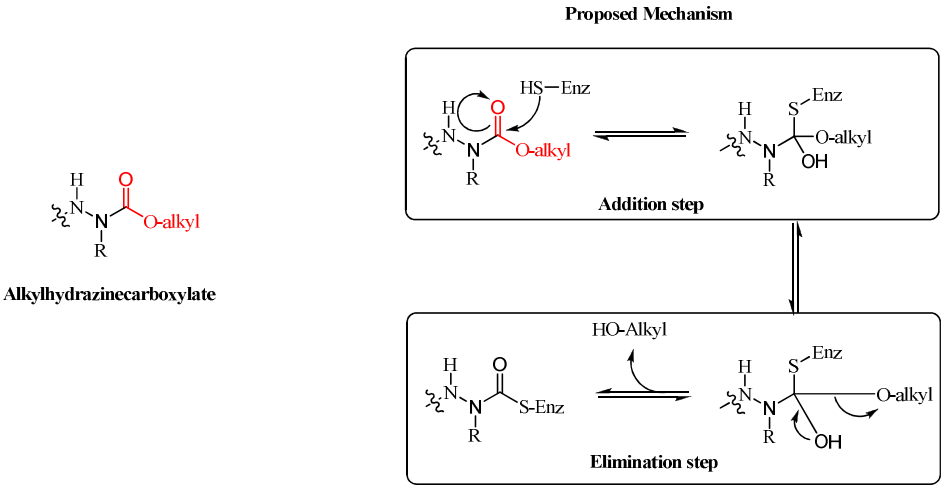

Figure 1.14. Overview of the two stage carbamoylating mechanism of alkylhydrazinecarboxylate warheads **54**.

Like other carbamates, these warheads were reported able to carbamoylate the target producing a carbamoylcysteine residue which, in some biological environments, can result stable to hydrolysis. This was

accomplished through a two stage reaction mechanism in which the nuclephilic attach of thiol leads to the formation of an unstable tetrahedral intermediate. After this, the tetrahedral structure of intermediate collapse and the alkyloxy leaving group is displaced away to produce the stable carbamoylated enzyme (Figure 1.4). The specific reactivity of this kind of warheads toward thiols was related to the low nucleofugicity of the alkyloxy leaving group. Indeed, among biological nucleophiles, only thiols are strong enough to efficiently displace this bad leaving group. This means that only thiol exposing biological targets could be efficiently carbamoylated by these warheads. The dependence of their carbamoylating potential to the nucleofugicity of oxygenated leaving group can be easily verified considering the serine-trapping activity of carbamate carrying more nucleofuge leaving group.[4] Despite the specific cysteine reactivity showed by alkylhydrazinecarboxilate warheads, no therapeutic applications were reported for such compounds. Nevertheless, the good solution stability of alkylhydrazinecarboxilate moieties allows their use as active site titrants for cysteine protease quantification or, once linked to a proper driver group, as tools for *in vivo* investigations.[4]

1.3 Cysteine-reactive compounds as drugs or pharmacological tools: some steps forward

As described in Chapters 1.2, cysteine-trapping compounds can be efficiently used as biological or pharmacological tools and as drugs as well. Next chapters will show how structure tailoring and/or warhead reactivity modulation strategies can be applied to cysteine trapping compounds in order to develop new covalent inhibitors for pharmacologically relevant cysteine-exposing targets like Epidermal Growth Factor Receptor (EGFR) (Chapter 2) or MonoAcylGlycerolLipase (MAGL) (Chapter 3). The development of a new covalent EGFR pro-drug, able to unmask its Michael acceptor warhead within the EGFR ATP binding side, will be reported too (Chapter 2).

Chapter 2

EGFR targeting

2.1 Introduction

Receptor protein kinases (RPTKs) play a central role in signal transduction pathways, regulating cell division and differentiation. Among them, the epidermal growth factor receptor (HER-1/ErbB1/EGFR), one of the most important member of ErbB protein family, is involved in the regulation of several key processes such as cell proliferation, survival, adhesion, migration, and differentiation. [51] Overexpression of EGFR tyrosine kinase was reported in a variety of human tumors and was associated with poor prognosis.[52,53] Therefore, inhibition of EGFR kinase activity has emerged as a promising new approach to cancer therapy and several small molecule tyrosine kinase inhibitors are currently in clinical use or development. Out of the numerous inhibitors of EGFR reported in the last few years, compounds competing with ATP for binding at the catalytic tyrosine kinase domain of EGFR are of special interest. Unfortunately, despite the clinical efficacy of some of these compounds as anticancer drugs, accumulated clinical experience indicates that specific populations of patients can develop resistance against these drugs due to expression of a mutated form of EGFR.[54] In order to overcome this occurrence some covalent irreversible EGFR inhibitors are synthesized by researchers. These derivatives act as non-competitive inhibitors binding the ATP-binding site of EGFR-TK domain by a covalent irreversible interaction with a solvent exposed cysteine residue. Despite these drugs are proven to be effective to overcome the drug resistance induced by EGFR mutation,[55] it is reported that their effective clinical efficacy is limited by occurrence of dose–limiting toxicity problems.[97] Since few kinds of warhead portions have been embedded to irreversible EGFR inhibitors tested until now,[31, 89-86] an expanded exploration of different cysteine-reactive warhead could help to achieve better toxicological profiles. In this way, a systematic

structure-reactivity relationship study could be carried out on these compounds to enhance their toxicity/efficacy ratio.

2.1.1 The HER receptor family: structure, expression and physiological functions

The human epidermal growth factor receptor (HER) family (also known as ErbB receptor family) is composed of EGFR/HER-1/ErbB1, HER-2/ErbB2, HER-3/ErbB3, and HER-4/ErbB4. These receptors share common structural features like an amino-terminal extracellular ligand-binding domain (except HER-2/ErbB2), a single transmembrane anchoring domain and a carboxy-terminal intracellular domain endowed with tyrosine kinase activity (except HER-3/ErbB3) and involved in regulatory functions (Figure 2.1).[53] Among HER receptor family, only HER-1, HER-3, and HER-4 bind canonical growth factor ligands while no ligands were identified for HER-2. Except HER-3, all other HER family members are active as tyrosine kinases.[53,56]

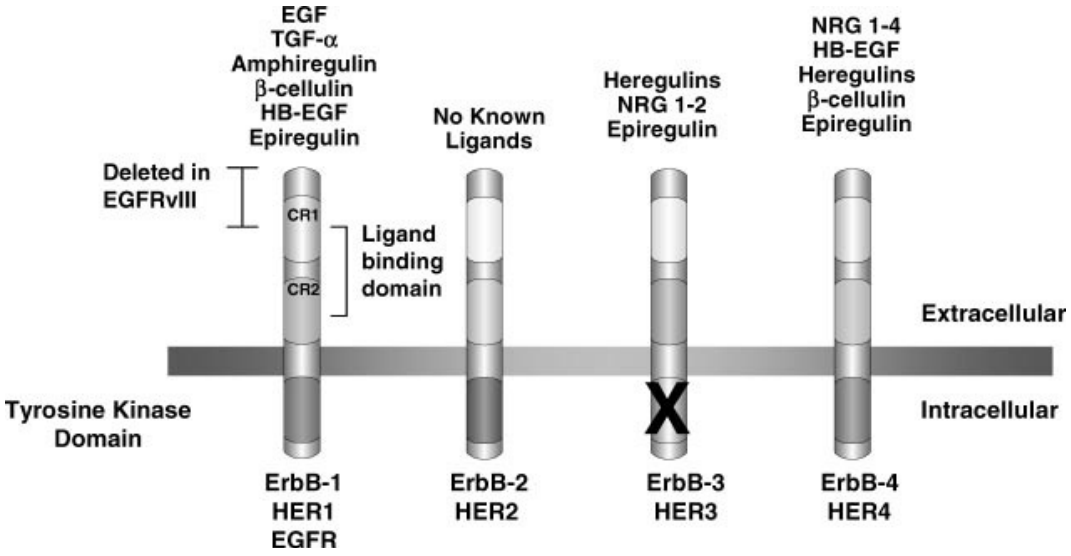

Figure 2.1. The HER family members. Known ligands are reported in the upper position for each depicted receptor.[57]

Each HER receptor is fundamentally an inactive monomer that dimerizes in response to ligand binding. The dimerization process activates the tyrosine kinase activity of the receptor and triggers a complex downstream signalling network involved to regulation of specific aspects of cell function[58] such as gene expression, cellular proliferation, angiogenesis, and inhibition of apoptosis (Figure 2.2)

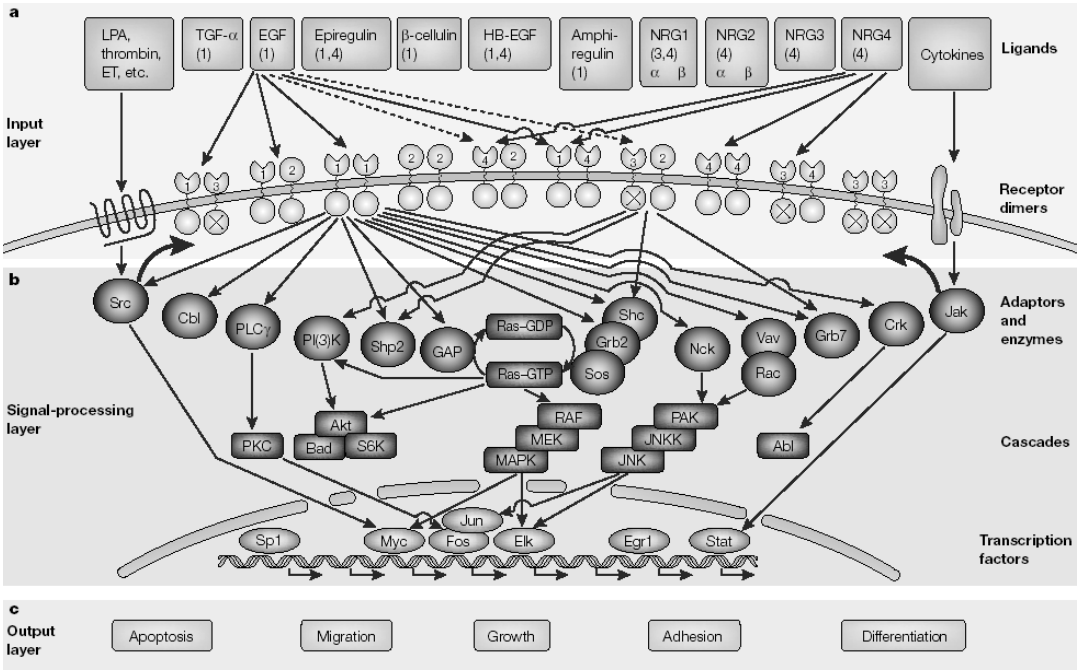

Figure 2.2. The EGFR signalling network.[53]

HER-1/ErbB1/EGFR could be considered the most studied and clinically important member of HER receptor family. A large spectrum of ligands can bind this receptor inducing its homo- or heterodimerization with remaining HER members (especially with HER-2) on the cellular surface. Once dimerized, the autophosphorylation of the intracytoplasmic EGFR portion take place. Phosphorylated tyrosine residues on EGFR intracellular domain serve as binding sites for the recruitment of signal transducers and activators of intracellular substrates which then stimulate an intracellular transduction cascade that transmit

signals to the cellular nucleus (Figure 2.2).[59,60] Finally, the EGFR signalling is mainly inactivated through endocytosis of the dimeric receptor-ligand complexes. The contents of the resulting endosomes are then either degraded or recycled to the cell surface[58,61]

2.1.2 The role of EGFR activation in human development and diseases

The HER family lies at the head of a complex signal transduction cascade that modulates cell proliferation, survival, adhesion, migration and differentiation. While growth-factor-induced EGFR signalling is essential for many normal morphogenic processes and involved in numerous additional cellular responses, the aberrant activity of members of this receptor family has been shown to play a key role in the development and growth of tumor cells. It is also reported that stimulation of EGFR pathways could also contribute to the development of malignancy of tumors,[51,62] promoting tumor cell motility, adhesion and metastasis. [63] In addition, a link between EGFR activation and angiogenesis, which is crucial to sustain tumor growth and invasion, has been described. [64,65]

2.1.3 Pharmacological potentials of EGFR inhibition

Over the recent years, much evidence has been collected to implicate the EGFR and its family members in the development and progression of numerous human tumors. The EGFR can results in tumor development by different mechanisms acting either separately or in combination. This includes receptor overexpression, gene amplification, activating mutations, and autocrine factor loops. Most epithelial tumors, such as head-and-neck, colorectal carcinoma, lung carcinoma, esophageal carcinoma, gastric carcinoma, and breast carcinoma,

overexpress the EGFR. The discovery of constitutive active mutations of the EGFR has been described, providing another mechanism for EGFR-induced tumorigenesis. The mutated EGFR variant EGFR (v) III, the best characterized and the most frequently found in human tumors, presents a constitutive-active, ligand independent tyrosine kinase activity that stimulates cell proliferation in the absence of activating ligands.[66,67] For the pivotal role of EGFR in tumor development and progression, this receptor has become a target for anticancer drug development, and several inhibitors of the EGFR are currently in clinical use or development. In addition, EGFR inhibition has been very recently proved to be pharmacologically exploitable as a new strategy to enhance the nerve regeneration in injured nervous tissues. Indeed, EGFR inhibition seems to slow down the formation of glial scars inhibiting the astrocytes proliferation and to promote nerve regeneration *in vitro* and *in vivo*.[68]

2.1.4 EGFR inhibition strategies

The evidence of significant involvement of EGFR in the growth of solid tumors provides a strong rationale for developing agents that target the EGFR signalling system. Various approaches have been described regarding EGFR-targeted therapies (figure 1.3). These include: (i) monoclonal antibodies (mAb) that compete with activating ligands at the extracellular domain, (ii) small molecule inhibitors that target the intracellular tyrosine kinase domain, (iii) immunotoxins conjugates, (iv) EGFR-targeted antisense oligonucleotides, and (v) downstream inhibitors of the EGFR signalling pathway.

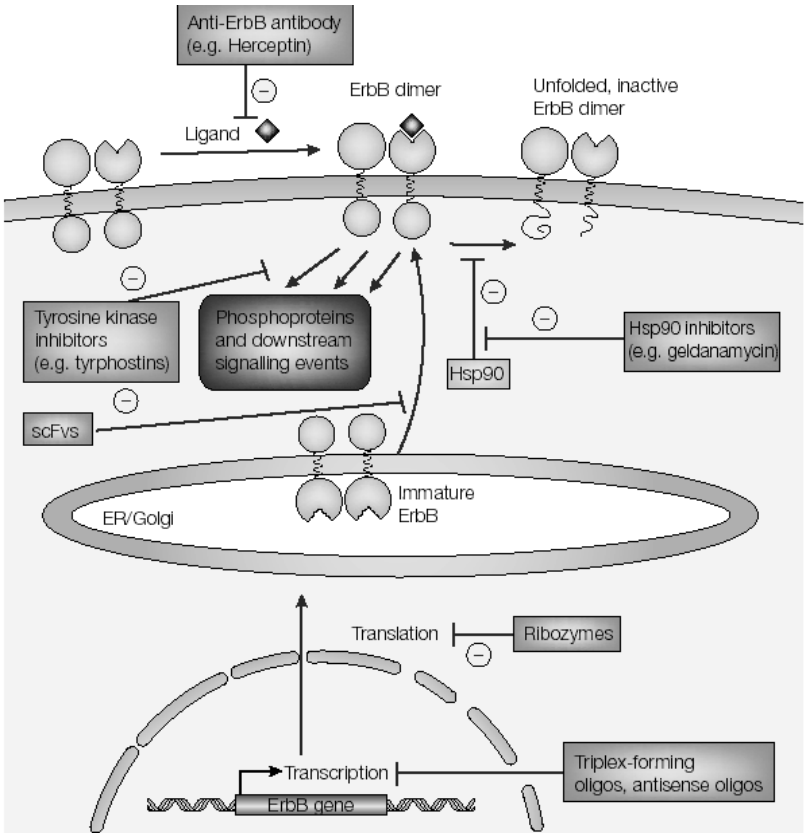

Figure 2.3. Therapeutic strategies for blocking the EGFR signalling network[53]

Among these approach, small-molecule compounds that interfere with intracellular EGFR tyrosine kinase activity are, together with monoclonal antibodies, the most extensively studied approach to block the EGFR signal. Small-molecule inhibitors target the intracellular tyrosine kinase domain of the receptor and inhibit the activation of downstream signalling pathways. These agents has shown many advantages over the other larger molecules directed to EGFR: they can be made more easily, they may show increased penetration into solid tumors, and they may have the advantage over targeting the extracellular region especially in cases where truncation of the extracellular domain of EGFR has led to ligand independent tyrosine kinase activity.

2.2 EGFR-TK domain inhibitors

Dependently to their binding mode with EGFR-TK domain, EGFR tyrosine kinase inhibitors can be classified in two different classes: 1) ATP-competitive inhibitors (reversible) and 2) ATP non-competitive inhibitors (irreversible or partially reversible).

The first class is populated by many structurally different compounds able to inhibit EGFR-TK activity by competing with ATP for binding at the catalytic domain of the enzyme. As a class, they interact with TK-domain in a reversible and non-covalent manner. Despite the clinical efficacy of some of these compounds as anticancer drugs in specific populations of patients with tumors harboring oncogenic forms of tyrosine kinases EGFR variant (v) III,[69] accumulated clinical experience on non-small-cell lung cancers (NSCLCs) indicates that most patients develop resistance due to expression of mutated EGFR.[54] The replacement of the gatekeeper threonine 790 by a bulkier methionine residue in this mutated EGFR (EGFR T790M) seems to increase the EGFR-TK affinity for ATP so to decrease the binding effectiveness of competitive reversible drugs for the same receptor binding site. Despite the potency decreasing induced by this mutation is not so dramatic, the intracellular ATP concentration become higher enough to push-out the drug from EGFR ATP-binding site so to restore the EGFR-TK functionality.[70]

In order to assure to these molecules an effective binding also in presence of T790M mutation, the second class of EGFR-TK inhibitors was developed by scientists. Compounds belonging to this class have structures still designed to mime ATP within the active site of EGFR-TK but they are equipped also with a warhead portion that allow them to covalently interact with a cysteine residue located within the ATP-binding site of EGFR-TK. Their covalent binding mode provides a non-competitive inhibition of EGFR-TK, overcoming in this way the drug

resistance induced by T790M. Moreover, the additional binding affinity provided by formation of covalent adducts often give to these compounds the ability to bind and to inhibit one or more receptors among the remaining catalytically active HER members. This expanded binding spectra could be used to turning off more completely the HER receptors signalling, especially when there are evidences that other HER receptors than EGFR are involved into tumor growing process. For instance, they could be useful in the treatment of breast cancer in which the overexpression of HER-2 was detected in about 30% of cases.[71]

2.2.1 EGFR-TK domain structure

As determined by crystallography,[82] the EGFR kinase domain (EGFR-TK domain) consists of two major lobes separated by a narrow cleft (hinge region) that defines the ATP-binding pocket and the site where ATP-mimetic inhibitors interact with the enzyme. The N-terminal lobe consists of mostly β-strands and one conserved α helix. The C-terminal lobe is largely helical and contains a segment, the activation loop, which includes the tyrosine residues that are phosphorylated for activity. The hinge region connects the two lobes (Figure 2.4 a).

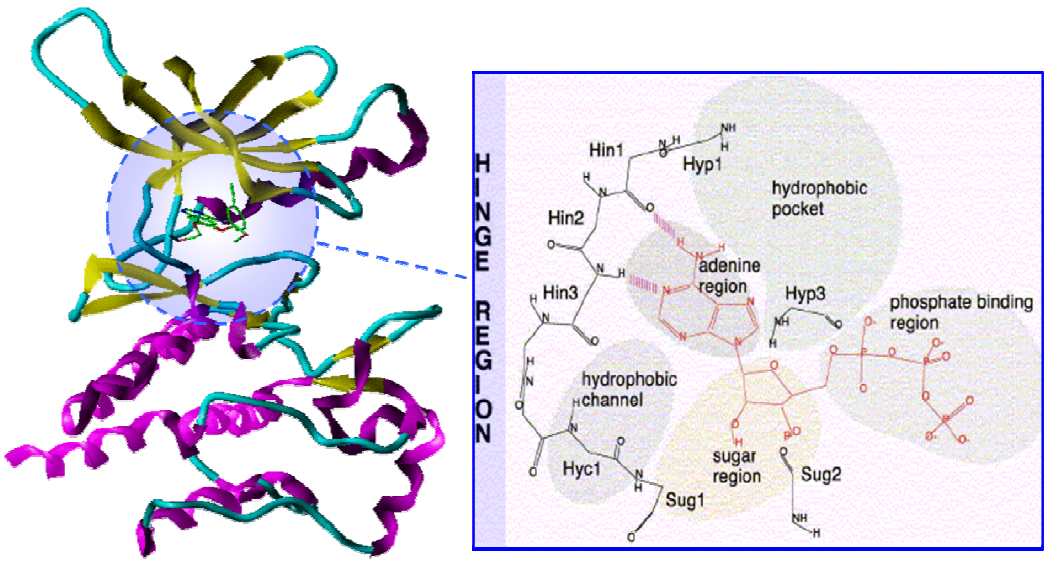

a b

Figure 2.4. (a) The structure of the catalytic domain of EGFR in complex with tarceva; (b) Structure of the ATP-binding site of EGFR.

The ATP-binding site of EGFR can be divided into five regions: the adenine region, the sugar pocket, two hydrophobic regions, and the phosphate binding region (Figure 2.4 b). In the adenine region, the adenine ring of ATP can engage hydrogen bond interactions with amino acid residues of the hinge region. The sugar pocket is of hydrophilic character, it contains the Cys773 residue, unique to the EGFR family of kinase, that could provide to covalent inhibitors both potency and selectivity (see below). The hydrophobic pockets are not normally occupied by ATP but may be used for the design of new inhibitors. Finally, the phosphate binding region has high solvent exposure and does not play a key role with respect to the binding affinity.

2.2.1 Reversible EGFR-TK inhibitors

Probably the erliest widely used EGFR inhibitor was the isoflavone genistein (Figure 2.5).[72] Genistein belong to the first class of EGFR-TK

inhibitors because inhibits EGFR in the submicromolar range by competing at the ATP-binding site of the enzyme.

Among these class members, the most advanced in clinical development are 4-anilino-quinazolines,[73,74] with two derivatives, gefitinib (Iressa™, AstraZeneca) and erlotinib (Tarceva™, Genentech/Roche), recently approved for clinical use in the treatment of non-small-cell lung cancer (NSCLC) (Figure 2.5).

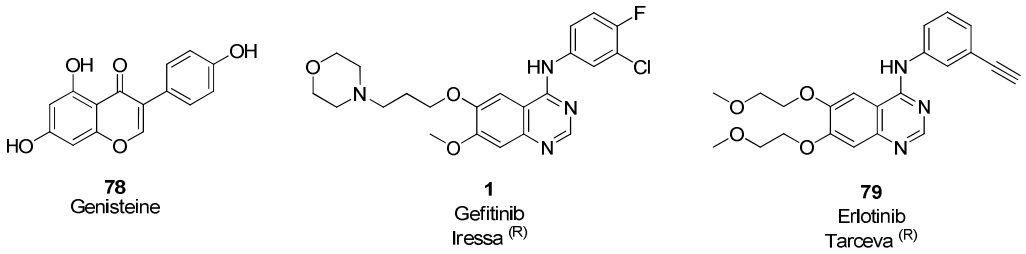

Figure 2.5. Chemical structures of some known reversible EGFR TK inhibitors.

4-Anilino-quinazolines represents a highly selective and potent class of ATP-competitive EGFR TK inhibitors with reported IC_{50} values in the nanomolar and subnanomolar range. Eventually, a number of alternative chemical classes were also shown to be equally efficient structural templates including other bicyclic pharmacophores such as pyridopyrimidines, [75] quinoline-3-carbonitriles, [76] pyrimidopyrimidines, [77] pyrrolopyrimidines, [78] and pyrazolopyrimidines, [79] as well as tricyclic molecules such as imidazoloquinazolines, pyrroloquinazolines, and pyrazoloquinazolines.[80,81]

Although many different chemical templates have been explored over the years, the more successful compounds possess certain common structural elements that are responsible for the tight-binding affinity to their targets. The disclosed structure of EGFR co-crystallized with the inhibitor erlotinib (Tarceva™),[82] as well as some of the earlier predictions for inhibitor-enzyme interactions using homology models of EGFR,[76,81,83]

have been used to explain how these inhibitors can achieve their remarkable affinity and selectivity.

The crystal structure of the kinase domain from the EGFR with the EGFR TK specific inhibitor erlotinib (Tarceva™),[82] provided direct structural evidences about how 4-anilinoquinazoline ATP-competitive inhibitors bind, at a molecular level, the catalytic domain of EGFR (Figure 2.6).

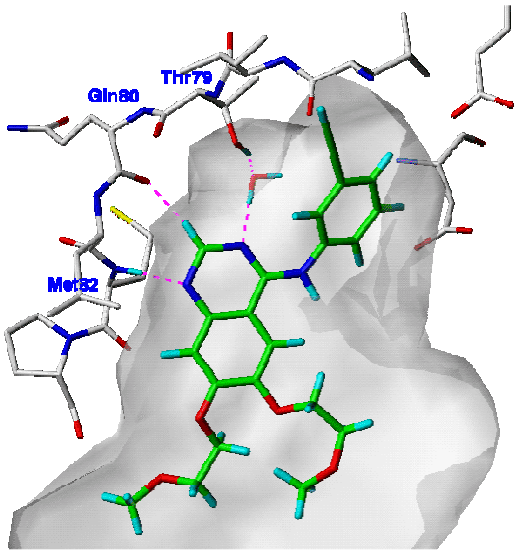

Figure 2.6. EGFR TK domain co-crystallized with erlotinib (Tarceva™).

The N1-C8 edge of the quinazoline nucleus is directed into the adenine pocket with the substituents at the C6 and C7 positions directed out toward the solvent and the aniline pointed into a hydrophobic pocket (Figures 2.6 and 2.7).

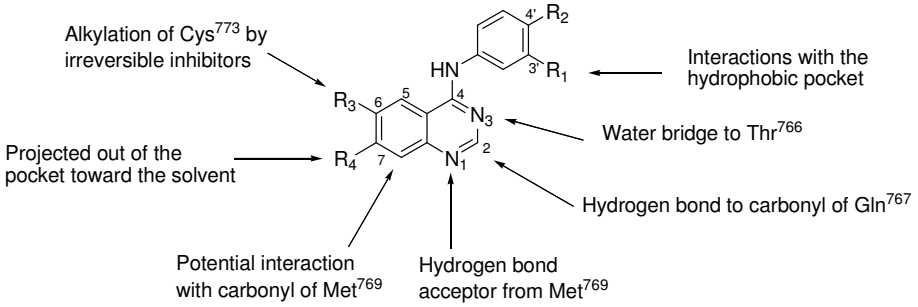

Figure 2.7. Interactions established by 4-anilino-quinazoline scaffold within the ATP-binding site of EGFR.

The N1 of the quinazoline points toward the amide NH of Met769, forming a stable hydrogen bond. The other ring nitrogen, N3, is involved in a second hydrogen bond with the side-chain hydroxyl group of Thr766 through a water molecule which bridges the two groups. Other protein interactions with the quinazoline template have been proposed for the C2 and C8 positions (figure 1.7). The 4-aniline group, including the 3' and 4' substituents, clearly plays an important role in the affinity and selectivity for 4-anilinoquinazoline inhibitors. The phenyl ring is tilted out of the plane of the quinazoline, allowing the substituent at the 3' position, which is an acetylene moiety in the case of erlotinib, to fit more precisely into a hydrophobic pocket. This well-defined hydrophobic pocket appears to be occupied by 4-anilinoquinazoline inhibitors but not by ATP, which might explain in part the much greater affinity for these inhibitors than the enzyme's natural substrate.

2.2.2 Covalent irreversible EGFR-TK inhibitors

These compounds belong to the previously defined second class of EGFR-TK inhibitors and are been designed mainly to overcome the drug resistance toward gefitinib or erlotinib treatment induced by the expression of EFGR T790M in tumor cells. Most potent and clinically advanced members of this class share a common 4-anilino-quinazoline or 4-anilino-3-cyanoquinoline core structure with reversible ATP competitive inhibitors and this confers to them the ability to bind the ATP binding site of EGFR-TK domain with high potency and specificity (Figure 2.8).

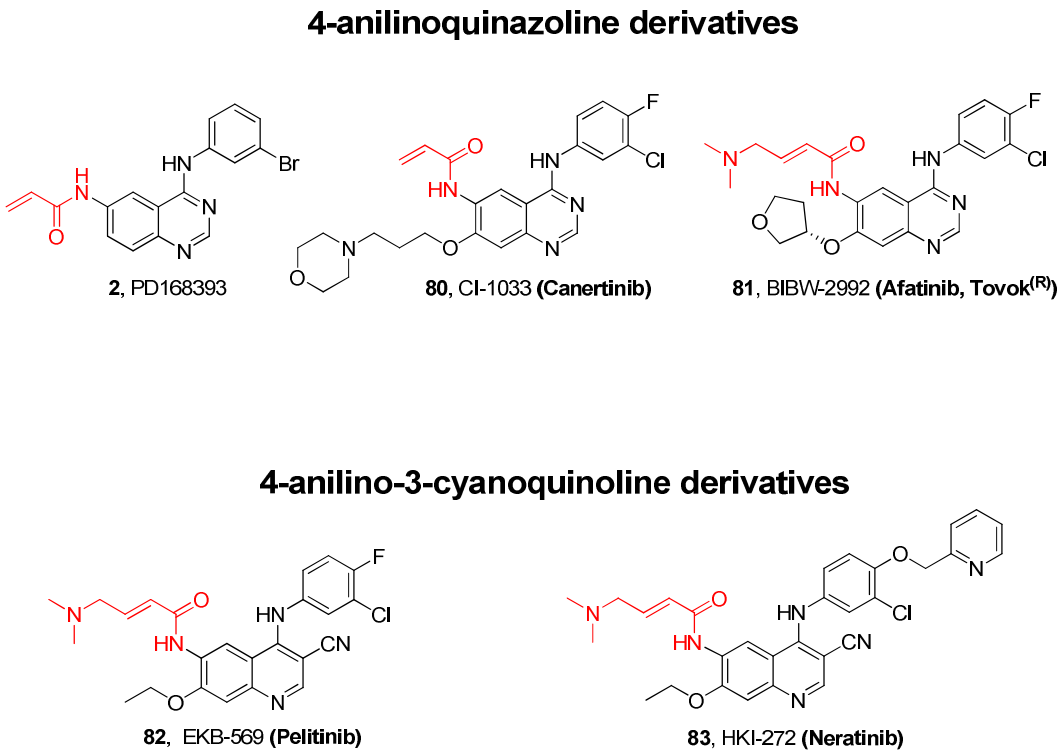

Figure 2.8. Collection of most representative irreversible covalent EGFR inhibitors with embedded warhead portions colored in red. Among them, brackets names indicate the most clinically advanced members.

On the other hand, the presence in these compounds of a reactive warhead portion (such as (1,2-dithiolan-3yl)alkylamide,[31] chloroacetamide, [84] acrylamide, [85] propargylamide [86] or vinylsulphonamide[85]) linked to the 6 position of the heterocyclic driver group give them the ability to covalently bind EGFR-TK, inhibiting it in a non-competitive manner (Figure 2.9.).

Disulfide bond forming warheads

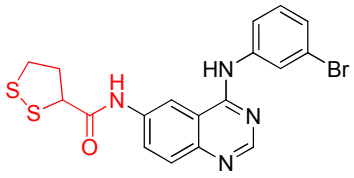

84

Alkylating warheads
(nucleophylic substitution-based mechanism)

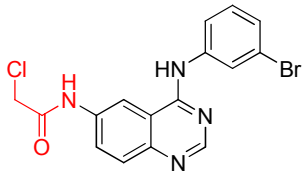

85

Alkylating warhead
(Michael addition-based mechanism)

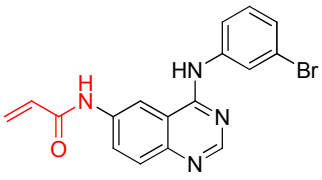

2, PD168393

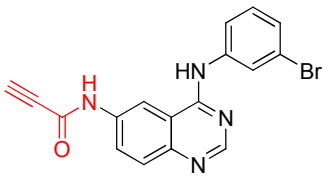

86

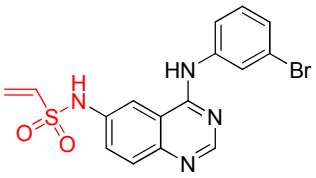

87

Figure 2.9. Warhead diversity among 4-anilnoquinazoline based irreversible ERGF-TK inhibitors.

Despite most of these covalent modifiers have been reported to irreversibly inhibit EGFR-TK activity, is important to underline that the ability of them to covalently bind the desired target cannot be considered a strictly requirement to achieve an irreversible action. Indeed, it has been reported that non-covalent inhibitors of EGFR-TK like lapatinib (Tykerb ®),[87] are able to irreversibly inhibit EGFR.

Since the enzyme activity depends on the presence of free and fully functional enzyme in the testing medium, there are two conditions that can lead to an irreversible target inhibition (Scheme 2.1):

1. The used inhibitor presents very a high K_{inhib} values (tight binding). In this case, most of free enzyme "E" is bound by the inhibitor "I" and converted to the inactive non-covalent complex **I**. This condition does not lead to a fully irreversible inhibition of the target because the enzyme activity can be recovered by addition of high amount of a proper ligand able to compete with the inhibitor "I" for the binding site. Despite this, compounds like these could act as irreversible inhibitors at least from a clinical point of view.
2. The used inhibitor is able to decrease the concentration of non-covalent drug-enzyme complex **I** available to regenerate the free active enzyme "E". This could occur when the complex **I** undergoes conversion to more stable complexes like covalent bound complex **II** or non-covalent stabilized complex **III** (the increased stability of the latter is often generated by conformational changes of bound enzyme). The formation of covalent stabilized complexes **II** (for which K_{cov} defines their formation ratio) can be usually induced by a covalent inhibitor whereas the formation of non-covalent stabilized complexes **III** (for which $K_{non\text{-}cov}$ defines their formation ratio) is more frequently hypothesized when non-covalent binders are used. However, also

inhibitors designed to covalently react with a given target could generate non-covalent stabilized complexes like complexes **III** rather than covalent bound complex like **II**.

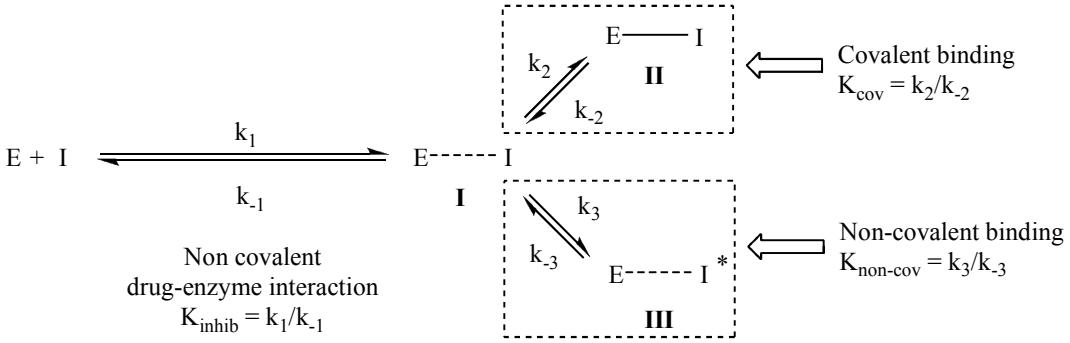

Scheme 2.1. Enzyme inhibition kinetics for covalent modifiers and non-covalent binder on a given enzyme "E".

The irreversible inhibition of EGFR-TK provided by lapatinib is due to the formation of a very stable non-covalent complex between the drug and the unactive conformation of EGFR-TK (complex type **III**, scheme 2.1). The high stability of this complex (it has been reported an estimated complex half-life of 300 min)[87] decrease the amount of free available enzyme "E" and provide a long lasting inhibition of EGFR-TK. On the contrary, covalent EGFR-TK inhibitors reported in literature decrease the amount of free available enzyme "E" forming with it covalent stabilized complexes (complex type **II**, scheme 2.1). Despite the equilibrium constant of covalent bound complexes (K_{cov}) is often so high to make this process irreversible, a good chemical stability for obtained complexes is a fundamental requirement to achieve an irreversible effect. Indeed, covalent complexes **II** could undergo chemical degradation (hydrolytic processes, etc.) that finally lead to the release of a modified inhibitor I' and to the catalytically active free enzyme "E" (Scheme 2.2).

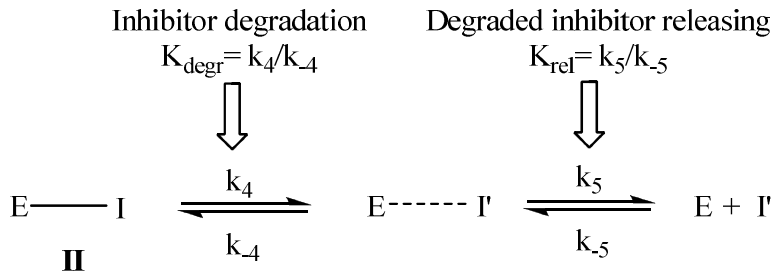

Scheme 2.2. Kinetic of covalent complex **II** chemical degradation.

Considering these assumptions, not all covalent EGFR-TK inhibitor can be automatically considered irreversible. From a kinetic point of view, irreversible EGFR-TK inhibitors can be achieved only using covalent modifier characterized by high K_{cov} values (Scheme 2.1) and low K_{degr} values (Scheme 2.2).

As described in Chapter 1.1.2, also for EGFR covalent modifiers described in literature a general functional structure defined by a driver portion, a linker and a warhead portion can be recognized. In addition, a "tuning portion" involved into pharmacokinetic profile tuning of such compounds can be identified too (Figure 2.10).

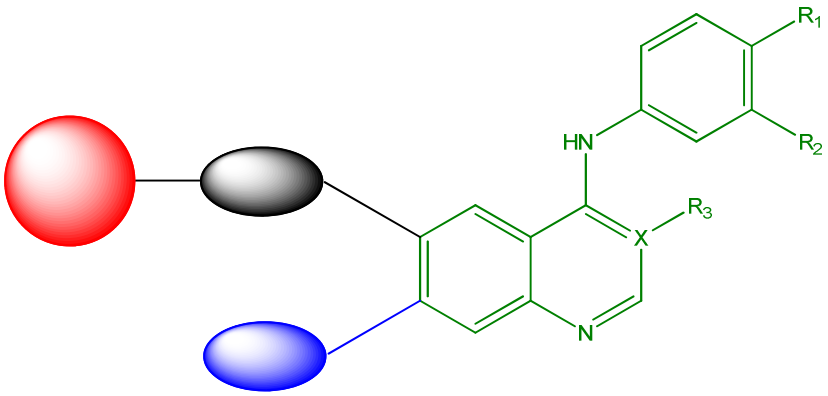

Figure 2.10. General structure of 4-anilinoquinazoline (X=N, R_3=not present) and 4-anilino-3-cyanoquinoline (X=C, R_3=CN) based covalent inhibitors: warhead portion in red, linker portion in black, driver portion in green and tuning portion in blue.

The 4-anilino-quinazoline or 4-anilino-3-cyanoquinoline core structure act as a "driving portion" for these compounds, driving the warhead reactivity to form covalent interactions mainly within the ATP binding site of EGFR-TK. Indeed, it provide, as previously described for the first EGFR-TK inhibitors class, an optimized non-covalent drug-target interaction that bring, together with the contribution of linker portion, the electrophilic-carbon atom of the warhead into close proximity with the nucleophilic thiol atom of target cysteine (Cys773 for EGFR-TK). This facilitates the rapid formation of the covalent drug-enzyme complex [88] reducing, in the same time, the occurrence of off-target risks. The stability of the established covalent interaction influences reversibility and duration of EGFR-TK inhibition. In this way, only warheads able to provide strong and stable covalent bonds with targeted cysteines would induce an irreversible inhibition of EGFR-TK, with duration that only depend from receptor turnover rate on cell surface. Among covalent inhibitors listed in Figure 2.9, alkylating derivatives are the best to leading an irreversible inhibition of EGFR-TK.[31] In particular, Michael addition-based mechanism inhibitors like PD168393 **2** are proved to inhibit EGFR-TK activity with high potency and a long-lasting effect by a stable alkylation of cysteine residue 773 inside the ATP binding site of EGFR-TK domain (figure 2.11).[89]

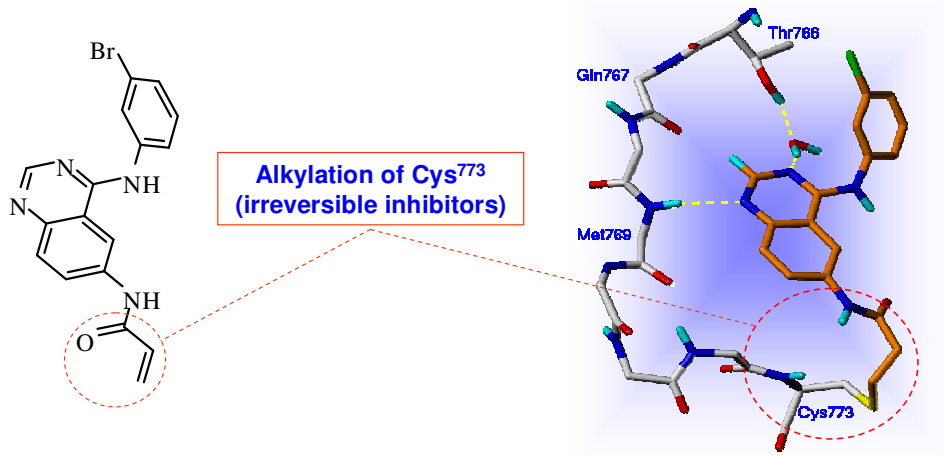

Figure 2.11. EGFR-TK domain co-crystallized with PD168393.[89]

This inhibition results insensitive to the intracellular ATP levels and represents the rational to explain why these compounds were found able to assure an effective inhibition of EGFR T790M tyrosine kinase activity. Moreover, the additional binding energy provided by formation of covalent drug-cysteine adducts decrease the number of non-covalent interactions usually needed to achieve the desired pharmacological potency.[2] In this way, these kind of compounds can bind their targets without needing a fine structural modulation of driver portion. For this reason, despite the high affinity of 4-anilinoquinazoline and 4-anilino-3-cyanoquinoline based driver groups for the ATP binding site of EGFR-TK, many of these covalent modifiers often inhibit multiple cysteine exposing targets inside and outside HER receptor family.[90] Despite this enlarged target spectrum could appear detrimental for the target selectivity of these compounds, it provide, on the contrary, additional selectivity to these inhibitors because force them to exert their biological activity only toward a short list of cysteine exposing targets (Table 1.1) without interfere with the activity of other kind of kinases. This is possible because, despite the primary sequence of ATP binding site is highly conserved among kinases, only few of them have a cysteine residue within the ATP binding site located in the same position of Cys773 in EGFR and so suitable to be bound by these inhibitors (Table 2.1).

EGFR_EGFR	V	Q	L	I	T	Q	L	M	P	F	G	C	L	L	D	Y	V	R
EGFR_HER2/ErbB2	V	Q	L	V	T	Q	L	M	P	Y	G	C	L	L	D	H	V	R
EGFR_HER4/ErbB4	I	Q	L	V	T	Q	L	M	P	H	G	C	L	L	E	Y	V	H
JakA_JAK3	L	R	L	V	M	E	Y	L	P	S	G	C	L	R	D	F	L	Q
Src_BLK	I	Y	I	V	T	E	Y	M	A	R	G	C	L	L	D	F	L	K
CAMKL_LKB1	Q	K	M	Y	M	V	M	E	Y	C	V	C	G	M	Q	E	M	L
Tec_BMX	I	Y	I	V	T	E	Y	I	S	N	G	C	L	L	N	Y	L	R
Tec_BTK	I	F	I	I	T	E	Y	M	A	N	G	C	L	L	N	Y	L	R
Tec_TEC	I	Y	I	V	T	E	F	M	E	R	G	C	L	L	N	F	L	R
Tec_TXK	L	Y	I	V	T	E	F	M	E	N	G	C	L	L	N	Y	L	R
Tec_ITK	I	C	L	V	F	E	F	M	E	H	G	C	L	S	D	Y	L	R

Table 2.1. Alignment of primary sequences of ATP binding site portions of kinases. Among kinases only eleven kinases have a cysteine residue located in the same position of Cys773 in EGFR (boxed residues).[90]

Moreover, the inhibition of additional HER receptors beyond EGFR could be useful for treatment of cancers forms in which other HER receptor members play an important role in tumor growth and immortalization. For instance, HER-2 was suspected to be an important player in the development of tumors because was found overexpressed in many kind of cancers,[91,71] and this occurrence is generally correlates with poor prognosis and decreased survival.

HER-2 is the most preferred partner for EGFR heterodimerizations and promotes tumors growth inducing enhanced proliferation, migration and resistance to apoptosis in cancer cells. Moreover, HER-2 containing dimers have features (like slow ligand dissociation, high stability, relaxed ligand specificity, slow endocytosis, rapid recycling and prolonged firing) that prolong and enhance the EGFR downstream signaling.[57]

Recently, a synergic pharmacological response induced by inhibition of both EGFR and HER-2 has been reported.[92] This multi target approach have provides better outcomes than traditional therapies only focused on selective EGFR or HER-2 inhibition[93] and it could represent the

rational for development of new multi target covalent modifiers for cancer treatment.

In vitro tests show that the most of clinically advanced irreversible EGFR-TK covalent inhibitors are able to inhibit multiple targets among HER members (Table 2.2).

Developer	Compound	Selectivity in vitro IC50 (nM)		
		EGFR	HER2	HER4
ParkeDavis-Pfizer	CI-1033, PD183805, canertinib	0.8	19	7
Boehringer Ingelheim	BIBW-2992	0.5	14	
Wyeth-Ayerst	EKB-569, pelitinib	39	1200	
Wyeth-Ayerst	HKI-272, neratinib	92	59	

Table 2.2. Target selectivity within HER receptor family of most clinically advanced 4-anilinoquinazolinic and 4-anilino-3-cyanoquinolinic irreversible EGFR-TK inhibitors. Except for EKB-569 (pelitinib) that binds EGFR selectively, IC_{50} values shown that almost of them can inhibits multiple targets.[94]

Among listed compounds, CI-1033 (canertinib) shows the most expanded target spectrum since it can irreversibly inhibits EGFR, HER-2 and HER-4 by irreversible alkylation of Cys773, Cys805 and Cys778 respectively. Inhibiting all catalytically active members of HER receptor family, this compound can theoretically completely shut down the HER receptors downstream signaling. Notably, canertinib was reported to induce poly-ubiquitinilation and degradation of HER-2 so to interfere with EGFR and HER-2 heterodimerization process. Therefore, together with the irreversible inhibition of EGFR, the high activity shown by this compound in preclinical models could be explained also considering this additional mechanism of action.[95]

In comparison to CI-1033 (canertinib), BIBW-2992 (afatinib, Tovok ®) and HKI-272 (neratinib) present increased target specificity, since they are reported as dual inhibitors of EGFR and HER-2 only. Between them, the higher HER-2 specificity showed by HKI-272 (neratinib) has been

addressed to the presence of the 2-pyridin-2-ylmethoxy decoration of the 4-anilino-3-cyanoquinoline driver portion.[96]

Finally, EKB-569 (pelitinib) represents an exception among these covalent modifiers because it has proved to be very selective for EGFR at nM concentrations.

Despite all of just described compounds are able to bind EGFR T790M mutants with high potency both *in vitro* and *in vivo* models, it is reported that their effective clinical efficacy, especially in patients with gefitinib and erlotinib-resistant NSCLC, is limited by occurrence of dose–limiting toxicity problems.[97] Indeed, since the ATP affinity for EGFR T790M and for wild type EGFR (wtEGFR), the concentration of irreversible inhibitors required to inhibit EGFR T790M will also effectively inhibits wtEGFR. The concurrent inhibition of wtEGFR results in side effects like skin rash and diarrhea that hamper the reaching of plasma concentrations sufficient to inhibit EGFR T790M.

In order to solve these problems, a second generation of EGFR irreversible inhibitors was very recently synthesized. It is composed only by three compounds at the moment: WZ4002, WZ3146, and WZ8040 (Figure 2.12a).[97] As described for other EGFR irreversible inhibitors, all of them present a warhead portion responsible of the covalent binding of Cys773 within the ATP binding site of EGFR. On the other hand, these compounds are characterized by a completely redesigned driver portion that increases their selectivity against EGFR T790M mutant rather than against wtEGFR (Figure 2.12b).

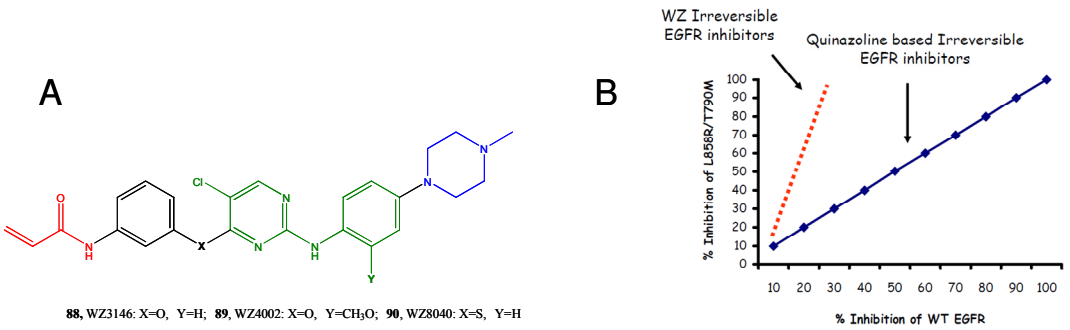

Figure 2.12. a) General structure of second EGFR covalent irreversible inhibitors generation: warhead portion in red, linker portion in black, driver portion in green. Despite authors haven't defined any tuning portion for these molecules, the piperidine moiety could be recognized as a possible tuning portion (in blue), useful to enhance the solubility of these inhibitors. b) Toxicity-Efficacy gap between EGFR covalent irreversible inhibitors belonging to the first and to the second generation respectively.

X-ray diffraction analysis of EGFR T790M co-crystallized with WZ4002 showed why these compound are so selective for EGFR T790M (Figure 2.13).

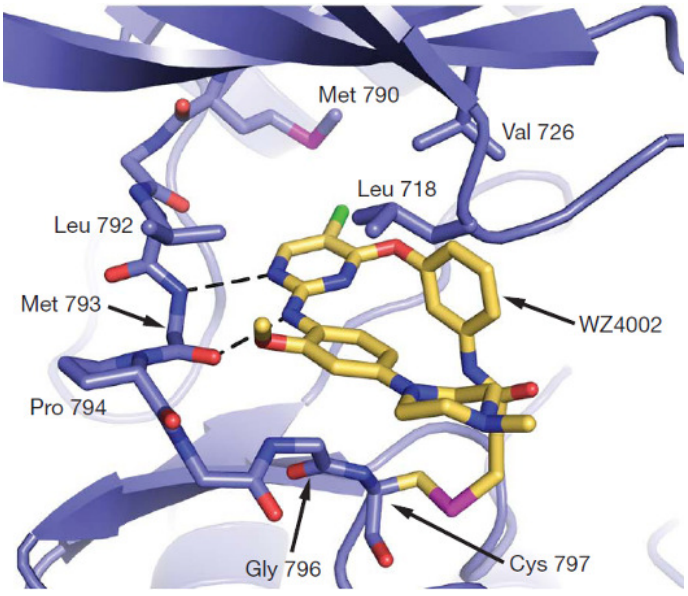

Figure 2.13. EGFR T790M co-crystallized with WZ4002. Dashed lines indicate main interactions with the "hinge" region of EGFR-TK domain. Observing the conformation of WZ4002, is easy to understand the importance of the phenyl linker portion to bring the acrylamide warhead close to Cys797 (Cys773 in an *alternative* numbering scheme).[97]

While the anilinopyrimidine driver portion of WZ4002 provide an effective interaction with the "hinge" region of ATP binding site of EGFR T790M by a bi-dentate hydrogen bonding interaction with Met793 residue, the chlorine substituent on the pyrimidine ring contacts the mutant gatekeeper residue Met790 through an hydrophobic interaction. This hydrophobic interaction could be responsible of the observed selectivity of WZ4002 for EGFR T790M rather than for wtEGFR. Indeed it can take place with the properly positioned Met 790 residue in EGFR T790M but it is disfavored when Thr790 is present in this position in wtEGFR. Beyond the driving portion, the linker portion is fundamental to allow to covalent inhibition of EGFT T790M. Indeed, the 'linker' phenyl ring lies roughly perpendicular to the pyrimidine core juxtaposing the acrylamide warhead with the thiol group of Cys797 (Cys773 in an alternative numbering scheme) and facilitating the covalent bond formation.[97]

These compounds were found effective toward *in vitro* and *in vivo* cancer models harboring EGFR T790M mutation. WZ4002 has been tested in mouse lung cancer models harboring EGFR T790M and it has provided a significant tumor regression without exert any significant inhibition of EGFR WT. The enhanced selectivity for EGFR T790M of these compounds could be useful for the clinical treatment of gefitinib-resistant cancers in human patient avoiding the occurrence of dose-limiting side effects related to wtEGFR inhibition. Furthermore, they could be administered before that the EGFR T790M occurs, in order to prevent it.

2.3 Synthesized EGFR inhibitors

2.3.1 Aim of the work

Considering the acrylamide moiety of 6-acrylamide-4-(3-bromoanilino)quinazoline [98] (**2**, PD168393, Figure 2.8 and 2.9) as a reference warhead fragment, the role of different cysteine reactive groups inserted on the 6-amino-4-(3-bromoanilino)quinazoline driver portion (**3**, Table 2.6) was explored in terms of covalent EGFR WT and EGFR T790M inhibition.[99]. Combining knowledge from existing covalent modifier drugs and late-stage clinical candidates, as well as from known EGFR tyrosine kinase inhibitors, new irreversible EGFR inhibitors **1**-**14** carrying different cysteine-reactive groups at position 6 (Scheme 2.4 and Table 2.6) were designed and synthesized. In particular, embedded warhead portions were designed to possess different reaction mechanisms toward nucleophiles: (i) nucleophilic addition (epoxides **4**, **5**, and **6**); (ii) nucleophilic substitution with *in situ* release of a leaving group (phenoxymethylamides **7**, **8**, and **9**); (iii) carbamoylation (carbamate **10**); (iv) Pinner reaction with formation of a thioimidate adduct (nitrile **11**); (v) disulfide bond formation (isothiazolinone **12**, benzisothiazolinone **13**, and thiadiazole **14**).

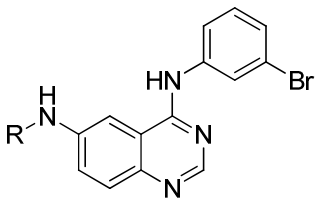

Compd	R	Proposed inhibition mechanism
2		Michael addition (reference compound for EGFR irreversible inhibition)

3		No covalent interactions (reference compound for EGFR reversible inhibition)
4	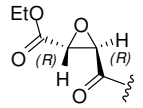	Nucleophilic Addition
5	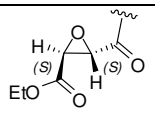	
6	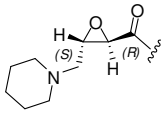	
7	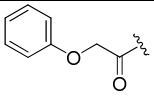	Nucleophilic substitution
8	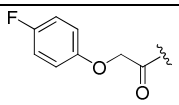	
9	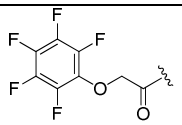	
10	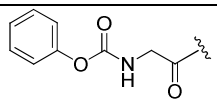	Carbamoylation
11	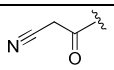	Pinner reaction
12	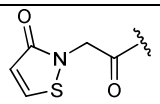	Disulfide bond formation
13	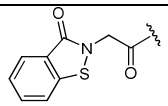	
14	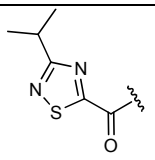	

Table 2.3. Overview of designed warheads. Proposed reaction mechanisms are reported too.

In some cases, warhead reactivity was also tentatively modulated by introduction of electron-withdrawing groups (**9** *vs* **8** and **7**).

In order to increase the target selectivity and, in the same time, to decrease the potential off-target toxicity of compounds **2**, the pro-drug **15** was synthesized too.

Compound	R	Proposed inhibition mechanism
15	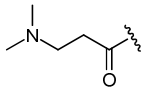	Michael addition (Pro-drug)

Table 2.4. Designed warheads overview. Proposed reaction mechanisms are reported too.

Compound **15** presents the *N,N*-dimethylethylamide side chain in place of acrylamide warhead of compound **2**. Despite the unsaturated β-aminoamide moiety of compound **15** lacks of reactive electrophilic centres to directly interact with nucleophiles species, it is known that, especially when exposed to basic conditions, β-aminocarbonyl compounds like **15** can undergo retro-Michael reaction so restore the acrylamide warhead of compound **2** (Scheme 2.3).[100,101]

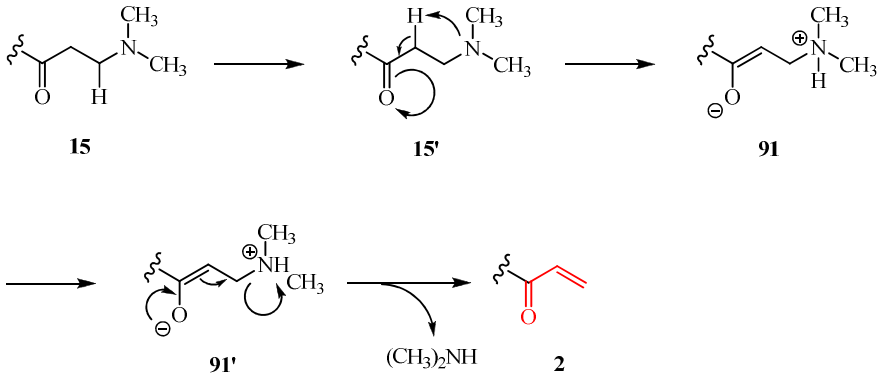

Scheme 2.3. Basic catalytic activation of compound **15**. Warhead portion of resulting acrylamide **2** is colored in red.

Indeed, in presence of a general base, the β-amino group becomes free to deprotonate the neighbouring α-carbon. The resulting tautomerization of compound **15** produces the enolate **91** and starts the β-elimination reaction to from the acrylamide final product **2**. In this way, deprotonation of the α-carbon can be recognized as the key step of this reactions sequence.

The enolization step can be induced using basic catalysis in solution but it could also take place within specific areas of a biological target in which a proper positioned basic residue could deprotonate the α-carbon and triggers the enolization process. In this way, only once the compounds **15** have bound the EGFR-TK active site, β-aminoamide portion could start to eliminate Et_2NH to unmasking the highly reactive acrylamide warhead of compound **2**. Then, the acrylamide moiety of compound **2** could react with Cys773 so to irreversibly alkylate and inactivate EGFR.

Despite some findings seems to confirm the involvement of this kind of enzyme-suicide reminiscent mechanism for the irreversible inhibition of Thyroid Hormone Receptor provided by a β-aminocarbonyl derivative,[102] no experimental data have been reported to support the hypothesis that β-aminoamide **15** could undergo a retro-Michael reaction within the hydrophilic sugar pocket of EGFR ATP binding site. If this hypothesis will be verified, the pro-drug behaviour of β-aminoamide **15** could drastically limit potential off-target toxicity normally associated to the use of acrylamides like compound **2**.

In order to test the nonspecific toxicity of warhead portions and the contribute of 4-(3-bromoanilino)quinazoline driver group to the observed inhibition potency, derivatives **16** and **17** (Scheme 2.5 and Table 2.5) were synthesized too. In these compounds, two of the cysteine-trap portions within the series were linked to a naphthalene based driver group that, because lacking the structural elements required for EGFR

ATP-binding interaction, should not be able to recognize the molecular target.

Compound	Structure	Proposed inhibition mechanism
16	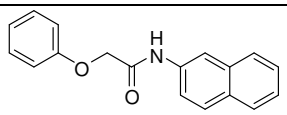	Nucleophilic substitution
17	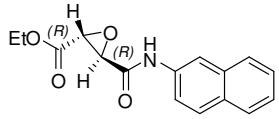	Nucleophilic substitution

Table 2.5. Designed warheads overview. Proposed reaction mechanisms are reported too.

Evaluation of EGFR tyrosine kinase inhibition potential of new synthesized compounds was carried out by enzyme-based and cell-based assays. While, enzyme-based assays were performed to evaluate the ability of synthesized compound to inhibit human EGFR as purified protein, cell-based assays were designed to obtain more information about their kinase inhibitor effectiveness on intact living cells.

The anti-proliferative and pro-apoptotic activities as well as their effects on downstream EGFR-dependent signaling pathways of synthesized compounds were also investigated in the gefitinib-resistant H1975 NSCLC cell line which expresses EGFR T790M. In order to identify new irreversible EGFR inhibitors active on a mutated gefitinib-resistant cell line, structure-activity relationships within the series of synthesized compounds were evaluated.

2.3.2 Chemistry.

The amides **4**-**14** and **16**-**17** of Table 2.6 were synthesized by coupling their precursor amines (**3** or **106**) with the appropriate

carboxylic acid (**92**, **93**, **95**-**101**), carboxylate (**94**), or carboxylic ester (**102**), as described in Schemes 2.4 and 2.5. 6-Amino-4-(3-bromoanilino)quinazoline **3** was prepared in three steps from 4-nitroanthranilonitrile **103** as previously described (Scheme 2.4).[99,103]

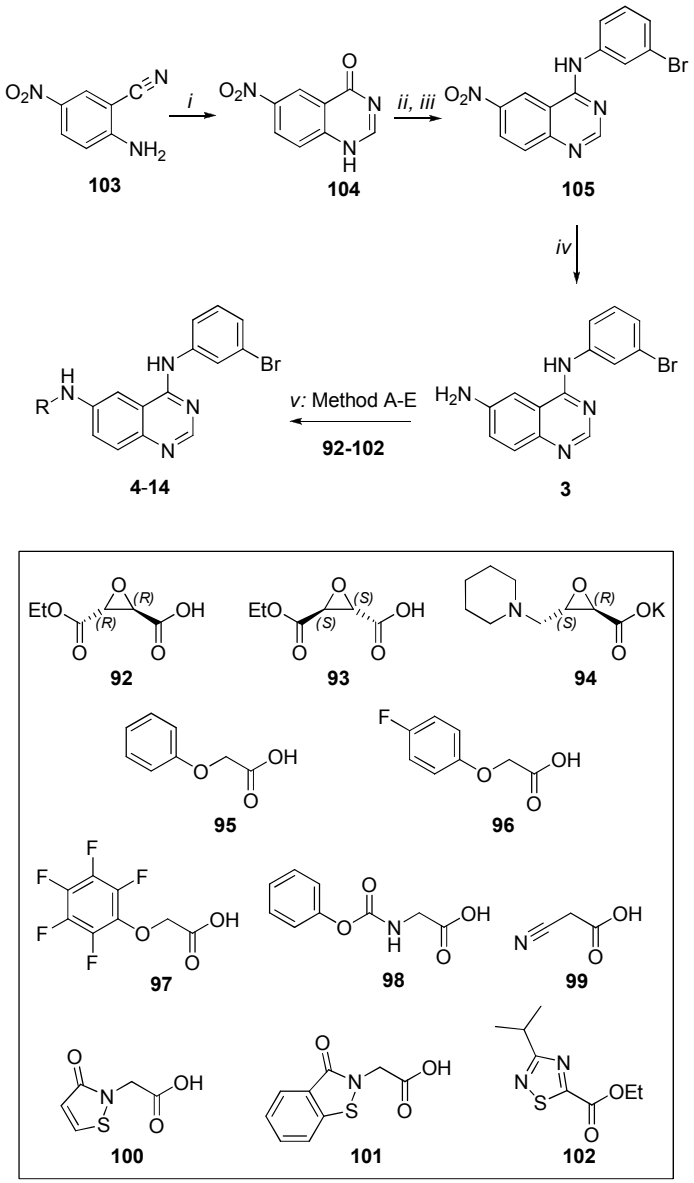

Scheme 2.4. Synthesis of compounds **3**-**14**. (i) H_2SO_4, formic acid, reflux; (ii) $SOCl_2$, dioxane, reflux; (iii) 3-bromoaniline, *i*-PrOH, 60 °C; (iv) Fe, AcOH, EtOH/H_2O, reflux; (v) Method A: dichloromethylene dimethyliminium chloride, $NaHCO_3$, **92** (for **4**) or **93** (for **5**), CH_2Cl_2, 0 °C; Method B: HBTU, DMF, **94**, rt. (for **6**). Method C; PCl_5, **95** (for **7**) or **96** (for **8**)

or **97** (for **9**) or **99** (for **11**), CH_2Cl_2, reflux. Method D; DCC, **98** (for **10**) or **100** (for **12**) or **101** (for **13**), DMF, 0 °C to rt. Method E; *t*-ButOK, **102** (for **14**), DMF, MW, 100 °C.

Briefly, **103** was refluxed in formic acid and sulfuric acid to give 6-nitro-4-oxoquinazoline **104**, which was chlorinated with thionyl chloride in dioxane and subsequently treated with 3-bromoaniline to yield 6-nitro-4-(3-bromoanilino) quinazoline **105**. Reduction of the 6-nitro group with iron and acetic acid in aqueous ethanol gave the 6-amino-4-(3-bromoanilino)quinazoline **3**.

The epoxy derivatives **4** and **5** were synthesized by coupling **3** with carboxylic acids **92** and **93**, respectively, using dichloromethylene dimethyliminiumchloride as the coupling reagent (method A, Scheme 2.4), while **6** was obtained from **94** with *O*-(benzotriazol-1-yl)-*N,N,N',N'*-tetramethyluronium hexafluorophosphate (HBTU) (method B, Scheme 2.4). Compounds **7**-**9** and **11** were prepared as described in method C (Scheme 2.4) from the amine **3** and the acyl chlorides obtained from **95** (for **7**), **96** (for **8**), **97**(for **9**), or **99** (for **11**). Derivatives **10**, **12**, and **13** were synthesized employing *N*,*N*-dicyclohexylcarbodiimide (DCC) as the coupling reagent and **98**, **100**, and **101**, respectively, as carboxylic acids (method D). Amide **14** was obtained by adding potassium *tert*-butoxide to a premixed mixture of ester **102** and amine **3** and exposing the reaction mixture to microwave irradiation (method E, Scheme 2.4).

Amides **16** and **17** were synthesized by reacting 2-naphthylamine **106** with carboxylic acids **92** (method A) and **95** (method C), respectively (Scheme 2.5).

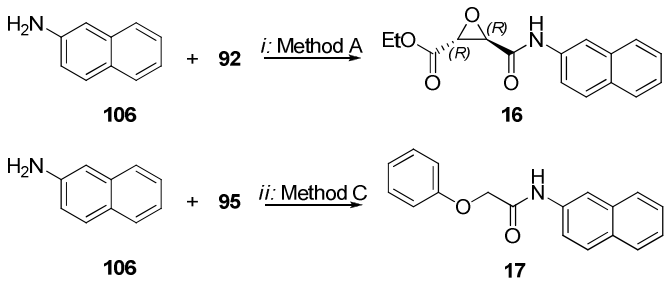

Scheme 2.5. Synthesis of compounds **16** and **17**. (i) Method A: dichloromethylene dimethyliminium chloride, $NaHCO_3$, CH_2Cl_2, 0 °C; (ii) Method C: PCl_5, CH_2Cl_2, reflux.

Finally, the amide **15** was prepared coupling the precursor amine **3** with 3-chloropropionic acid and displacing the chlorine atom in β-position of compound **118** with dimethylamine (Scheme 2.6)

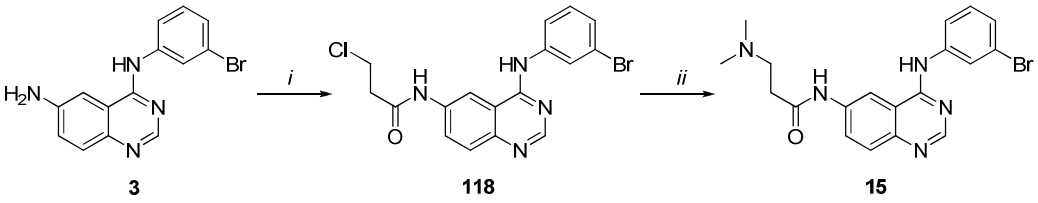

Scheme 2.6. Synthesis of compound **15**. (i) 3-chloropropionyl chloride reflux; (ii) Et_2-NH 33% v/v, NaI, EtOH abs, reflux.

Carboxylic acids **95**-**99** were commercially available, while **92**-**94**, **100**, **101**, and the ester **102** were prepared as shown in Schemes 2.7 and 2.8.

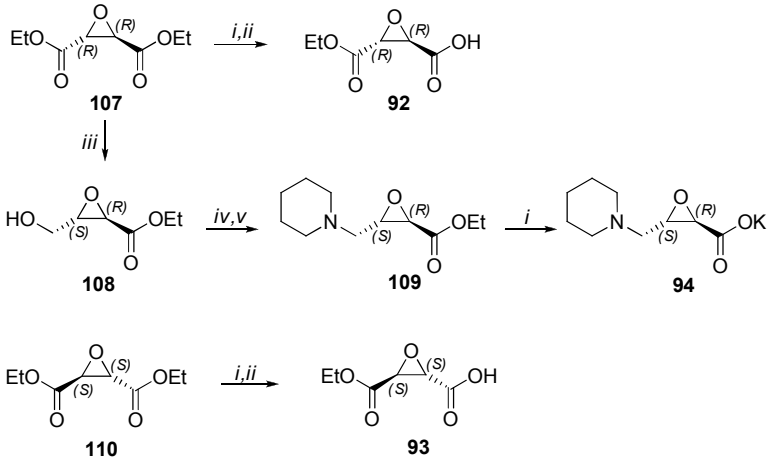

Scheme 2.7. Synthesis of warheads **17**-**19**. (i) KOH, abs. EtOH, 0 °C; (ii) 5% $KHSO_4$, rt; (iii) $NaBH_4$, EtOH, 0 °C; (iv) MsCl, Et_3N, CH_2Cl_2, 0 °C to rt; (v) anhydrous piperidine, KI, DMF, 0 °C to rt.

The (2*R*,3*R*)-epoxy diester **107**[104] was partially hydrolyzed to the desired (2*R*,3*R*)-monoethyl ester **92**[105] or selectively monoreduced to the hydroxyl ester **108**.[106] Mesylation of the alcohol **108** and substitution with piperidine gave the epoxy ester **109**, which was hydrolyzed to afford the desired carboxylate **94**. The (2*S*,3*S*)-monoethyl ester **93** was synthesized by partial hydrolysis of the proper (2*S*,3*S*)-epoxy diethyl ester **110**.[107] The isothiazolinone derivative **100** was synthesized as shown in Scheme 2.8.

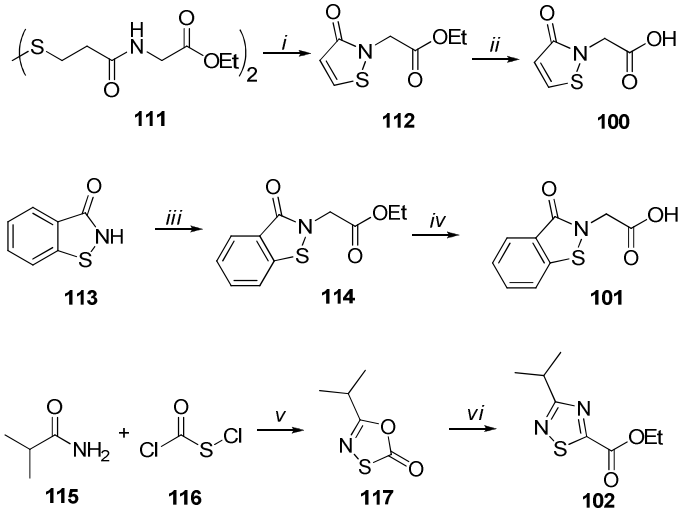

Scheme 2.8. Synthesis of Warheads **100**-**102**. (i) SO_2Cl_2, $ClCH_2CH_2Cl$, rt; (ii) 1 M TFA, reflux; (iii) $BrCH_2COOEt$, Et_3N, THF, rt; (iv) HCl reflux; (v) CH_2Cl_2, reflux; (vi) NCCOOEt, p-xylene, reflux.

3,3'-Dithiodipropionamide **111**[108] was cyclised with sulfuryl chloride to isothiazolinone **112**,[109] which was hydrolyzed to the desired carboxylic acid **100** by refluxing in 1 M trifluoroacetic acid. The benzisothiazolinone carboxylic acid **101** and the ethyl 3-isopropyl-1,2,4-thiadiazole-5-carboxylate **102** were prepared as described in Scheme 2.8, according to literature methods.[110, 111]

2.3.3 Results and discussion

As described in chapter 4.1.3 (Experimental section), the effects of synthesized compound on the tyrosine kinase activity of human EGFR were investigated. These assays were carried out on membrane associated EGF receptor on living human cell line (cell-based assays) as well as on purified protein (enzyme-based assays). Cell-based assays were used to estimate the reversibility of EGFR tyrosine kinase activity inhibition and the antiproliferative effect provided by tested compounds. On the other hand, their inhibitory potencies (IC_{50}) were calculated from data obtained from cell-based as well as enzyme-based assays.

Despite compound **15** was tested too, the collected biological data are still under evaluation. For this reason, no experimental data about compound **15** will be reported in this PhD thesis.

A preliminary direct evaluation of the inhibitory potency of synthesized compounds on human EGFR was carried out by an enzyme-based assay. In this test, the EGFR-dependent phosphorylation of a suitable peptide substrate was quantified by time-resolved fluorimetric measurements in presence or in absence of inhibitors. The determined IC_{50} values are reported in Table 2.6.

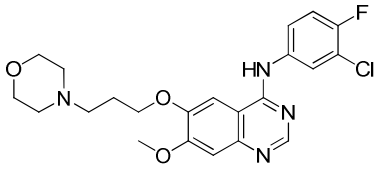

1, Gefitinib

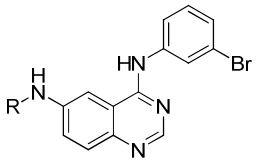

2-14

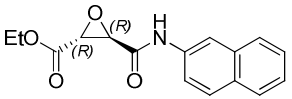

16

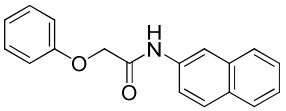

17

Compd	R	kinase assay[a]	autophosphorylation assay[b]			
		IC_{50} (nM)	% inhibition (1 μM)		IC_{50} (μM)	
			1 h	8 h	1 h	8 h
2		1.69 ± 0.16	98.6 ± 1.4	93.6 ± 6.3	0.012 ± 0.004	0.152 ± 0.037
3	H	n.d.	98.5 ± 1.5	0.0 ± 0.1	0.030 ± 0.010	>10.00
4	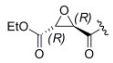	0.50 ± 0.12	100.0 ± 0.0	96.6 ± 1.1	0.011 ± 0.007	0.145 ± 0.030
5	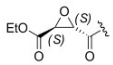	0.49 ± 0.04	96.7 ± 3.3	95.7 ± 1.3	0.034 ± 0.009	0.068 ± 0.009
6	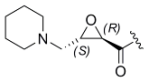	1.24 ± 0.13	99.4 ± 0.6	96.3 ± 1.5	0.007 ± 0.001	0.044 ± 0.010
7	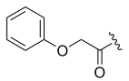	9.25 ± 0.71	93.5 ± 7.5	71.4 ± 7.2	0.076 ± 0.054	0.292 ± 0.068
8	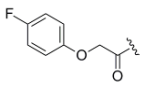	8.43 ± 0.16	97.4 ± 1.8	77.6 ± 10.1	0.031 ± 0.008	0.291 ± 0.011
9	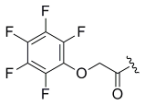	23.6 ± 1.75	91.5 ± 4.3	91.4 ± 7.6	0.084 ± 0.037	0.078 ± 0.032

10	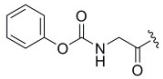	0.37 ± 0.05	95.2 ± 0.2	79.9 ± 16.4	n.d.	n.d.
11		0.17 ± 0.02	95.0 ± 3.2	23.6 ± 9.6	n.d.	n.d.
12	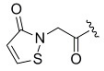	0.36 ± 0.08	79.6 ± 8.1	24.7 ± 14.7	n.d.	n.d.
13	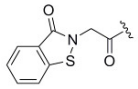	0.85 ± 0.05	69.0 ± 16.3	30.7 ± 14.3	n.d.	n.d.
14	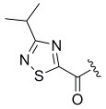	129 ± 17.3	82.3 ± 9.1	66.9 ± 13.8	n.d.	n.d.
15	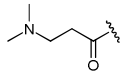	Not reported.	Not reported	Not reported	Not reported	Not reported
16		n.d.	0.0 ± 0.1	0.0 ± 0.1	n.d.	n.d.
17		n.d.	0.0 ± 0.1	0.0 ± 0.1	n.d.	n.d.

Table 2.6. EGFR tyrosine kinase and autophosphorylation inhibition in A431 cells. [a] Concentration to inhibit by 50% EGFR tyrosine kinase activity. IC_{50} values were measured by the phosphorylation of a peptide substrate using time-resolved fluorimetry (see Experimental Section). Mean values of three independent experiments ± SEM are reported. [b] Inhibition of EGFR autophosphorylation was measured in A431 intact cells by Western blot analysis. Percent inhibition at 1 μM concentration and IC_{50} values were measured immediately after and 8 h after removal of the compound from the medium (1 h incubation). Mean values of at least two independent experiments ± SEM are reported.

Reported kinase assay data show that substitution of the acrylamide warhead of reference compound **2,** with an epoxy- (**4**-**6**), a carbonylic- (carbamate **10** and nitrile **11**), or a (benzo)isothiazolinonic- (**12** and **13**) one do not impact so much on the observed inhibition potency on purified enzyme, leading to equally potent or more potent inhibitors. Despite showing slightly decreased inhibition potency, also compounds carrying phenoxyacetamidic warheads (compounds **7**-**9**) potently inhibit EGFR with IC_{50} values in the low nanomolar range. On the contrary, in the tested conditions, kinase inhibition potency is notably reduced by the introduction of a 1,2,4-thiadiazole warhead (**14**).

All these findings are in agreement with previously published SAR profiles of the 4-anilinoquinazoline ring[85,112,113,114] in which the ATP-binding site of EGFR seems tolerant to the introduction of differently sized and shaped substituents at position 6 of this heterocyclic driver group.

In order to obtain more information about the biological activity of synthesized compounds on living cell, enzyme-based assays were replaced by cell-based assays. In this way, the reversibility of EGFR inhibition provided by these compounds was investigated on A431 human epidermoid cancer cell line by Western blotting (Figure 2.14 and Figure 2.15). This cell-based assay was carried out incubating A431 cells, which overexpress wild type EGFR, with each synthesized inhibitor for 1 h and washing them free of drug. The degree of EGFR autophosphorylation was measured either immediately after or 8 h after removal of the inhibitor from the medium.[88]

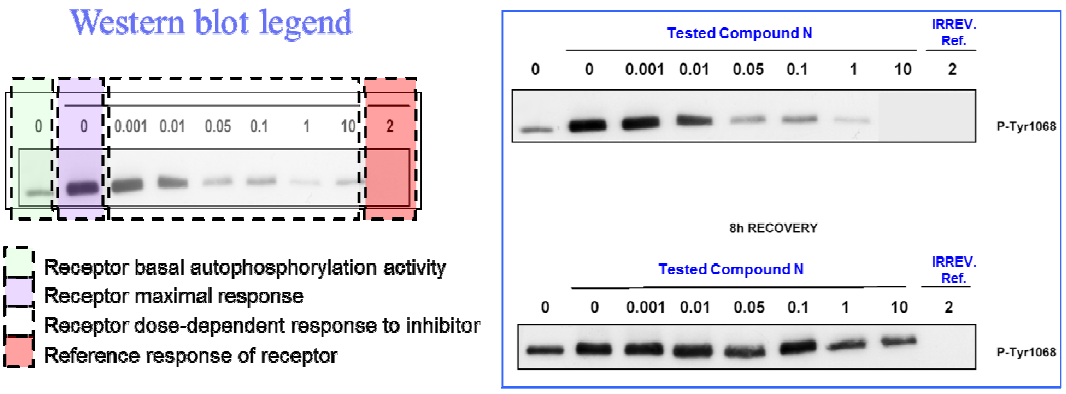

Figure 2.14. Autophosphoriyation test in A431 cells. The inhibition of EGFR autophosphorylation is determined using a specific anti-phosphotyrosine anti-body by Western blot analysis and compared with some reference results as (1) the basal EGFR autophosphorylation activity (- EGF / - EGFR inhibitor; green colored boxed area), (2) the maximum EGFR autophosphorylation response (+ EGF / - EGFR inhibitor; violet colored boxed area), (3) the EGFR autophosphorylation inhibition provided by a fixed amount of reference compound **2** (+ EGF / + reference irreversible EGFR inhibitor; red colored boxed area). An example of an autophosphorylation inhibition result is offered too. The upper line of this Western blot image shows the TK inhibition immediately after incubation whereas the lower one shows the TK-inhibition 8h after.

Among tested compounds, irreversible and reversible EGFR inhibitors can be recognized comparing their results with those observed for irreversible and reversible reference compounds **2** and **3** respectively. Indeed, as previously reported,[98] compounds showing 80% or greater EGFR inhibition 8 h after their removal from the medium are recognizable as irreversible inhibitors whereas compounds showing 20-80% of residual inhibition can only be considered as partially irreversible ones. Only for compounds that showed the highest inhibitory potencies toward EGFR at 1 μM concentration on A431cell line, dose-dependency was investigated (Figure 2.15) and IC_{50} determined (Table 2.6).

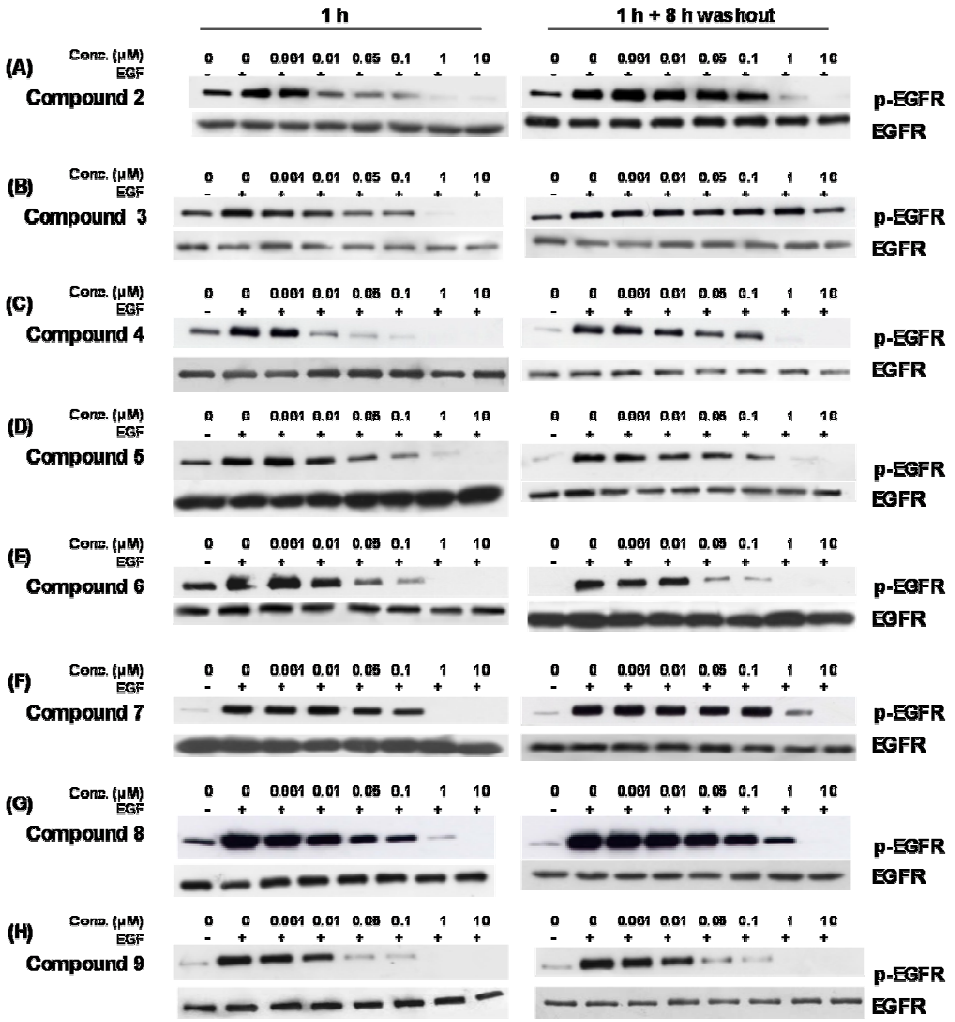

Figure 2.15. Irreversible inhibitory actions of compounds **4-9** on EGFR autophosphorylation. A431 cells were incubated with the investigated compound for 1 h and stimulated with EGF either immediately after or 8 h after removal of the compound from the medium. Western blot analysis was done using monoclonal antibodies directed to p-Tyr1068. **2** and **3** were used as irreversible and reversible reference compounds, respectively. Representative blots of three independent experiments are shown. Total EGFR is shown as loading control.

While the reference compound **3** does not exert any irreversible inhibition, reference irreversible compound **2** as well as many of the newly synthesized derivatives like epoxides **4**-**6** and phenoxyacetamide **9**, irreversibly inhibit EGFR activity, with inhibition values higher than 90%

after 8 h washout. On the other hand, only a partially irreversible inhibition was provided by compounds **7-8** and **10-14** under the testing conditions, with percent inhibition of EGFR autophosphorylation between 24 and 80%. (Table 2.6)

The irreversible inhibition provided by compounds **4**-**6** could be addressed to the ability of their epoxide rings to undergo nucleophilic attack by Cys773 so to generate a stable enzyme-bound addition product.[85,98] Compounds **4**-**6** showed dose-dependent inhibition of EGFR autophosphorylation in A431 cells with IC_{50} values comparable to that of **2**. Despite compounds **4** and its (2*S*,3*S*) enantiomer **5** showed similar affinity for purified human EGFR, they inhibit EGFR tyrosine kinase activity differently 1 h after and 8 h after the removal of the compound from the reaction medium. If compared with compound **4**, compound **5** was slightly less potent to inhibit EGFR after 1 h treatment but showed slightly higher potency 8 h after its removal. Despite these limited differences may not allow the establishment of accurate structure-activity relationships, different contribution in term of reversible and irreversible binding could explain these IC_{50} value changes. Indeed, the IC_{50} value at 1 h could be addressed to both reversible binding to the EGFR catalytic site, by weak interactions at the enzyme surface, and to irreversible binding, due to the formation of a covalent bond with an exposed cysteine. On the other hand, the IC_{50} value measured 8 h after ligand removal only would depend to the extent of irreversible covalent binding.

In agreement with reported data about acrylamide and propargylamide derivatives,[115,116] the introduction of a basic group in the warhead portion improved inhibitor potency of compound **6**. Despite, the presence of the piperidine group did not improve the affinity toward purified EGFR enzyme with respect to the epoxysuccinate **4**, the introduction of this basic group increased the inhibitory activity of

compound **6** (Figure 2.15 entry E and Table 2.6). The amino group could act as (i) an intramolecular catalyst for nucleophilic additions to the cysteine-reactive center, (ii) a water-solubilizing group, (iii) an additional site for hydrogen bond recognition with acidic residues within the EGFR binding site. The former option was proposed [117] considering the protonated nitrogen of the piperidine ring able to provide an additional hydrogen bond with the acidic group of Asp800.[118,119] In this way, the piperidine group should facilitate the nucleophilic attack at the epoxy ring by Cys773[116] rather than improving the recognition of **6** at the active site.

6-phenoxy-acetamide derivatives **7**-**9**, designed to undergo a nucleophilic attack by Cys773 on their α-methylene activated portion, irreversibly and potently inhibit EGFR. Similarly to what had been reported for α-chloro-acetamides,[84] they could irreversibly alkylate Cys773 with subsequent *in situ* releasing of the phenolic leaving group. Since the reactivity of their α-methylene portion mainly depends on the phenol leaving group activation, a different decoration of this aromatic ring can modulate the reactivity of these classes of inhibitors.

Following this concept, while the introduction of one electron-withdrawing fluorine atoms on the phenoxy aromatic ring did not significantly change the inhibitory effect of compounds **7** and **8**, the penta-fluoro substitution (compound **9**) greatly increased the α-methylene portion reactivity versus Cys773 so to provide a significantly increase of the EGFR inhibition after 8 h (IC_{50} 0.078 μM, lower than the reference compound **2**, Figure 2.15 entry H and Table 2.6). These results indicate this kind of warhead suitable for further chemical optimization focused on modification of the stereoelectronic features of the phenolic leaving group. Beyond this, phenoxy-acetamide derivatives could be also designed to release pharmacologically active leaving groups inside cells subsequently to their binding with EGFR-TK. In this way, phenoxy-

acetamide warheads could be suitable to provide a multi-target approach. [120,121]

Despite both compounds **10** and **11** were designed to establish covalent but reversible interactions with nucleophilic cysteine residues, carbamate derivative **10** showed a quasi-irreversible inhibition EGFR while only a residual effect was observed 8 h after treatment with compound **11**. These findings could be explained hypothesizing that the thiocarbamate adduct resulting from the interaction between Cys773 and compound **10** would more stable than the thioimidate ester produced, in the same way, by compound **11**. If this is true, carbamoylating agents should be considered more promising than nitrile based derivative in terms of suitability for further structural optimizations focused to achieve a full irreversible inhibition of EGFR.

Again, despite sulphenamide armed compounds **12**-**14** should share a common binding reaction mechanism toward Cys773, only the 1,2,4-thiadiazole **14** was able to provide a potent, yet partial, irreversible inhibition of EGFR. Isothiazolinone **12** and benzisothiazolinone **13** armed derivatives, indeed, reversibly inhibited EGFR. These compounds should covalently react with Cys773 forming a mixed disulfide bond by breaking of the sulfenamide bond and subsequent ring opening[8,21]. Also in this case, because of their common covalent inhibition mechanism, a way to explain the different reversibility shown by these compounds could be to hypothesize a different stability for their covalent disulfide products in the testing conditions.

To evaluate the contribution of 4-anilinoquinazoline driving portion to the observed EGFR-TK inhibition effects, compounds **16** and **17** (Scheme 2.5 and Table 2.6) were synthesized and tested by cell-based assays. In these compounds two of the most active cysteine-trap portions of the series were linked to a simple naphthalene nucleus as driver group. Since naphthalene lacks the structural elements required for

interaction with the ATP-binding site of EGFR[81], these compounds should not be able to recognize the desired molecular target providing, in this way, a direct evaluation of warhead reactivity contribution to the observed inhibition activity. As expected, compound **16**, carrying an epoxysuccinic group analogue to compound **4**, and compound **17**, containing the same side chain as compound **7**, did not inhibit EGFR autophosporylation in A431 human epidermoid cancer cell line, demonstrating that target specificity of the series is due to driver-portion recognition within the EGFR active site. Moreover, compounds **16** and **17** exhibited less than 10% inhibition of A431 cell proliferation at concentrations up to 10 μM, indicating no relevant aspecific cellular toxicity for tested warheads. To assess the intrinsic chemical reactivity of warheads characterizing the most promising synthesized candidates toward thiol nucleophiles, the formation of conjugates with glutathione was evaluated in aqueous buffered solution by LC-UV and LC-ESI-MS (see Experimental Section, Chapter 4.1.4). Neither the epoxy-derivatives **4** and **15**, nor the phenoxyacetamides **7** and **17** gave any measurable adduct with GSH after 1 h incubation. On the other hand the acrylamide **2** showed conversion of 36.2 ± 1.9% (mean ± SD; n = 3) of the starting compound to its GSH-conjugate ($[M+H]^+$ = 676.11) under the same conditions.

In order to evaluate the ability of synthesized compounds to irreversibly inhibit T790M EGFR as well as wtEGFR, the antiproliferative activities of compounds that exhibited highest irreversible inhibition potency toward A431 cell line (overexpressing wild type EGFR) was quantified on gefitinib-resistant H1975 NSCLC cell line (harboring T790M EGFR). The antiproliferative activity of tested compounds was reported in table 2.7 and it was determined by MTT assay. As already done for the set-up of the autophosphorylation assay on A431 cell line, also in this case some reversible and irreversible reference compounds, derivatives

2-4, **6** and **8-9** respectively, were tested together with the investigated compounds, in the same testing conditions. Since H1975 NSCLC cell line are known to be resistant to gefitinib (Table 2.7, entry 1, reference compound), also this drug was tested as clinically used reference.

Compound	H1975 Cell line IC_{50} (μM)
1 (Gefitinib)	8.26 ± 1.11
2	0.61 ± 0.05
3	19.5 ± 2.46
4	6.76 ± 0.60
6	1.72 ± 0.47
8	7.82 ± 1.19
9	11.0 ± 1.08

Table 2.7. Viability inhibition potency of NSCLC H1975 gefitinib-resistant cell line was reported as concentration to inhibit by 50% their proliferation. The cell proliferation was determined by the MTT assay, after 72 h of incubation with compounds (0.1–20 μM). Mean values of three independent experiments ± SEM are reported.

As reported in Table 2.7, calculated IC_{50} values for all investigated compounds were greater than IC_{50} value calculated for the irreversible reference compound **2**. On the other hand, all tested compounds could clinically inhibit H1975 cell proliferation with potencies magnitude equal or higher than reversible reference compounds **1** or **3** respectively. Notably, the introduction of the basic piperidine group on the reactive side chain of compound **4** made compound **6** four times more active than **1** on H1975 cells (Figure 2.16 and Table 2.7), with an antiproliferative IC_{50} of 1.72 μM. In this way, compound **6** showed the best potency profile among investigated derivatives.

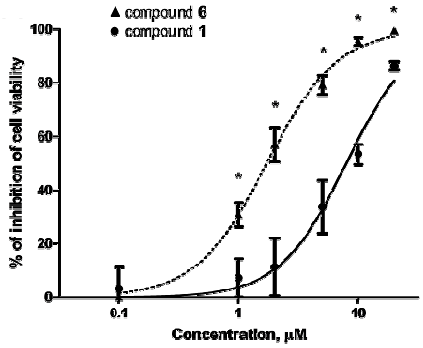

Figure 2.16. Effectiveness of irreversible EGFR inhibitor **6** in H1975 NSCLC cell line. Antiproliferative effects of compound **6** (▲) in comparison with **1** (●) on H1975 cell line, harboring the resistance-associated mutation T790M. Cell proliferation was determined by MTT assay, as described in the Experimental Section (Chapter 4.1.3). Results are reported as the mean ± SD of three independent experiments. *, $P < 0.01$ for each dose versus **1**; n = 3. (B) Comparison of compounds **6**, **1**, and **2** in their ability to suppress EGFR autophosphorylation (p-EGFR), erbB2 autophosphorylation (p-erbB2) and phosphorylation of downstream effectors AKT (p-Akt) and MAPK (p-p44/42) in H1975 cells. Total EGFR, erbB2, AKT and MAPK are shown as loading controls.

The ability of compound **6** to inhibit EGFR signaling in the NSCLC cell line H1975 (harboring the T790M mutation) was investigated by Western blot analysis. Once again, compounds **1** and **2** were used as reference compounds in this test and collected results of Western blot analysis are illustrated in Figure 2.17. While **1** showed marginal activity on EGFR and erbB2 in H1975 cells up to 10 µM, compound **6** was found to produce a dose-dependent inhibition of EGFR and of erbB2 autophosphorylation with complete inhibition at 1 µM concentration. Moreover, compound **6** was also considerably more effective than **1** to inhibit the two major EGFR dependent signaling pathways like the PI3K/AKT/mTOR and the RAS/RAF/MAPK cascades that were recognized to have a pivotal role in controlling cell survival, cell growth and proliferation (Figure 2.17).

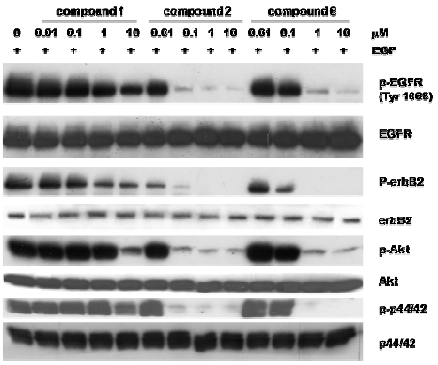

Figure 2.17. Effectiveness of irreversible EGFR inhibitor **6** in H1975 NSCLC cell line. Comparison of compounds **6**, **1**, and **2** in their ability to suppress EGFR autophosphorylation (p-EGFR), erbB2 autophosphorylation (p-erbB2) and phosphorylation of downstream effectors AKT (p-Akt) and MAPK (p-p44/42) in H1975 cells. Total EGFR, erbB2, AKT and MAPK are shown as loading controls.

Moreover, compound **6** was found to be more effective than compound **1** to induce apoptosis in living cells (25-30% at 5 μM concentration) (Figure 2.18A) and it was associated with caspase-3 activation (Figure 2.18B).

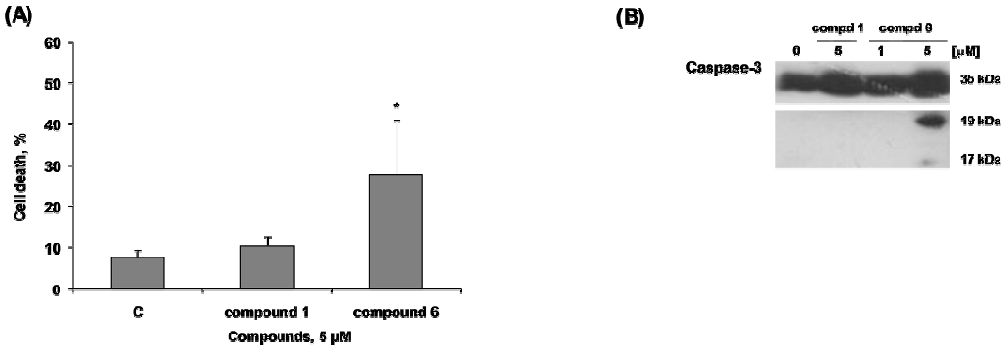

Figure 2.18. Effect of compound **6** on H1975 cell death. (A) H1975 cells were treated with the indicated concentration of compound **1** and compound **6** for 72 h and then analyzed with propidium iodide/ Hoechst 33342 staining to assess cell death. (*), $P < 0.01$ for each dose versus control; n = 3. (B) At the same time the cleavage of procaspase-3 was assessed on lysate proteins by Western blotting. The migration positions of each full-length procaspase and of its processing products are indicated.

Taken together, these results suggest that irreversible inhibitor **6** could exert both a cytostatic and a cytotoxic effect on the H1975 cancer cell line. On the other hand, compound **6** proved to have a weak cytotoxic profile on a cell line where proliferation is not driven by EGFR activity, excluding off-target cytotoxic effects. In fact, compound **6** at 10 μM inhibited less than 50% of SW620 human colon carcinoma cell proliferation, similarly to what observed for **1** and for the epoxysuccinic derivative **4**. On the opposite, the acrylamide derivative **2** was found more toxic, giving an IC_{50} of 8.23 ± 1.08 μM (Table 2.8).

Compound	SW620 cells proliferation IC_{50} μM[a]
1	>10
2	8.23±1.08
4	>10
6	>10

Table 2.8. Viability inhibition of SW620 cell line. [a] Concentration to inhibit by 50% the proliferation of SW620 cells. The cell proliferation was determined by the MTT assay, after 72 h of incubation with compounds. Mean values of at least two independent experiments ±SD are reported.

Conclusions

The results here described extend the chemical diversity of new irreversible EGFR inhibitors and represent a good example of the application of cysteine reactive compounds to the drug development process. In this case, covalent target modification was desired to increase the binding affinity of synthesized inhibitors toward T790M EGFR in order to develop new EGFR inhibitors able to overcome the drug resistance shown by gefitinib-resistant cancer cells.

Presented inhibitors were designed to react with cysteine through different kind of reaction mechanism like nucleophilic addition (epoxides

4-**6**), nucleophilic substitution (phenoxyacetamides **7**-**9**), carbamoylation (carbamate **10**), Pinner reaction (nitrile **11**) and disulphide bond formation (isothiazolinone **12**, benzisothiazolinone **13**, thiadiazole **14**). Among them, compounds from different chemical classes proved efficient in irreversibly inhibiting EGFR autophosphorylation.[122] Epoxy-derivatives **4**-**6** showed potencies comparable to the acrylamide reference **2**. Moreover, the introduction of a terminal basic group (compound **6**) significantly improves the inhibition potency of epoxyde derivatives both in EGFR autophosphorylation and in cell proliferation assays. These results indicate that the identified epoxydes could be considered good starting points for further structure-based optimization.

Compound **6** inhibited the EGFR downstream signaling pathways showing cytostatic and cytotoxic activities on gefitinib-resistant NSCLC cells (H1975). Notably, the independence of observed cytotoxicity of compound **6** on H1975 cell line to off-target general cytotoxic effects suggests that this compound could induce apoptosis in H1975 cell line mainly by EGFR inhibition. Beyond its clinical utility, this finding provide one more supporting example of how the aspecific reactivity of covalent modifier can be selectively driven toward a desired target by proper structural modifications, limiting the occurrence of off-target toxicity.

The potency as well as the irreversibility of inhibition provided by compound **9** makes the phenoxyacetamide warhead interesting for EGFR irreversible inhibition. Moreover, since each phenoxyacetamide carrying compound can release a leaving group subsequently to Cys773 targeting, these derivatives may be considered for a multi-drug approach in cancer treatment. Promising results were also observed with the carbamate **10** and the 1,2,4-thiadiazole **14**.

Chapter 3

MAGL targeting

3.1 Introduction

N-**A**rachidonoyl**E**tanol**A**mmine (**AEA**, **119**, Figure 3.1) and **2**-**A**rachidonoyl**G**lycerol (**2-AG**, **122**, Figure 3.1) are the most representative members of a class of endogenous ligands named endocannabinoids that are able to activate cannabinoids receptors (CBs) expressed by neurons and cells belonging to the immune system. Once released, AEA and 2-AG act as retrograde neuromudulators, inhibiting multiple neurotransmission pathways across the brain by presinaptical CB_1 receptor activation. Their removal from peri-synaptic space by reuptake mechanisms or by rapid enzymatic deactivation,[123] finally terminate their signalling.

Altogether, the cannabinoid receptors, their endogenous ligands, and their respective catabolic enzymes constitute the endocannabinoid system.[125] The endocannabinoid system plays important roles in various aspects of neural functions including learning and memory, anxiety, depression, addiction, appetite and feeding behaviour, nociception, and neuroprotection.[124] Despite the therapeutic exploitability of some of these responses, it is still difficult to uncouple beneficial effects from undesirable ones when an enhanced cannabinoid neurotransmission is pharmacologically induced. Moreover, lack of knowledge about the physiological role of each single endocannabinoid neuromodulator in central nervous system (CNS) and peripheral nervous system (PNS) makes the dissection of their contribution to the observed effects difficult.

Since 2-AG has been considered the true on-demand released endocannabinoid ligand for CB_1 receptor,[124,137] understanding of physiological role of 2-AG in CNS is crucial to effectively manipulate the endocannabinoid system. Unfortunately, due to its short half-life, it is not possible to use 2-AG as therapeutic agent by *in vivo* direct administration. So, a promising way to explore and promote its therapeutic potential

could be the selective inhibition of MAGL, the enzyme responsible of 2-AG degradation. Despite this, few potent and selective MAGL inhibitors are available until now.

The use of covalent modifier to inhibit MAGL could represent a good strategy to develop new highly potent and selective pharmacological tools for the endocannabinoid system investigation. Beyond this, the establishment of a proper covalent interaction with MAGL could provide to these inhibitor high basal potency and selectivity for the target, constituting a good starting point for their further structural optimizations. Combined together, these strategies could lead to the development of new effective drugs which are able to selectively induce beneficial effects like analgesia, neuroprotection or orexigenic responses through an enhanced endocannabinoid neuromodulation.

3.1.1 Structure and physiological role of endocannabinoids

The endocannabinoids are a family of polyunsaturated fatty acid amides or esters (Figure 3.1) derived from arachidonic acid (compound **120**, Scheme 3.1).

Figure 3.1. Structure of most representative endocannabinoids.[124]

Endocannabinoids, mainly represented by anandamide (**119**, AEA) and 2-arachodonoylglycerol (**122**, 2-AG), aren't stored in vesicles like other neurotransmitters but generated on-demand through stimulus-dependent cleavage of membrane phospholipidic precursors and quickly released into peri-synaptical space by neurons belonging to CNS

and PNS.[125] Once released, AEA and 2-AG are free to reach the pre-synaptic terminal by a retro diffusion process to activate $G_{i/0}$ protein coupled receptors like CB_1 and CB_2 which are expressed by neighboring cells. It was reported that AEA and 2-AG act toward CB_1 as partial agonist and as full agonist respectively. [126 ,132] After their action, endocannabinoids are removed from peri-synaptic space by reuptake mechanisms or by rapid enzymatic deactivation (Figure 3.2).[123] Because of their non-synaptic production and fast elimination, endocannabinoids are thought to act in CNS and PNS as short-range modulators of cells and synapses activity rather than classical hormones or neurotransmitters.[127]

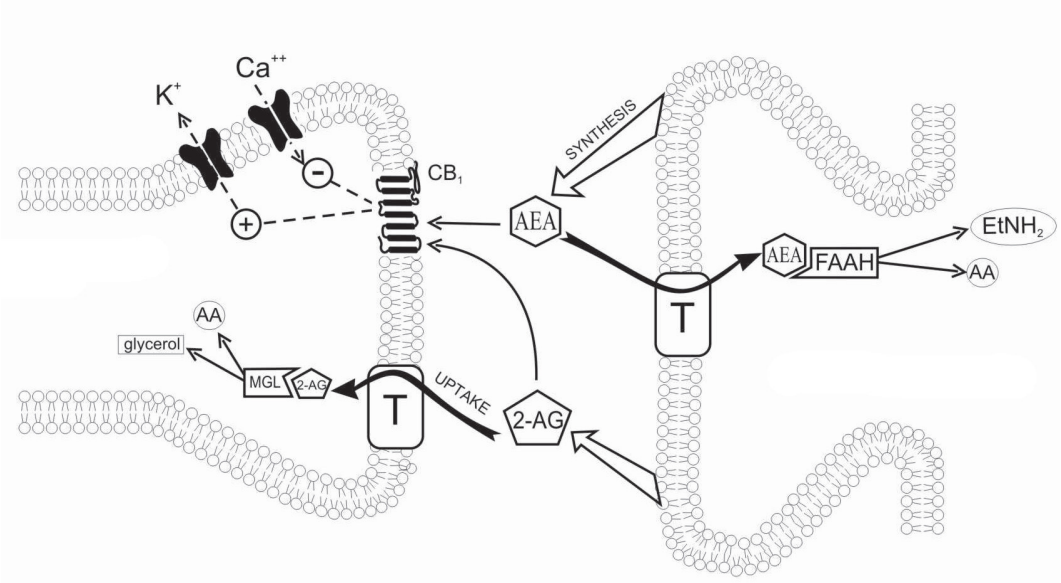

Figure 3.2. Overview of endocannabinoid signaling.[125] Hydrolytic inactivation of AEA and 2-AG, mainly due to the activity of FAAH (Fatty Acid Amide Hydrolase) and MAGL (MonoAcylGlycerol Lipase) enzymes respectively, is recognized as the main bioinactivation mechanism responsible of endocannabinoid signaling termination.

The endocannabinoid neuromodulation plays important roles in various aspects of neural functions including learning and memory,

anxiety, depression, appetite and feeding behaviour, nociception, neuroprotection[124] and movement control.[128] Among neural functions that involve endocannabinoid signalling, nociception, food intake modulation and neuroprotection represent the most studied and pharmacologically exploitable functions which can be used to develop some new analgesic, orexigenic and neuroprotective drugs respectively. Considering that CB_2 receptors are predominantly present in tissues belonging to immune systems (such as spleen, tonsils, lynphonodes, macrophages and microglia) and that CB_1 receptors are abundantly expressed in CNS (cortex, hippocampus, amygdala, basal ganglia outflow tracts and cerebellum) and in PNS, [129] it is though that endocannabinoids could modulate pain, emesis and food intake through CB_1 receptor activation.[124] Since CB_1 receptors are expressed by peripheral terminals of primary sensory neurons, by dorsal horn synapses and by encephalic neurons involved to pain sensation modulation, it is thought that endocannabinoids take part in a natural CB_1 receptors dependent anti-nociceptive system. It was reported that cannabinoids, through CB_1 receptor activation, may potentiate the activity of supraspinal descending inhibitory pathways as well as activate dynorphin containing interneurons located to dorsal horns of the spinal cord. In this way, they could induce analgesia modulating the neurotransmission between primary afferent fibers and spinothalamic neurons. Indeed, CB_1 activation in brain stem areas like RVM (rostral ventromedial medulla) and PAG (periaqueductal gray) provide analgesia by over-activation of descending inhibitory neurotransmission (figure 3.3)[130]

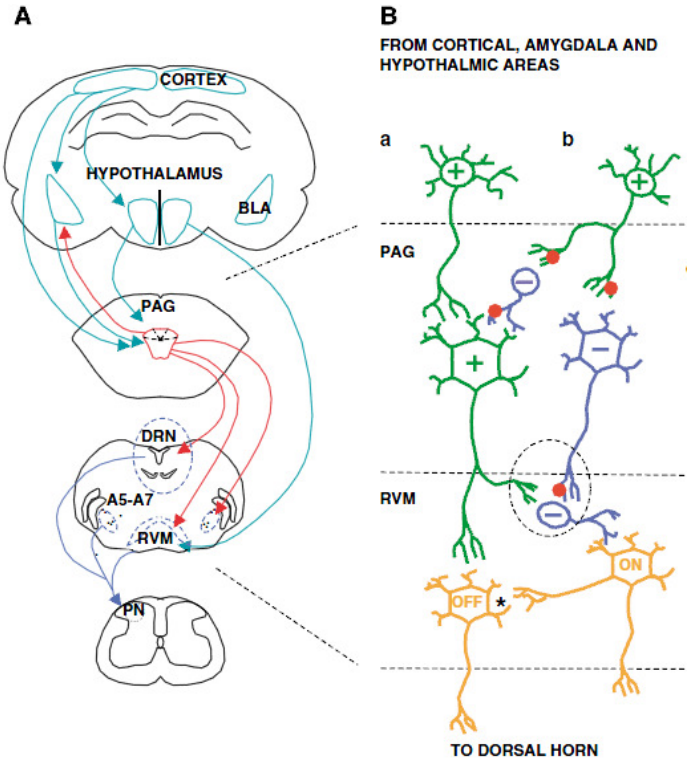

Figure 3.3. Possible mechanism for endocannabinoid-mediated control of nociception.[130] (A) Diagrammatical representation of some of the interactions between various brain regions of the descending pain pathway. The PAG have a pivotal role in the modulation of this kind of neurotransmission (BLA=Basolateral Amygdala; DRN=Dorsal Rafe Nucleous; PAG=Peri-Aqueductal Gray; RVM= rostral ventromedial medulla, PN= Peripheral neurons). (B) Two possible outcomes of this net. The final effect on the input of ON and OFF cells to the dorsal horn is neutral when no painful stimuli is perceived. It is proposed that painful stimuli selectively activate pathway (b) that lead the activation of ON cells and the simultaneous inhibition of OFF cell so to allow the full nociceptive perception. On the other hand, anti-nociceptive neurotransmission is mainly exerted through pathway (a) in which excitatory neurons in the PAG are activate by pathways upstream the PAG. These excitatory neurons, in turn, activate the firing of OFF cells and, in the same time, inhibit the firing of ON cells through GABAergic interneurons.[130]

It was proposed that the endocannabinoid system could also modulate the food-intake behaviour interacting with the orexigenic

(e.g., orexins) and anorexigenic (e.g., leptin) mediated neurotransmission at mesolimbic level.[124]

Moreover, the CB_1 activation mediated by endocannabinoids has been shown to exert neuroprotection in a variety of *in vitro* and *in vivo* animal models of neurodegeneration. [124] Despite the neuromodulation provided by endocannabinoids is mainly achieved by activation of a common receptor (CB_1), different neurological responses to AEA or 2-AG increased level in CNS have been reported.[131] Beyond the differential selectivity exerted by these endocannabinoids toward CB_1 or CB_2, a possible explanation of the phenomena could be provided by several different hypotheses:

1. State-dependent selectivity of neurons activation: it is reported that the physiological action of endocannabinoids in CNS may be dependent to the pre-built sensitivity of some neuronal network toward cannabinoid ligands. Indeed, it was hypothesized that intracellular signalling induced by cannabinoids may vary across different neuronal environments dependently to changes in CBs receptors expression, changes in endocannabinoid deactivating proteins expression (hydrolytic enzymes or reuptake pumps), or to CBs receptor/G protein/downstream effectors proteins coupling effectiveness differences (Figure 3.4).[132] Thus, a given ligand may act, for instance, as a partial agonist in well coupled tissues but as an antagonist in tissues where receptor coupling and/or G protein-dependent effectors activation are less well coupled.

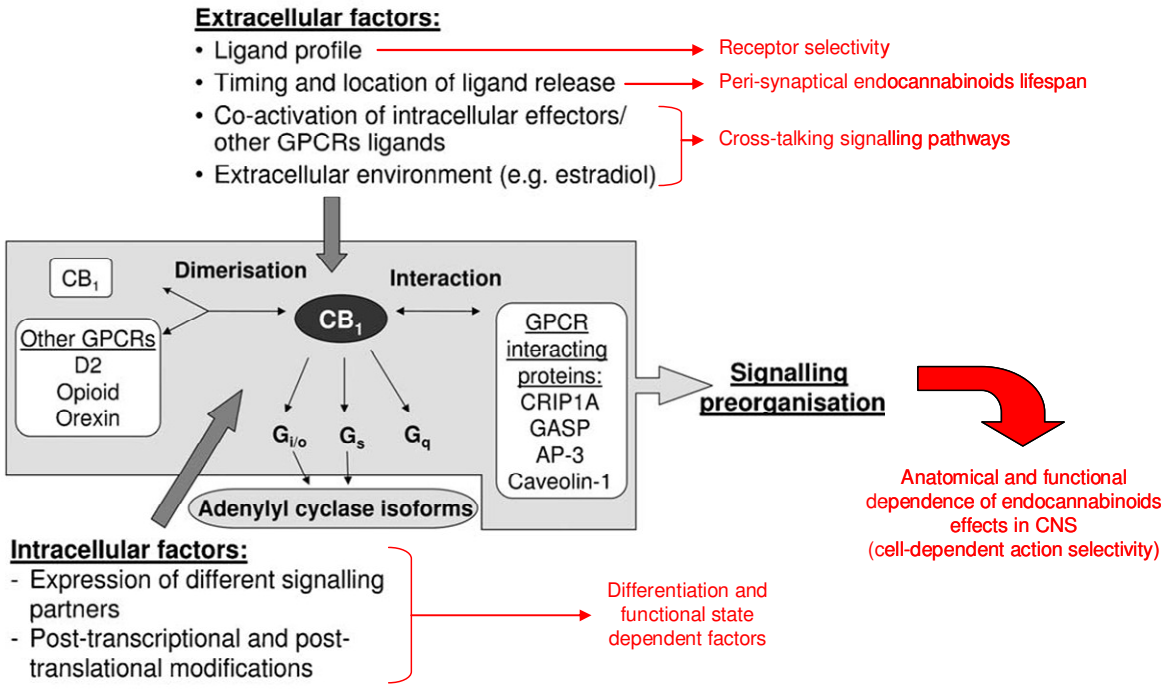

Figure 3.4. Different levels of CB_1 signalling modulation. Due to a fine-control by intra- and extracellular factors, the signalling cascades regulated by CB_1 cannabinoid receptor are cell-specifically pre-organised. In this way, coupling efficiency and receptor trafficking control can precisely modulate cellular responses to endocannabinoids (cell-based selectivity).[132]

2. Activation of non-CB_1/CB_2 receptors: it was reported that the activation of some non-CB_1/CB_2 receptors by endocannabinoids could imply a possible cross-talk between the endocannabinoid and endovanilloid systems.[124]. There are some differences between AEA and 2-AG in terms of affinity for non-CB_1/CB_2 receptors like Transient Receptor Potential Vanilloid Type 1 (TRPV1) channels or the orphan GPR55 receptor. For instance, AEA is physiologically able,[133] unlikely 2-AG, to bind and activate TRPV1 channel in brain, probably modulating the nociceptive perception.[134] On the other hand, the neurophysiological role of endocannabinoid-mediated activation of GPR55,[124] widely expressed in CNS and PNS areas like frontal cortex,

cerebellum, striatum, hypothalamus, brain stem and dorsal root ganglia neurons,[135] is still unclear.

Although AEA may tonically control pre-synaptic CB_1 receptors,[136,142] most experimental evidences support the hypothesis that 2-AG could be considered the most important retrograde messenger involved to on-demand induction of short- and long-term synaptic depression through CB_1 activation. Indeed, the tissue levels and the production rate of 2-AG in stimulated nervous tissues and cells are higher than those of AEA so to indicate 2-AG as a fast signaling molecule.[137]
Moreover, 2-AG has been proposed as the true physiological endogenous ligand for CBs receptors[124] because, unlikely AEA, it acts as a full agonist toward CB_1 and CB_2 receptors without activating other receptor classes like TRPV1.

3.1.2 Endocannabinoids synthesis and metabolism

AEA and 2-AG are produced following an increased intracellular Ca^{2+} concentrations subsequent to cell depolarization, or caused by $G_{q/11}$ protein-coupled receptors dependent mobilization of intracellular Ca^{2+} stores.[143] AEA is mainly synthesized from pre-existing *N*-arachidonoyl phosphatidylethanolamine (NAPE), whereas 2-AG can be synthesized via multiple pathways. Indeed, 2-AG can be produced from arachidonic acid-containing diacylglycerol by the action of a diacylglycerol lipase (DAGL)(route I), by hydrolysis of lysophosphatidylinositol (lyso-PI) by a specific phospholipase C (route II) or by hydrolysis of arachidonic acid-containing lysophosphatidic acid by the action of a phosphatase (route III) (Figure 3.5).[138]

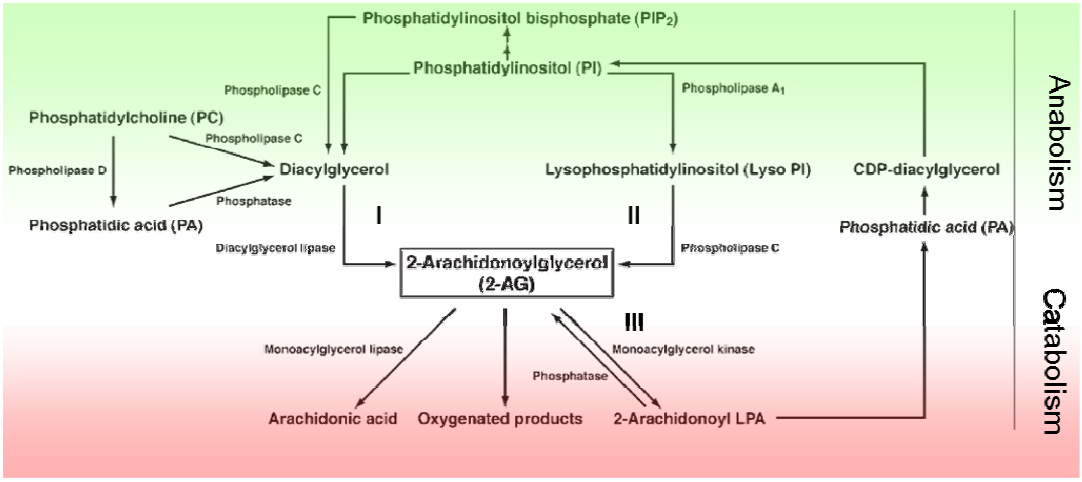

Figure 3.5. Metabolic pathways for 2-AG.The most physiologically important synthetic pathway of 2-AG seems to be mediated by diacylglycerol lipase (route "I").[138]

AEA and 2-AG signalling can be shut off by a two-step process: 1) transport of endocannabinoids from the extracellular to the intracellular space; and 2) intracellular hydrolytic degradation or oxidation. Despite some experimental evidences suggest the existence of a common protein-facilitated mechanism responsible for intracellular accumulation of 2-AG and AEA, protein (s) involved in this mechanism are still unknown.

Whereas FAAH is responsible of hydrolysis of AEA yields arachidonic acid and ethanolamine,[139] the major enzyme responsible for 2-AG metabolism seems to be the serine hydrolase MAGL.[140] The latter enzyme is expressed in a variety of human, rat, and mouse tissues[141] and mediated hydrolysis of 2-AG giving arachidonic acid **120** and glycerol **123** as products (Scheme 3.1).[144]

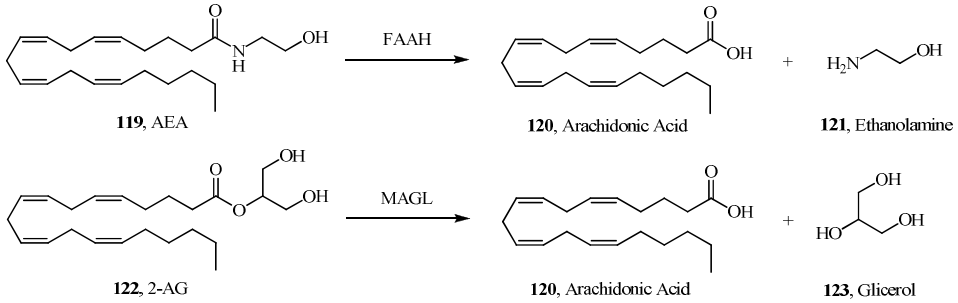

Scheme 3.1. Hydrolysis of AEA **119** and 2-AG **122** by FAAH and MAGL respectively.[143]

Considering the post-synaptic expression of FAAH and the presence of MAGL on pre-synaptic terminals of different neuronal populations, it was suggested that FAAH might be involved in the regulation of AEA resting levels close to its sites of synthesis whereas MAGL might help to inactivate 2-AG close to its sites of action.[127,142]

Despite the hydrolysis represents the main deactivation mechanism of AEA and 2-AG,[127] it is reported that these neuromodulators can also undergo oxidative metabolism mediated by enzyme like COX-2 (cyclooxygenase type 2), 12-LOX (12-Lipooxygenase) and 15-LOX (15-lipooxygenase. [143] Since it is reported that oxidized product of endocannabinoids activate receptors outside the "endocannabinoid system", it is still unclear if oxidative catabolism of AEA and 2-AG represents an additive way to terminate endocannabinoid signalling or, instead, to start another kind of cells cross talking.

3.1.3 Structure and expression of MAGL enzyme

MAGL is a cytosolic serine hydrolase that cleaves 2-arachidonoylglycerol (2-AG) into fatty acid and glycerol through a catalytic mechanism that involves a classical serine-aspartate-histidine triad.[144] MAGL hydrolyses medium- and long-chain fatty acids, such as palmitic acid, oleic acid, and arachidonic acid from the position 2 of monoglycerides, with the highest hydrolysis rate for arachidonic acid.[145]

The primary structure of MAGL is defined by a 303-long amino acid sequence[146] that shares a high degree of homology in mouse-, rat-, and human. Thus, in term of amino acid homology degree, human and mouse MAGL (hMAGL and mMAGL respectively) are 84% identical,[144] whereas mouse and rat MAGL (rMAGL) are 92% identical.[140]

Very recently, the crystals of a dimer of human MAGL (hMAGL) in a "open" conformation (see the text below) was obtained and solved at

2.2 Å of resolution by X-ray diffraction (Figure 3.6).[147] MAGL presents the hallmarks of the α/β hydrolases superfamily like a central β-sheet core, constituted of seven parallel and one antiparallel strands, surrounded by six α helices (Figure 3.6). A wider U-shaped cap domain covers the structurally conserved β-sheet core and the MAGL active site in which the catalytic triad, made up of residues Ser122, Asp239 and His269, is located.

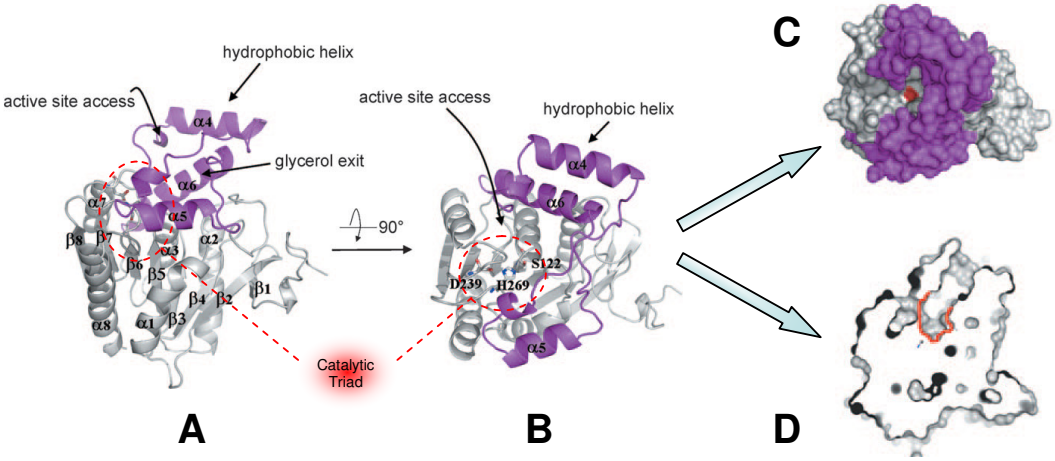

Figure 3.6. Overall structure of hMAGL monomer in "open" conformation with catalytic triad represented as sticks, and cap domain colored magenta (A) Side view, ribbons representation. (B) Top view (90° rotation), ribbons representation. (C) Top view, surface representation (nucleophilic Serine 122 colored in red). (D) Transverse section highlighting the near environment of the nucleophilic serine (lined in red)[147]

As for other human lipase like human pancreatic lipases (hPL), it has been speculated that the cap domain in MAGL serves as a lid domain that, once the proteins come into contact with lipid droplets or 2-AG, allows the enzymes to unveil their otherwise unreachable hydrophobic active site (interfacial activation). This process should allow the enzyme to exist in two main conformation, a "closed" and an "open" form. Moreover, it has been suggested that the hydrophobic and flexible α4 helix of MAGL cap domain may help the soluble cytosolic form of MAGL

either to get in close contact with or to anchor in the cytoplasmic membrane in order to reach its lipophilic substrates. Despite this could explain why MAGL was sometimes considered a cytosolic enzyme and sometimes a membrane-associated one,[127, 148 ,150b] no interfacial activations has been described for MAGL, neither there isn't any evidence that alternative biological conformations might exist.

Beneath the MAGL cap domain, a highly hydrophobic pocket connecting the MAGL surface to its catalytic site, deeply buried in the protein, has been recognized. This cavity (~25 Å in length and ~8 Å in width)[149] becomes wider as one moves away from the catalytic triad environment towards the surface of the protein and seems suitable for recognition and accommodation of the long and flexible chain of MAGL substrates during their catalyzed hydrolysis process. Another narrow cavity (about 5 Å of diameter) was recognized to connects the active side to the outside of the protein. The architecture formed by loops connecting α4 to α5 and α5 to α6 helices, and the last portion of the α5 helix, is responsible of the formation of this narrow hole. This small channel lies perpendicularly to the trajectory that leads from the hydrophilic pocket to the membrane binding site and might act as putative exit door for the glycerol moiety, released after 2-AG hydrolysis.[147]

Some site-directed mutagenesis studies were carried out in order to understand which aminoacid residues are essential to the catalytic activity of MAGL. Not surprisingly, carrying out an alanine scanning based mutagenesis the catalytic triad members Ser122, Asp239 and His269 (red circled in Figure 3.7), were recognized as essentials for catalysis.[144] Moreover, using a glycine scanning based mutagenesis, three cysteine residues like Cys242, Cys201 (yellow circled in Figure 3.7) and Cys208 (green circled in Figure 3.7), were suggested to have a big impact on the basal activity of MAGL.[179] Involvement of one or more cysteine residues on MAGL catalysis regulation was also suggested by

previous studies in which the ability of unselective cysteine reactive agents like p-chloromercuribenzoic acid (p-CMB) to shut down the catalytic activity of MAGL were reported. [150] Recently, an X-ray diffraction study has localized these cysteine residues on MAGL (Figure 3.7). Cys242 was located into the active site of MAGL with its sulphur atom very closely positioned to catalytic Ser122 whereas Cys201 and Cys208 were found far away from the catalytic serine. Cys201 and Cys208 was found solvent-exposed and located at the liphophilic tunnel's wide entrance or in the vicinity of the putative glycerol exit hole, respectively.[149]

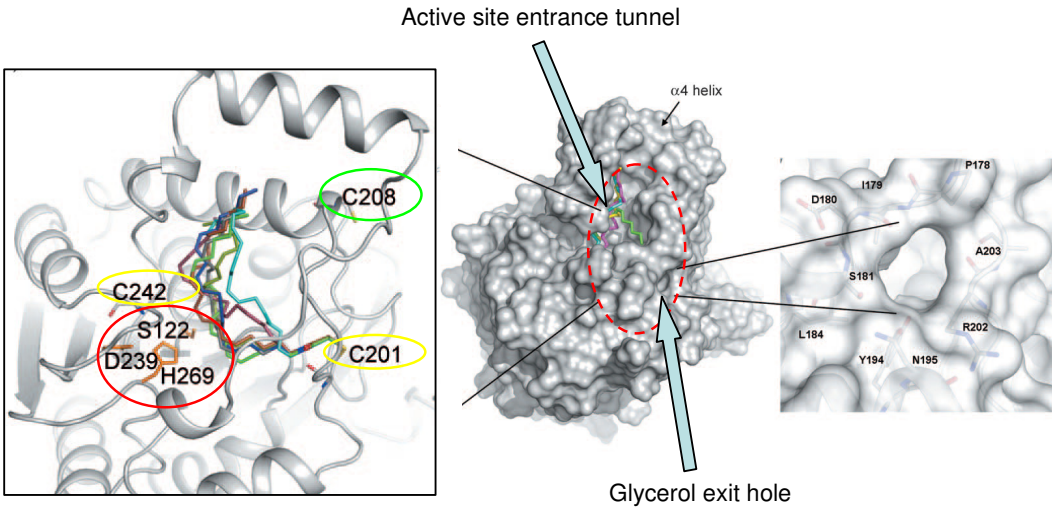

Figure 3.7. hMAGL top view (crystal structure, surface representation) with lid domain in opened conformation. [147] Right: highlighted nucleophilic residue targeted by covalent inhibitor of hMAGL(crystal structure, ribbon representation). A Cys201 covalently binded molecule of *N*-ArachidonylMaleimide (NAM), a cysteine trapping MAGL inhibitor, is docked inside the active site of MAGL. Left: putative glycerol exit hole (crystal structure, surface representation).[147]

MAGL seems to be expressed in a variety of cells and tissues. In human neutrophils, the enzyme activity was detected in granules within the cytoplasm and, after stimulation with calcium, close to the plasma membrane. In white fat and liver, MAGL is thought to catalyze the final step of the lipolytic cascade that releases fatty acids from triacylglycerol

stores[151] but the primary role of MAGL in the brain is to carry out the deactivating hydrolysis of 2-AG. MAGL is expressed more predominantly in the cortex, hippocampus and cerebellum.[127]

3.1.4 Pharmacological potentials of MAGL inhibition

It is known that exogenous administration of cannabinoids (obtained from natural sources like plants or synthetically produced) can induce a wide range of neuropharmacological effects mainly related to neurotransmission modifications in CNS by CB_1 receptor activation.[152,153] For instance, *in vivo* administration of (-)-Δ^9-tetrahydrocannabinol (Δ^9-THC), a well-known highly potent CB_1/CB_2 partial agonist present in *Cannabis* genus plants, produce behavioral responses like hypomobility, analgesia, catalepsy and hypothermia (collectively defined as "Martin's tetrad")in mice[154] and can induce antiemetic and hyperfagic effects in human [155] and in rats [156] respectively. Unfortunately, until now, the understanding of the endocannabinoid neurotransmission physiology is far to be completed and this doesn't allow us to entirely know how these responses are induced and how to uncouple beneficial and untoward properties of exogenous cannabinoid administration. Indeed, considering that both AEA an 2-AG act across the CNS mainly activating the same CB receptor subtype, it is easy to understand that one of the bigger problem that affects the study of endocannabinoid system physiology is to dissect the individual role of these endocannabinoids in CB_1 mediated signaling. Adding complexity to this topic, effects like catalepsy were reported after intravenous AEA administration in male CB_1/CB_2 receptor deficient mice ($Cnr1^{-/-}/Cnr2^{-/-}$) providing an evidence that some effect of Martin's triad could be mediated by activation of other kind of receptor than CBs.[157] Despite the induction of some CB_1 mediated neurological effects by administration of exogenous CB_1 agonists could be useful for the treatment of chronic pain, emesis and

anorexia, the occurrence of a number of undesirable side effects such as locomotor or cognitive impairments limits the clinical utility of these compounds as therapeutic agents.[131] In the same way, the exogenous administration of CB_1 agonist induce an unselective CB_1 activation across brain regions so that these agents cannot be used as pharmacological tools to unveil the individual physiological role of AEA and 2-AG in the endocannabinoid system framework. Since *in vivo* administration of AEA[157,158,159,160] and 2-AG as therapeutic agents are hampered by their fast hydrolytic bio-inactivation,[160] inhibitors of AEA and 2-AG degradation offers a potential alternative strategy to stimulate in a more physiological way the endocannabinoid system.[131] Despite a significant number of FAAH inhibitors have been developed, [161] MAGL inhibitors have lagged historically. Considering that 2-AG has been proposed as the true physiological endogenous ligand for CBs receptors,[124,137] it is easy to understand how the development of a selective inhibitor of MAGL could be useful not only to obtain a more effective pharmacological manipulation of endocannabinoid neurotransmission but also to dissect the overlapping effects of AEA and 2-AG signaling.[123] Because most of known MAGL inhibitors lack either potency and/or selectivity towards FAAH or other hydrolase, new selective MAGL inhibitors are required to allow the therapeutic exploitation of MAGL enzyme and to specifically investigate the 2-AG dependent signaling in the brain.

Moreover, Nomura K. and coworker (2010) have recently reported a MAGL overexpression in many kinds of cancer cells that seems correlated with an increased production of FFA (Free Fatty Acids) inside them. [162] Since increased levels of FFA are believed to promote cancer cells migration, survival and *in vivo* tumor growth, selective and potent MAGL inhibitors could be useful also to develop new anti-cancer drugs based on a completely new action mechanism.

3.1.5 MAGL inhibition strategies

As previously reported in Chapter 1.1.1 of this thesis, a covalent binding inhibition mechanism often provide high pharmacological potency also to ligands not properly structurally optimized for the receptor fitting. In this way, a large number of covalent reactive non-optimized "hit compounds" for a given biological target can be easily discovered and quickly submitted to further structural refinement studies. Thus, covalent modifiers might be helpful to quickly overcome the historical lack of highly potent and selective MAGL inhibitors.

MAGL covalent inhibitors reported in the literature can be classified on the base of their preferred targeted residues. These compounds can alternatively bind:

1. the catalytic triad residues (Ser122-His269-Asp239: red circled in figure 3.7) within the MAGL active site, [131,141,145,151,165]
2. the cysteine residues Cys242 and/or Cys201 (yellow circled in figure 3.7) located close to Ser122 in the active site or in the vicinity of the putative glycerol exit hole, respectively, [145,149]
3. The cysteine residues Cys242 (yellow circled in figure 3.7) and/or Cys208 (green circled in figure 3.7) located close to Ser122 or at the entrance of the wide liphophilic active site entrance tunnel, respectively.[33,32, 149,179.]

While compounds that target the catalytic triad residues act directly disrupting the activity of Ser122, the mechanism through remaining cysteine trapping agents inhibit MAGL is not so easy to understand. On the base of the mutual position of cysteine residues respect to catalytic active Ser112, it was proposed that covalent inhibitors that bind Cys242 or Cys201 could disrupt the enzymatic activity of MAGL hindering the active site or the putative glycerol exit hole, respectively.[149] In this way, compounds able to bind Cys242 or

Cys201could decrease the MAGL activity hampering the access of 2-AG or the fast exiting of cleaved glycerol to the active site.[149] On the other hand, compound able to selectively bind Cys208 wouldn't be able to directly modify the active site environment. After their covalent binding, they could hamper the substrate access to active site hindering the main liphophilic tunnel entrance. Otherwise, they could allosterically modulate the hydrolytic activity of MAGL,[147] perhaps hampering the postulated "interfacial activation" of MAGL provided by cap domain conformation changes.

3.2 Covalent MAGL inhibitors

Another classification of available covalent MAGL inhibitors can be carried out considering the reversibility of established inhibitor-enzyme interaction. Generally, covalent and non-covalent interactions concur to define both binding affinity and reversibility of a given inhibitor. On the other hand, considering that for a covalent modifier the largest part of binding energy are from the covalent bond formation, the reversibility of MAGL inhibition provided by these compounds mainly depend to the chemical and biological stability of established covalent interactions. In this way, among described inhibitors, alkylating agents form the most stable covalent interaction and can be always considered as irreversible inhibitors. Carbamoylating agents bind MAGL forming middle-range stable covalent bonds and provide MAGL inhibition that range from irreversible (at least from a pharmacological point of view) to partially reversible. Finally, despite disulfide bond forming agents and acylating agents should form the most easily breakable covalent interactions from a chemical and biological point of view, the reversibility of their action can easily range from irreversible to completely reversible, dependently to the macro or micro environment in which their respective covalent interactions take place. The reversibility of covalent interaction of THL (**55**, Orlistat ®, Figure 1.4) toward human pancreatic lipase (hPL) and human pancreatic carboxyl-ester lipase (hCEL) could represent a good example of how much the environment impacts on the stability of neo-formed acylated residues. Indeed, it was reported that THL is able to acylate the catalytic serine residue in the active sites of both enzymes,[163] but a covalent irreversible inhibition was reported only for hPL,[20] because of the hydrolytic instability of esterified serine within the hCEL active site.[163]

3.2.1 Reversible MAGL inhibitors

To date, only β-lactone OMDM169 (**124**, Figure 3.8) has been reported as MAGL reversible inhibitor.[164] Despite this compound presents the same β-lactone warhead of the well-known and structurally similar covalent modifier THL (**55**, Orlistat ®, Figure 4.1),[20] the covalent binding mode of **124** toward MAGL wasn't investigated until now. In this way, **124** could interact with its target by a non-covalent as well as covalent reversible mechanism.

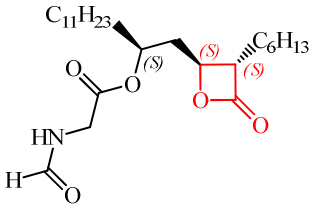

124, OMDM169

Figure 3.8. Structure of β-lactone OMDM169, the only putative covalent reversible MAGL inhibitor known until now.

It was reported that OMDM169 **124** *in vitro* inhibits MAGL and hPL at low μM concentrations without interact with other endocannabinoid system members (α-DAGL, FAAH and CB receptors). Intra-peritoneal *in vivo* administration of a dose as little as 2.5 mg/Kg of **124** was able to induce cannabinoid receptor-mediated antinociceptive effects *in vivo*.[164]

3.2.2 Irreversible MAGL inhibitors

Basing our classification of their inhibition mechanisms, two kinds of covalent irreversible MAGL inhibitors can be recognized. The first one is represented by compounds able to covalently bind MAGL catalytic Ser122, directly disrupting the MAGL hydrolytic activity. Among them,

despite these compounds provide the most affective MAGL inhibition, only few derivatives have shown high selectivity for the desired target. For instance, highly reactive serine-binding fluorophosphonates **125**-**130** or fluorosulphonates **131**-**133** (Table 3.1) are able to block MAGL activity with high potency[165] but are also able to inhibit other serine-dependent enzyme inside and outside the "endocannabinoids system" with comparable efficiency.

Warhead	R_1	R_2	Name	#	MAGL IC_{50} (nM)	FAAH IC_{50} (nM)	AchE IC_{50} (nM)	CB_1 IC_{50} (nM) *In vitro*
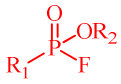	C_8H_{17}	Me	MOFP	**125**	3.0±02[166]	0.79±0.15[166]	N/A	N/A
	C_8H_{17}	Et	EOFP	**126**	3.0±07[166]	0.60±0.05[170]	120±7[170]	11000±5000[167]
	$C_{12}H_{25}$	Me	O-1778	**127**	N/A	3.0±02[168]	N/A	N/A
	$C_{12}H_{25}$	*i*-Pr	IDFP	**128**	0.76±0.33[166]	2[169]	N/A	1.8±0.8[169]
	$C_{20}H_{41}$	Me	O-1624	**129**	N/A	137±22[168]	N/A	N/A
	$C_{20}H_{33}$ (arachidonyl)	Me	MAFP	**130**	22±0.3[a]	0.10±0.02[170]	124±17[170]	530±130[167]
	C_8H_{17}	/	OSF	**131**	140±2[166]	1.9±0.2[166]	>500.000[170]	1300±300
	$C_{12}H_{25}$	/	N/A	**132**	200±75[166]	2[170]	N/A	6.9±3.6[169]
	$C_{20}H_{33}$	/	N/A	**133**	N/A	N/A	N/A	304±23[171]

Table 3.1. *In vitro* inhibition of mMAGL, FAAH, AchE (acetylcholinesterase) enzymes and of mouse CB_1 receptor by different fluorophosphonate and fluorosulphonate agents. All inhibition values are indicated as Mean±SE (n=3-6). [a] rMAGL in vitro inhibition data from Saario S.M. *et al.*; *Biochem. Pharmacol.* **2004**, *67*, 1381–1387.

In vivo administration of fluorophosphonate like MAPF **130** induces an increasing of 2-AG endogenous levels in rat CNS by inhibition of MAGL[i] but, on the other hand, increases endogenous AEA levels too by FAAH inhibition. Moreover, it is reported that some agents like these can covalently bind CB_1 receptors acting as uncompetitive CB_1 inhibitors.[168]

This produces an undesirable complex pharmacological response from which is difficult to selectively define the 2-AG contribution to the observed biological effects. Furthermore, the ability of these fluorophosponate derivatives to inhibit multiple serine-dependent enzymes[ii] is often responsible to high off-target toxicity, sometimes so severe to kill the treated subject. For instance, probably by inhibition of NeuropathyTargetEsterase (NTE) enzyme in CNS, it is reported that mice acutely treated with IDFP die within 48h after treatment.[131]

Despite the low target selectivity shown by these labeling compounds does not allow their use as drugs and limit their use as pharmacological tools, their impressive MAGL inhibitory potency have induced many scientists to develop more druggable and specific serine-trapping agents.

Recently these efforts are results in a series of carbamoyltetrazoles and carbamates and that have shown to covalently inhibit hMAGL with high potency and with enhanced selectivity (Table 3.2).

---

i) These kinds of compounds are able to inhibit other 2-AG deactivating enzymes such as ABHD6. The contribution of this additive inhibition to the 2-AG levels in CNS is very little because 85% of 2-AG is metabolized mainly by membrane-associated MAGL (Blankman J. L. *et al.*; *Chem. Biol*. **2007**, *14*, 1347-1356).

ii) They also inhibit the Hormone Sensitive Lipase (HSL), the ether-lipid metabolic enzyme KIAA1363 and the Neuropathy Target Esterase (NTE) (Long, J.Z. *et al*.; *Proc Natl Acad Sci* **2009**,*106*(48), 20270-20275.).

#	Name	Structure	hMAGL IC_{50} (nM)	Irrev. inhibition	Specificity for MAGL inhibition
134	LY2318912[176]	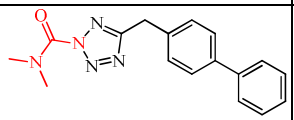	0.9	NO[172]	N/A
135	LY2183240[173]	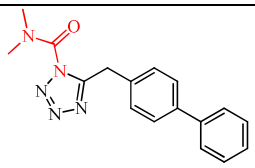	5.3	YES	NO
136	WWL152 (R_1=F)[131] WWL162 (R_1=Ome)[131]	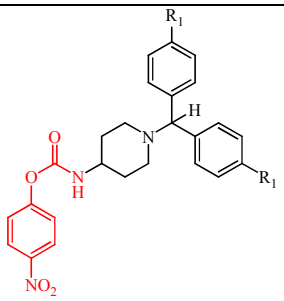	N/A	N/A	Partial (ABHD6 inhibition)
137	N/A[174]	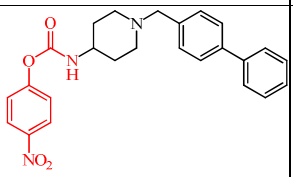	15	N/A[a]	YES
138	JZL175[131]	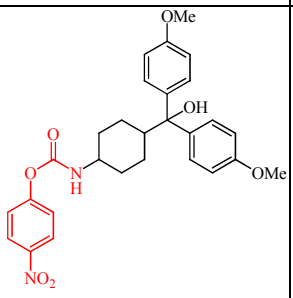	N/A	YES	YES

139	JZL184[131]	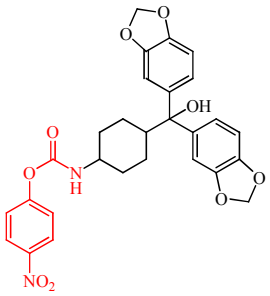	8	YES	YES (very high)

Table 3.2. *In* vitro potency of most selective irreversible MAGL serine-trapping inhibitors. [a] Covalent modification of MAGL was only hypothesized for this compound on the base of observed covalent binding of MAGL shown by other carbamates with similar structure[141]

Among them, JZL184 (**139**, Table 3.2) has shown the best potency/selectivity profile. It irreversibly inhibits MAGL and FAAH with IC_{50} values of 8 nM and 4 μM respectively.[141] It was reported that *in vivo* administration of **139** increases 2-AG levels in mice CNS by covalent irreversible MAGL inhibition without significantly interact with other component of "endocannabinoids systems".[131] When administered in mice, **139** evoke a clinically useful strong and prolonged analgesia but some side effects like hypomotility and hypothermia were also observed. Noteworthy, no catalepsy was detected in mice treated by **139** so to prove the ability of these compounds to evoke only a specific subset of Martin's tetrad responses.[131,141]

The second kind of covalent irreversible MAGL inhibitor is represented by compounds able to indirectly disrupt the MAGL hydrolytic activity, covalently binding critical cysteine residues that, even if not directly involved in the catalytic hydrolysis mechanism,[172] may exert a regulatory effect on MAGL catalytic activity. [175] *N*-substituted maleimides represent a good example of irreversible cysteine-trapping MAGL inhibitors. These molecules present a lipophilic portion linked to a heterocyclic warhead characterized by the presence of a broadly conjugate double bond that act as a highly activated Michael

acceptor system (Scheme 3.2). The *in vitro* inhibition potency of these compounds against rMAGL increases as lipophilicity increases and *N*-arachidonylmaleimide (**140**, NAM, Scheme 3.2) was found the most potent compound with IC_{50} magnitude in the range of nM.

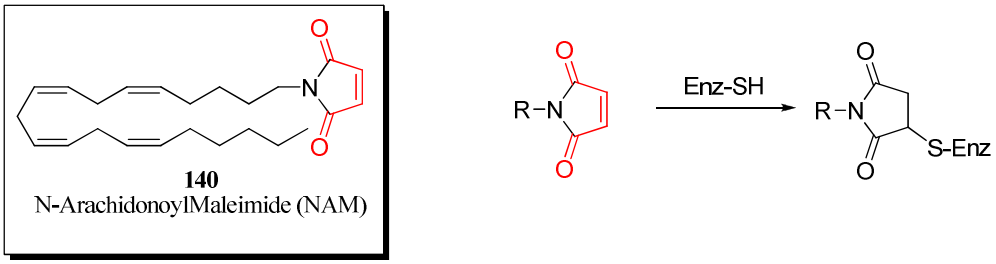

Scheme 3.2. Michael addition of Cys201 or Cys242 of MAGL to the conjugated carbon-carbon double bond of NAM **140**

Several *in vitro* studies have shown that **140** covalently inhibits hMAGL through an irreversible Michael addition of Cys201 (or Cys242 as secondary target),[147] without exerting any trapping activity toward the catalytic triad at tested concentrations (the latter finding has been reported for rMAGL).[145] The importance of Cys201 and Cys242 for NAM inhibitory binding on hMAGL was confirmed by glycine-scanning[175] and alanine-scanning[147] based mutagenesis independent studies. On the other hand, since only alkylated Cys208 (22-26% of alkylation degree) and Cys242 (74-78% of alkylation degree) residues were detected inside of tryptic fragments of rMAGL (wild type)incubated with NAM, [176] the exact identity of cysteine residues targeted by this compound is still debated. Even if the MAGL inhibition provided by NAM cannot be addressed to direct disruption of Ser-Hys-Asp triad catalytic activity, it could be alternatively explained by several other mechanisms. Dependently to the kind of bound cysteine residue, NAM could act a) obstructing the lipophilic tunnel that allow to 2-AG to reach the active site of the enzyme (binding of Cys208), b) obstructing the putative glycerol narrow hole that allow to glycerol to exit from the active site

once cleaved (binding of Cys201), c) sterically hindering the active site so to prevent the contact between catalytic Ser122 and the endogenous substrate (binding of Cys242). Despite its *in vitro* potency, *in vivo* administration of NAM does not produce any observable cannabinoid effects belonging to the Martin's tetrad. On the other hand, it was reported that *in vivo* intra-peritoneal NAM/2-AG mixed administration in mice induce a complete expression of Martin's tetrad responses. This "permissive" effect exerted by NAM about exogenous administration of 2-AG, normally hampered by short half-life of this endocannabinoid, was though due to a reduced 2-AG breakdown by covalent and irreversible MAGL inhibition.[177]

Among cysteine trapping inhibitors of MAGL, disulfiram (**68**, Scheme 1.8 and Figure 3.9) was reported able to in *vitro* potently inhibit MAGL (hMAGL IC_{50} ≈ 0.363 μM) by covalent binding of a not yet defined cysteine residue on the enzyme. The disulfidic nature of this covalent interaction was confirmed by the complete and dose-dependent reversibility of observed MAGL inhibition after addition of the reducing agent DTT. [178] The disulfiram analogue bis(4-methylpiperidinylthiocarbonyl)disulphide was recently reported able to selectively and irreversibly *in vitro* inhibit hMAGL (hMAGL IC_{50} ≈ 1.26 μM; hFAAH IC_{50} ≈ 363 μM) by formation of a covalent disulfide bond with Cys208 or Cys242.[33] Considering that also simple disulfides, bis(dialkylamino)disulfides and bis(alkylthiocarbonyl)disulfides were reported as *in vitro* MAGL potent inhibitor,[33] disulfide-containing molecules could represent a new promising class of irreversible, or at least partially reversible, cysteine trapping inhibitor of MAGL (Figure 3.9).

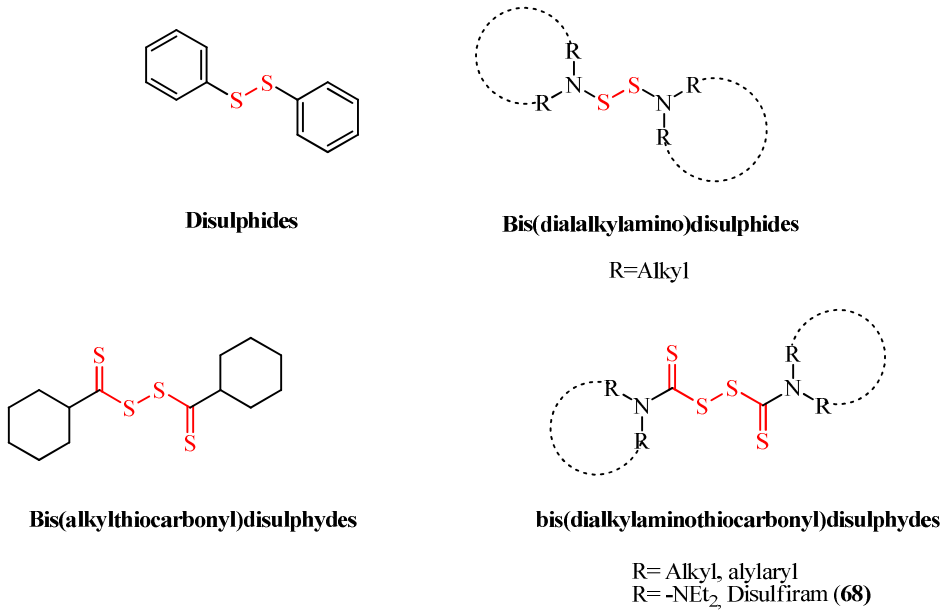

Figure 3.9. Overview of disulfide containing inhibitor of MAGL.

The high MAGL inhibitory potency and selectivity shown by some of covalent inhibitors described in this chapter make them excellent examples of selective labeling agents suitable for pharmacological investigation. On the other hand, their long-lasting inhibitory effect on MAGL could be detrimental for their clinical use because of eventually responsible of the occurrence of behavioral side effects.

Indeed, it is suggested that side effects like hypothermia and hypomotility induced by JZL184 administration would probably due to an over-physiological increase of 2-AG levels in the CNS resulting from prolonged irreversible block of MAGL.[141] In this way, these side effects could be pharmacologically uncoupled from beneficial one like analgesia by titrating the magnitude of *in vivo* MAGL inhibition.[141] In this way, reversible (Chapter 3.2.1) or partially reversible (Chapter 3.2.3) MAGL inhibitors like OMDM169 and isothiazol-3(2*H*)-one related compounds respectively could be useful to mildly modulate MAGL inhibition across brain regions. This mild approach could be helpful to

unveil physiological functions of 2-AG-dependent neurotransmission and to validate MAGL as a target for therapeutic drugs.

3.2.3 Partially reversible MAGL inhibitor

Only one class of covalent partially reversible MAGL inhibitors has been reported until now. This inhibitor class, recently discovered by Prof. Mor's research group, [179] is populated by disulfide-bond forming compounds such as isothiazol-3(*2H*)-one and benzo[d]isothiazol-3(*2H*)-one derivatives. These compounds were discovered as "hit compounds" during the screening of a short panel of cysteine trapping derivatives toward recombinant rMAGL. These reactive molecules (Figure 3.10) were chosen to exert their cysteine trapping activity through different kind of reaction mechanisms like Michael addition, mixed disulfide formation and nucleophilic substitution.

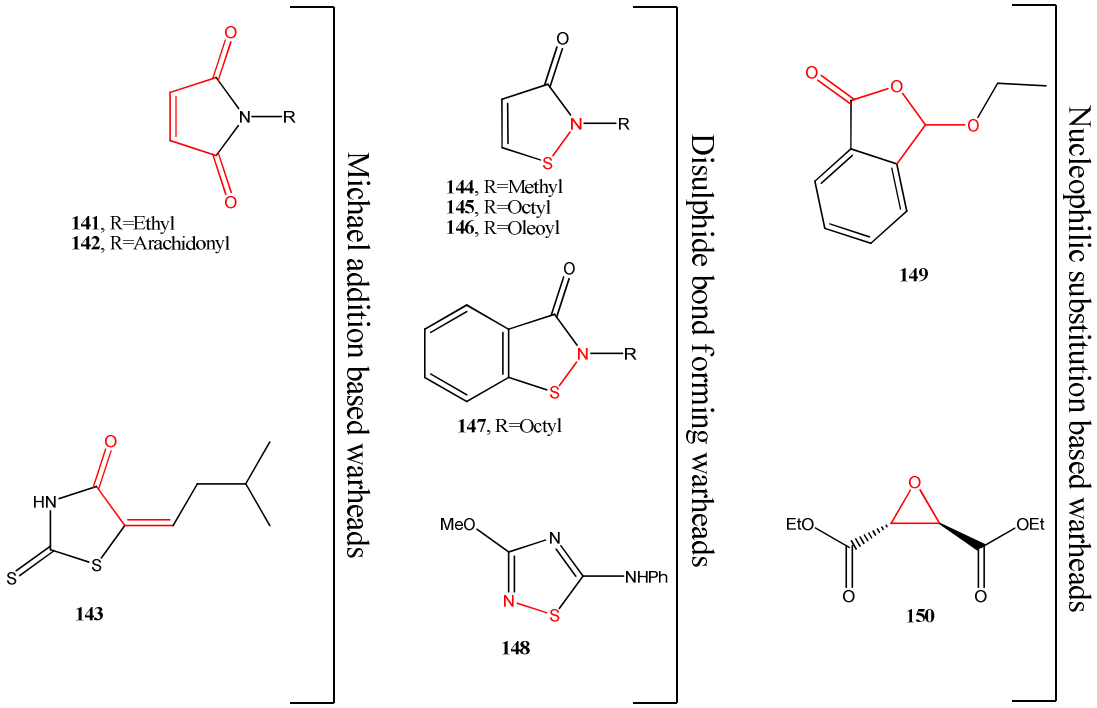

Figure 3.10. Red colored portions should be responsible of the cysteine related reactivity of depicted warheads.

Among them, except *N*-substituted maleimides **142** and **143** that were used by authors as reference standards for MAGL irreversible inhibition evaluation, only isothiazol-3(2*H*)-one and benzo[d]isothiazol-3(2*H*)-one derivatives have been shown to potently *in vitro* inhibit rMAGL with IC_{50} values ranging from low μM to nM concentrations. In order to evaluate the reversibility of the MAGL inhibition provided by these agents, a rapid dilution assay [180] of rMAGL, pre-incubated with the isothiazol-3(2*H*)-one derivative ochtylinone **145,** has been carried out. Collected data indicates that MAGL was inhibited by ochtylinone **145** with a partially reversible mechanism (Figure 3.11)

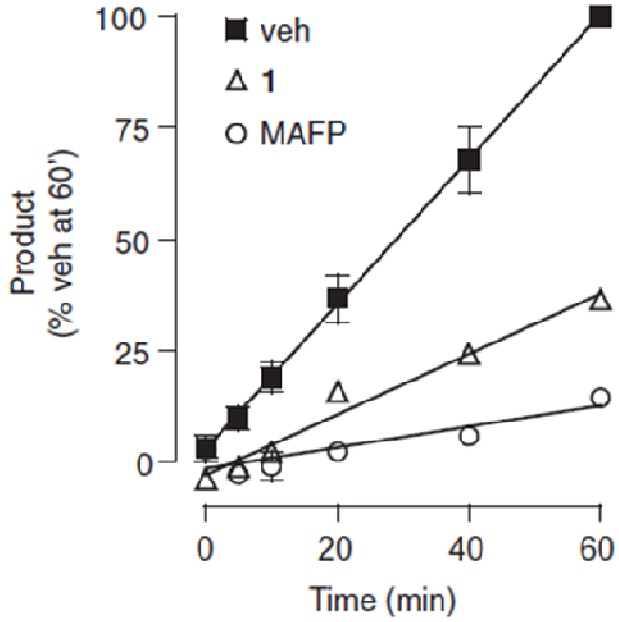

Figure 3.11. Reversibility of monoacylglycerol lipase (MAGL) inhibition by octhilinone. (A) Rapid dilution assays of purified MAGL in the presence of vehicle (dimethylsulphoxide, final concentration 2%), octhilinone or methyl arachidonylfluorophosphonate (MAFP). Results are expressed in percentage of product generated after a 60 min incubation with vehicle (mean ± SEM, n = 3).

A glycine scanning based mutagenesis study has suggested that their inhibition mechanism involve a covalent interaction between the sulfenamidic system and the Cys208 residue of MAGL (Figure 3.12).

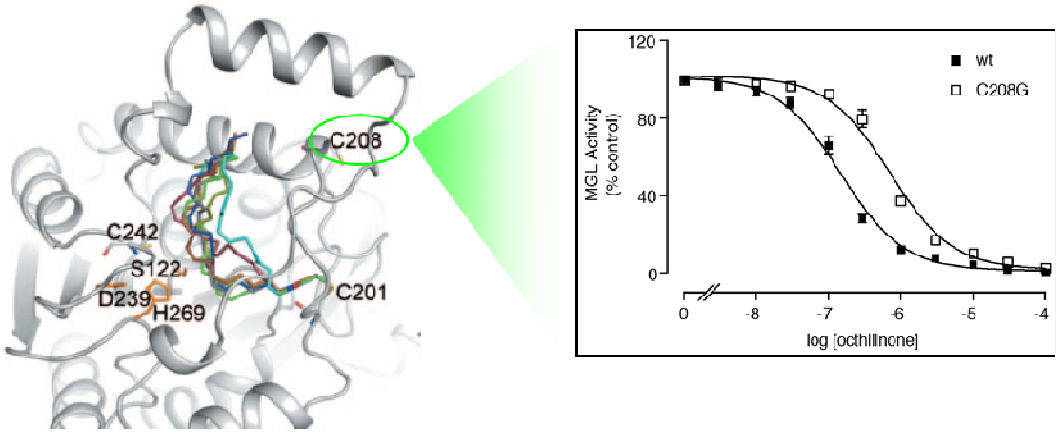

Figure 3.12. Concentration-response curves for the inhibition of MAGL activity by octhilinone in wild-type MAGL (wtMAGL) and C208G MAGL mutants. Results are expressed in percentage of control activity (dimethylsulphoxide, final concentration 1%) (mean ± SEM, n = 3–5).

It is proposed that this interaction takes place by a nucleophylic attach of Cys208 toward the sulfur atom of sulfenamidic system producing a subsequent nitrogen displacement[181] with formation of a mixed disulfide bond (Scheme 3.3).[175]

The proposed dependence of MAGL inhibition to the formation of a mixed disulfide bond rather than to a Michael addition of Cys208 to the isothiazol-3(2*H*)-one carbon-carbon double bond was in agreement with previous published results about reactivity of isothiazol-3(2*H*)-one warhead,[8] and it is also supported by two different experimental findings. The first one is represented by the observation of a 47-fold decreased inhibitory potency of ochtylinone **145** when rMAGL was incubated in absence or in presence of a low concentration of DTT. The second one is represented by the fact that 2-octyl benzo[d]isothiazol-3(2*H*)-one **147**, which cannot undergo Michael addition because of its conjugated

double bond is involved in benzene aromaticity, was as potent as ochtilinone **145** to inhibit MAGL activity.

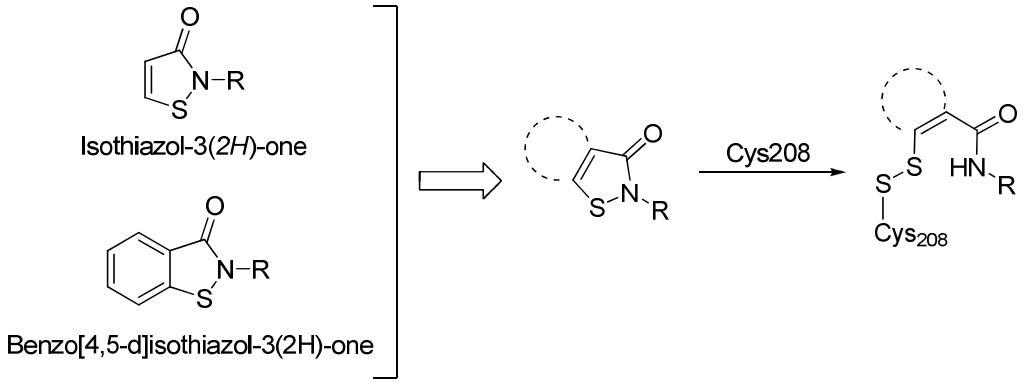

Scheme 3.3. Hypothesized cysteine trapping dependent inhibition mechanism of MAGL provided by isothiazol-3(*2H*)-one and benzo[d]isothiazol-3(*2H*)-one derivatives.

Further information about the reactivity these sulfenamidic warheads, their cysteine trapping related toxicity and their uses in medicinal chemistry are already reported in Chapter 1.2.1 of this PhD thesis.

3.3 Synthesized MAGL inhibitors

3.3.1 Aim of the work

Discovery of isothiazol-3(2*H*)-one and benzo[d]isothiazol-3(2*H*)-one derivatives as hit compounds for MAGL inhibition has provided the fundamentals for the development of new potent and partially reversible MAGL inhibitors. Like for other covalent modifier, the targeting of Cys208 on MAGL provide to these compounds a high binding affinity for the target that does not depend so much to a proper receptor fitting. The resulting high basal biological activity, represents a good starting point to set up a SAR study. Indeed, the establishment of a stable covalent bond between the target and tested compounds allows to freely expand the diversity of decorating groups around the warhead core with reduced risk of binding loss. In this way, the diversity of decorating group around the isothiazol-3(2*H*)-one and benzo[d]isothiazol-3(2*H*)-one warhead was expanded in order to:

1. explore the pharmacophoric space around the targeted Cys208 to enhance the selectivity of designed inhibitors for MAGL versus other hydrolytic enzymes (e.g. FAHH);

2. modulate the reactivity of the considered sulfenamidic warheads to optimize their druggability and to achieve a better activity/toxicity ratio.

Hypothesizing that the partial reversible character of MAGL inhibition shown by ochtilinone (**145**, Figure 3.10) could be a common feature of isothiazol-3(2*H*)-one and benzo[d]isothiazol-3(2*H*)-one based compounds, the use of these kind of warheads for the development of new partially reversible inhibitors of MAGL could provide a new and

more physiological way to increase 2-AG levels in CNS without induce unwanted side effects like those observed after JZL184 administration.

In this way, several compounds sharing a common structure motif were designed. They were characterized by the presence of (figure 3.13):

- a driver group (green colored) lipophilic enough to assure a good basal affinity for the enzyme to the synthesized compounds. This portion is also designed to modulate the reactivity of sulfenamidic warhead through a differential contribution to its electronic distribution.
- an isothiazol-3(*2H*)-one and benzo[d]isothiazol-3(*2H*)-one based cysteine-reactive warhead (red colored) linked to the lipophilic driver group R.

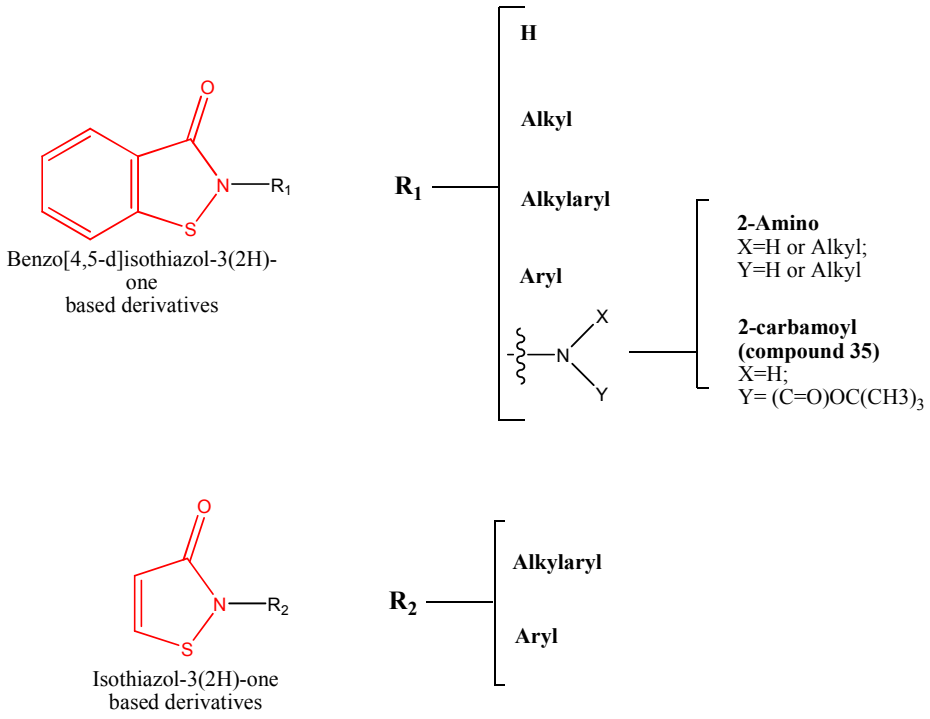

Figure 3.13. Overviev of synthesized cysteine-reactive compounds.

In order to evaluate the impact of a modified receptor fitting on the MAGL inhibition potency, the structure of the driver group of compounds sharing a common kind of warhead was broadly changed.

However, the inhibition potency and specificity of these isothiazol-3(2*H*)-one and benzo[d]isothiazol-3(2*H*)-one derivatives may not only depend from the receptor fitting but they could be also affected by warhead's reactivity changes. Nevertheless, the sulfenamidic system reactivity may probably exert a not negligible impact on warhead's chemical or metabolic stability.

In order to study these dependencies, a preliminary panel of *N*-substituted benzo[d]isothiazol-3(2*H*)-ones was synthesized (Table 3.3).

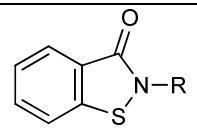

#	R	#	R	#	R	#	R
18		24	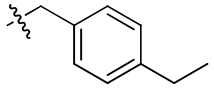	28	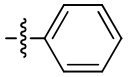	32	
19		25	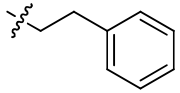	29	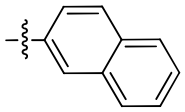	33	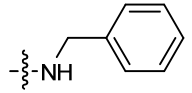
20	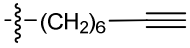	26	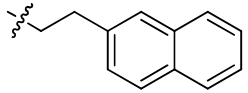	30	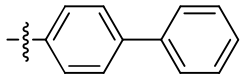	34	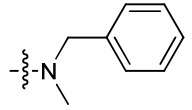
21	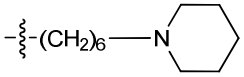	27	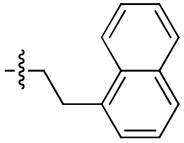	31	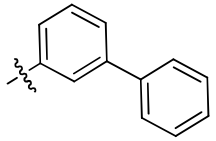	35	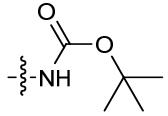
22	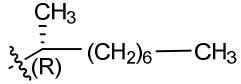	13	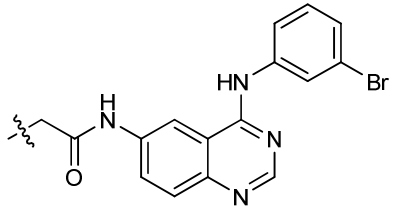				
23	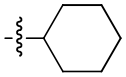						

Table 3.3. Synthesized benzo[d]isothiazol-3(*2H*)-one based MAGL inhibitors.

A brief look-over to the just reported summarizing table (Table 3.3) easily shows that this preliminary panel of synthesized compounds is characterized by the same structurally conserved benzo[d]isothiazol-3(2*H*)-one warhead. Despite this, these compounds should not possess the same chemical reactivity because of different steric hindrance and of electronic inductive effects exerted by the N-substituent "R" on the nitrogen atom of sulfenamidic system. Five different subsets of compounds should share similar warhead reactivity:

- *Cluster 1*: 2-alkyl and 2-alkylaryl derivatives belong to this cluster. Alkyl and alkylaryl substituents should exert the same inductive effect on sulfenamidic nitrogen so to confer to these compounds a similar warhead reactivity.
- Cluster 2: only 2-aryl derivatives populate this cluster. The direct conjugation of the aryl substituent to the sulfenamidic nitrogen lone pair should exert an electron withdrawing effect on the sulfenamidic system, probably increasing its reactivity toward nucleophils. This "activating" effect has been previously reported for *N*-arylpyrido[5,4-b]isothiazol-3(2*H*)-ones , where it was proposed to be responsible of metabolic instability.[182]
- Cluster 3: 2-amino derivatives populate this cluster. In these compounds the amino group at 2 position should exert an electron withdrawing effect on the sulfenamidic system increasing its reactivity toward nucleophils. Notably, the exocyclic nitrogen of these compounds could enhance the water solubility of these derivatives and it could be protonated under acidic conditions. The latter occurrence could enormously increase the electron withdrawal effect of exocyclic nitrogen on sulfenamidic system, overactivating it. For this reason, these clusters could collect high cysteine reactive derivatives.

- Cluster 4: only compound **35** populate this cluster (Table 3.3 and Figure 3.14). It should possess the strongest warhead reactivity among synthesized compound (at least in neutral conditions) because of the high electronic shortage of carbamoylated exocyclic nitrogen. Despite its structure seems close to those of "Cluster 3" members this compound cannot be grouped with them mainly because the carbamoyl moiety presence. This fragment could act as a serine trapping warhead so to make this compound able to bind multiple residues on MAGL.

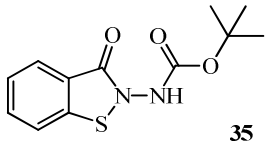

35

Figure 3.14. Structure of carbamate **35**

- Cluster 5: only compound **18** populate this cluster. Compound **18** should differ from all other synthesized compounds in term of reactivity because of the unsubstituted nitrogen atom on the benzisothiazol-3(*2H*)-onic structure. Lack of bulky "R" substituents on sulfenamidic nitrogen probably decreases the binding specificity of compound **18** toward MAGL but, in the same time, allows the existence of a prototropic equilibrium between the nitrogen and the oxygen atoms of isothiazol-3-onic warhead portion. [183] This hydrogen transfer induces the isothiazol-3-onic system aromatization and produces a fully aromatized 3-hydroxybenzisothiazole **151** (Scheme 3.4).

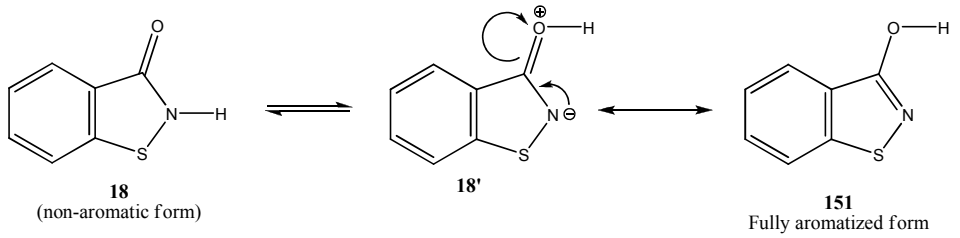

Scheme 3.4. The prototropic equilibrium of isothiazol-3-onic portion of benzisothiazol-3(2*H*)-one **18**.

In this form, the sulfenamidic system should not present any reactivity toward nucleophiles. Indeed, the S-N bond cleavage induced by a nucleophilic attack on 3-hydroxybenzisothiazole sulfur atom is unfavored in this molecule because it would lead to the disruption of heterocyclic system aromaticity. Thus, compound **17** should be less reactive that other synthesized *N*-substituted compounds, presenting a better chemical and/or metabolic stability.

Considering that members of each described cluster share a common reactivity, each biological activity variations detected among compounds belonging the same cluster should be only dependent to receptor fitting changes induced by driver portion structural changes. In this way, the contribution of lipophilicity of "R" driver group to the observed MAGL inhibition could be roughly evaluated comparing the biological activities shown by compounds belonging to the "Cluster 1" (table 3.4, all compounds). In the same way, differences in the observed inhibitory potency of these derivatives could provide information about the tolerability of a steric hindrance in α position to the sulfenamidic nitrogen (Table 3.4, compounds **20**, **22**, **23**) or about a different positioning of the hindering aromatic systems in these molecules (Table 3.4, compounds **13**, **24-27**).

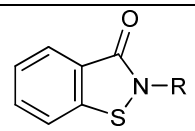

#	R	#	R
19		**24**	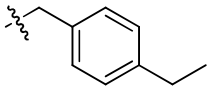
20	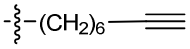	**25**	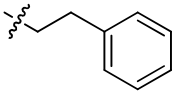
22	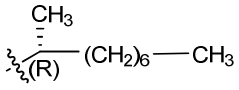	**26**	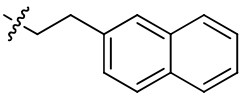
23	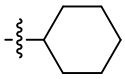	**27**	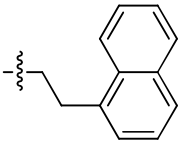
21	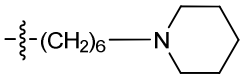	**13**	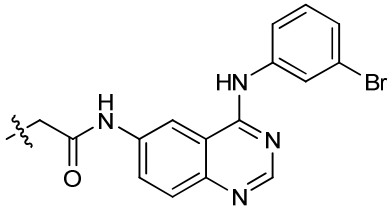

Table 3.4. Structural comparison of driver groups possessed by members of cluster 1.

Similar considerations can be done for compounds belonging clusters 2 and 3. In this way, compounds **28-31** could provide information about the influence of the presence of different shaped aromatic systems (Table 3.5-A, all compounds) or about the tolerability of a steric hindrance in α position to the sulfenamidic nitrogen (Table 3.5-B, all compounds).

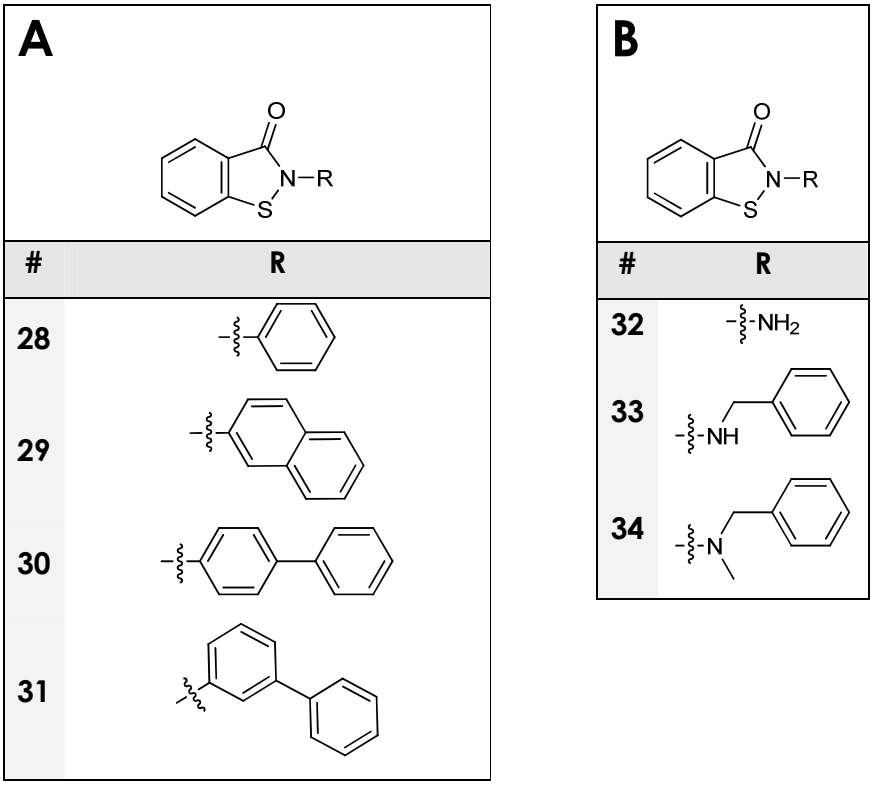

Table 3.5. Structural comparison of members belonging to A) cluster 1 and B) cluster 2.

On the other hand, compounds that possess different warhead reactivity but that share a similar driving portion structure can be grouped performing an orthogonal clustering process. For instance, some 2-aryl (compounds **19** and **22-24**) and 2-amino derivatives (compounds **28** and **32-34**) possess similar topological features but different warhead reactivity because of the different electron inductive effect provided by their driver groups (Table 3.6). A comparison of MAGL inhibitory potency values furnished by these compounds could define the contribution of the covalent warhead reactivity to the observed biological activity of these derivatives.

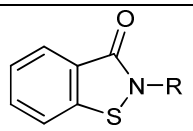

#	R	#	R
19		**32**	
23	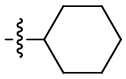	**28**	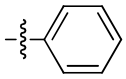
24	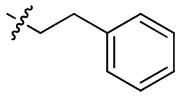	**33**	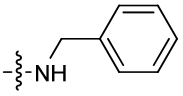
22	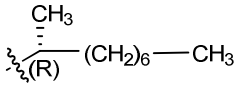	**34**	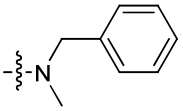

Table 3.6. Structural comparison of MAGL inhibitors possessing topologically similar driver group and different warhead reactivity (differential driver group contribution). Listed compound are member of clusters 1-3.

With the same strategy in mind, in order to evaluate if the reactivity of isothiazol-3(*2H*)-one and benzo[d]isothiazol-3(*2H*)-one warhead would differently contributes to the observed biological activity, some isothiazol-3(*2H*)-one derivatives (**36** and **37**) were also designed and synthesized. The compared structures are reported in Table 3.7.

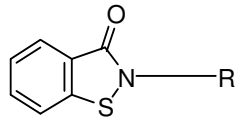		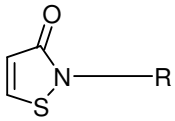	
#	**R**	**#**	**R**
24	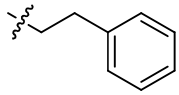	**36**	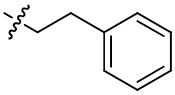
30	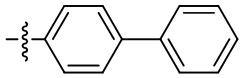	**37**	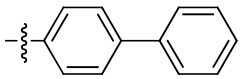

Table 3.7. Structural comparison of MAGL inhibitors possessing topologically similar driver group and different warhead reactivity (different warhead type).

Finally, in order to understand if the cysteine-trapping activity could be a fundamental requirement for the MAGL inhibition exerted by designed benzo[d]isothiazol-3(2*H*)-one-based compounds, two 3-alkyloxybenzo[d]isothiazoles (compounds **38** and **39**, Table 3.8), structurally very close to some previously shown 2-alkyl and 2-alkylaryl benzo[d]isothiazol-3(2*H*)-ones (compounds **19** and **26**, Table 3.8), were synthesized. The compared structures are reported in Table 3.8.

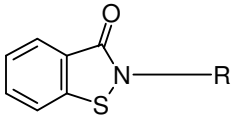		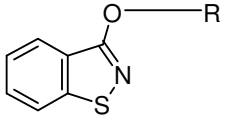	
#	**R**	**#**	**R**
19	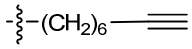	**38**	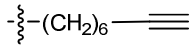
26	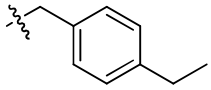	**39**	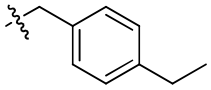

Table 3.8. Structural comparison of MAGL inhibitors possessing topologically similar driver group and different warhead reactivity (different warhead type).

For the same reasons considered for the aromatized form **151** of compound **18**, compounds **38** and **39** should be inactive as cysteine-

trapping agents because of their stable and fully aromatized heterocyclic warhead.

If this kind of compounds will result active as MAGL inhibitors, the cysteine-trapping feature possessed by tested benzo[d]isothiazol-3(*2H*)-one derivatives cannot be defined as "essential" for MAGL inhibition anymore. In this case, an alternative non-covalent MAGL inhibition mechanism will be proposed to explain the collected experimental data about this compound class.

3.3.2 Chemistry

Except for the purchased unsubstituted benzo[d]isothiazol-3(*2H*)-one **18** and for EGFR inhibitor **13** (see Chapter 2.3.2), all synthesized compounds were prepared following five different synthetic strategies that are summarized in Table 3.9. The synthetic route used to synthesize compound **13** was already reported in Chapter 2.3.2.

Strategy Code	Strategies overview
A	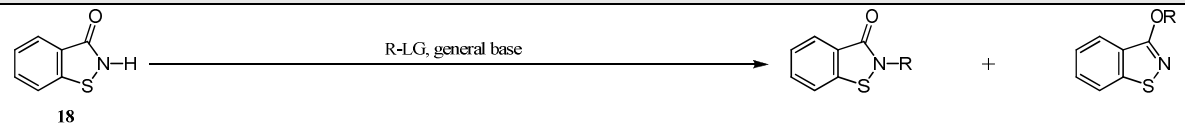
B	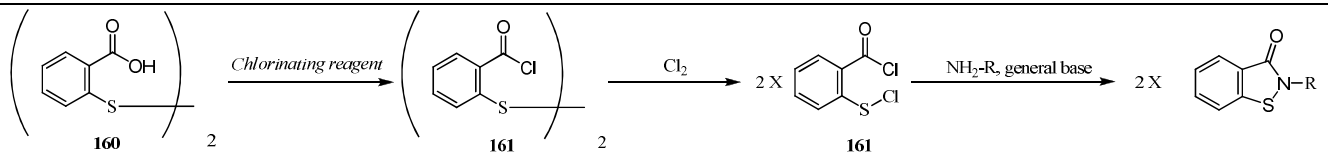
C	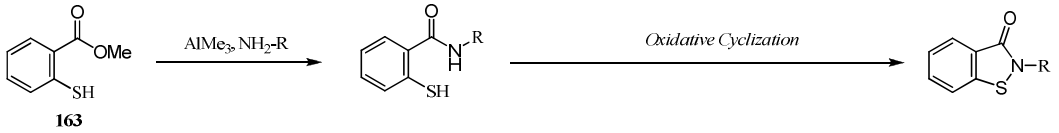
D	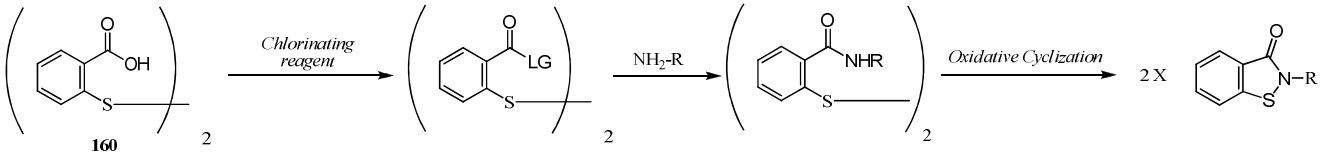
E	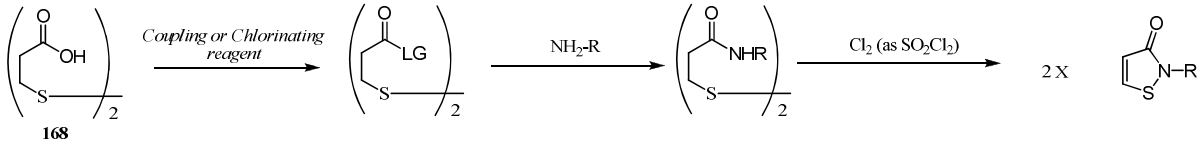

Table 3.9. Synthetic strategies overview.

Except for strategies **A** and **B**,[110] all other synthetic strategies were based on the activation of carboxylic moiety of the commercially available starting materials to produce isolable amides that were subsequently oxidatively cyclized to obtain the desired warhead portion. Strategies **A** and **B**, indeed, did not allow the isolation of any stable intermediate and produced desired *N*-alkylated products from commercially available precursors by a one-pot procedure (except for compound **21**). On the other hand, even the **D** strategy allowed the isolation and the purification of amidic intermediates, using I_2/Et_3N mixture as the oxidative cyclization agent [184] a one-pot and very effective modification of this sequence was developed and applied during this PhD thesis. When not commercially available, drivers groups were synthesized through properly designed synthetic routes.

Final compounds **19**, **20**, **21**, **24**, **38** and **39** (boxed in scheme 3.5) were synthesized following **A** strategy.

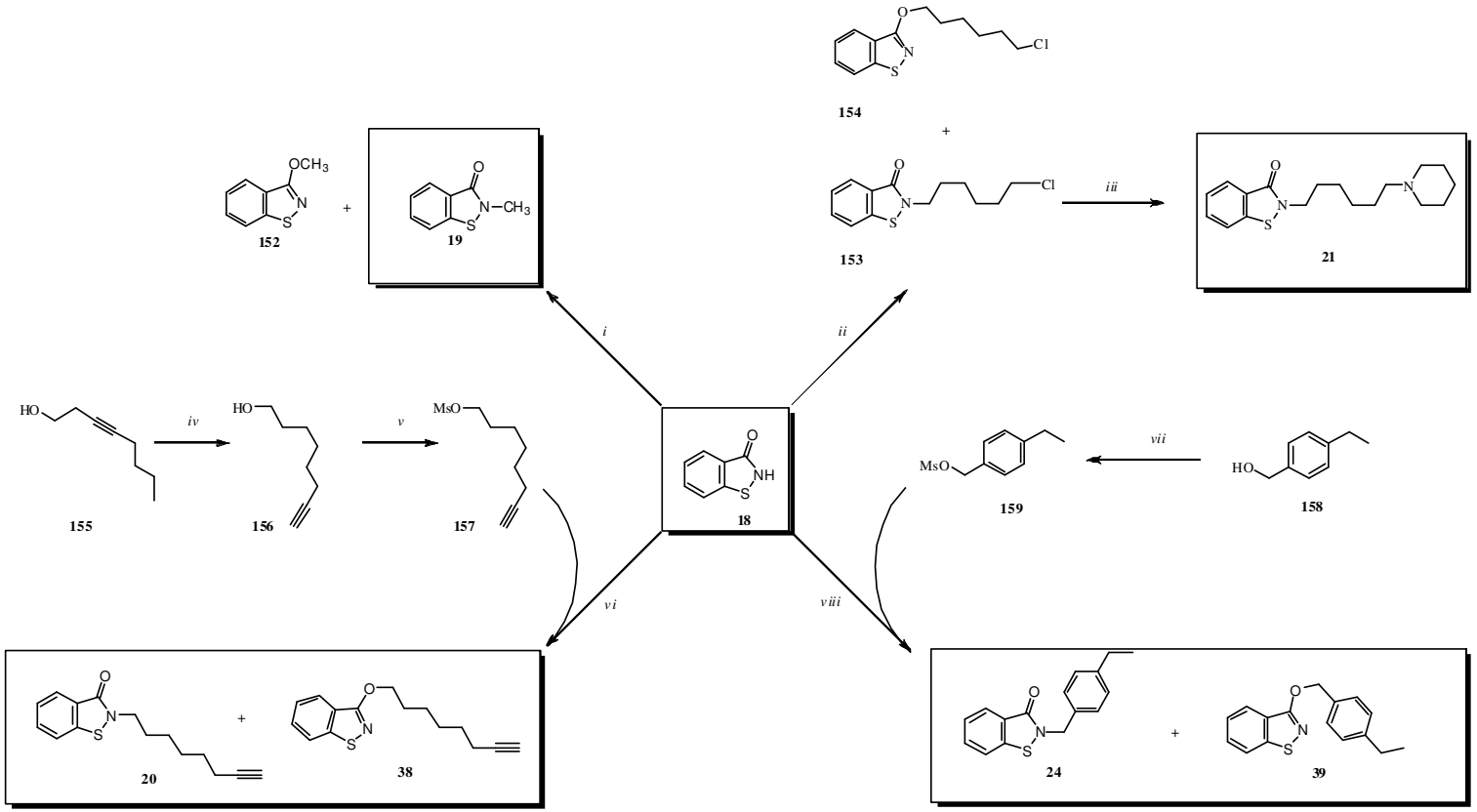

Scheme 3.5. Main synthetic scheme for compounds synthesized with method A. (i) CH_3I, K_2CO_3, KI, CH_3CN, RT; (ii) K_2CO_3, 1-chloro-6-Iodohexane, CH_3CN, RT; (iii) K_2CO_3, KI, piperidine, CH_3CN, 60°C; (iv) 1,2-ethylendiamine, NaH, RT 1h then 3-octyn-1-ole **155**, 65°C; (v) methanesulfonyl chloride, Et_3N, CH_2Cl_2, 0°C to R.T; (vi) K_2CO_3, CH_3CN, reflux, 1h; (vii) methanesulfonyl chloride, Et_3N, CH_2Cl_2, R.T; (viii) K_2CO_3, CH_3CN, reflux, 30 min.

Thus, they were synthesized by a simple nucleophilic substitution reaction between commercially available benzo[d]isothiazol-3(2*H*)-one **18** and a proper electrophilic side chain.[185] This reaction was carried out activating the benzo[d]isothiazol-3(2*H*)-one **18** in basic conditions so to *in situ* obtain the activated benzo[d]isothiazol-3(2*H*)-one nucleophilic salted form. Since a basic environment is required to deprotonate the nitrogen of benzo[d]isothiazol-3(2*H*)-one, because of occurrence of elimination side reactions, this synthetic strategy was not suitable to obtain final compounds in which aliphatic driver groups were joined to the heterocyclic warhead by a secondary carbon. While the electrophilic activated side chain of compound **153** was commercially available, side chains **156** and **158** were activated as reactive electrophiles by mesylation of the primary hydroxyl group[186] to obtain compounds **157** and **159**, respectively. p-ethylbenzylalcohol **158** was commercially available whereas the precursor **156** was synthesized by a contrathermodynamic isomerization of the commercially available internal alkynyl alcohol **155** following the methodology developed by Brown, C.A. and Yamashita, A.[187] Compound **153** was converted to final product **21** by a simple displacement of chlorine atom using piperidine as nucleophile species.[188,189]

Despite strategy **A** was resulted straightforward to quickly obtain several final compounds, the formation of O-alkylated side products, often present in 1:1 ratio with the desired product in the reaction mixture, was every time observed. Even if this occurrence was exploited in some case to obtain useful final compounds (like in the case of compounds **20**, **38**, **24**, **39**), the formation of these side products have lowered the yields of reactions carried out to specifically obtain *N*-alkylated final products (like in the case of compound **19** and **153**). In order to move around to this side reaction occurrence and to achieve a good synthetic

methodology for the preparation of *N*-aryl derivatives, other synthetic routes were carried out.

In this way, further *N*-alkyl and *N*-aryl benzo[d]isothiazol-3(2*H*)-one derivatives were synthesized using **B** strategy[110] using a very cheap commercially available starting material like dithiosalicylic acid **160**. This one-pot methodology has furnished desired products **25**,[42a] **26, 27** and **30** (boxed in scheme 3.6) very quickly but, unlike as reported in literature, with low reaction yields.

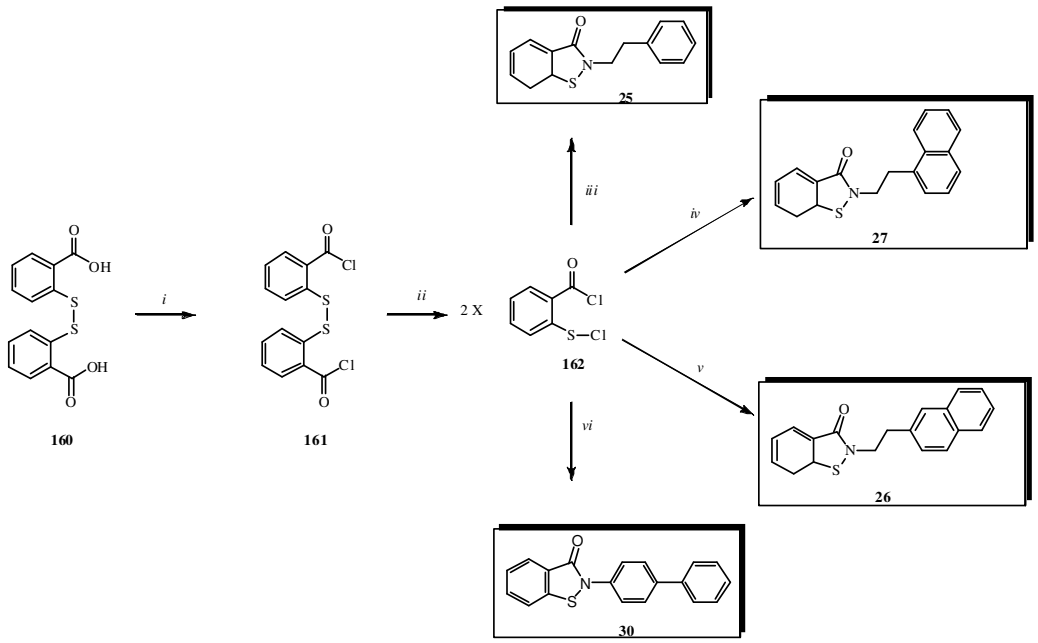

Scheme 3.6. Main synthetic scheme for compounds synthesized with method B. (i) $SOCl_2$, reflux, 3h; (ii) Cl_2, CCl_4, RT; (iii) 2-phenylethylamine, dry Et_3N, dry CH_2Cl_2, RT; (iv) 2-(napht-1-yl)ethylamine hydrochloride, dry Et_3N, dry CH_2Cl_2, RT; (v) 2-(napht-2-yl)ethylamine hydrochloride, dry Et_3N, dry CH_2Cl_2, RT; (vi) *p*-phenylaniline, dry Et_3N, dry CH_2Cl_2, RT

Considering the high toxicity of employed reagents, and the intrinsic instability of involved intermediates (intermediates **161** and **162**), this strategy was quickly abandoned in order to find a more safe and

effective synthetic strategy to obtain the remaining benzo[d]isothiazol-3(*2H*)-one derivatives.

In this way, final compound **28, 29** and **31** (boxed in scheme 3.7) were synthesized from commercially available compound **163** following the C strategy.[190] In this case, the amide coupling step is assisted by a strong Lewis acid like $AlMe_3$ affording the desired amides **164**-**166** with good yields. The final oxidative cyclization step was accomplished using an hypervalent-iodine species like phenyliodine bis(trifluoroacetate) (PIFA) leading to *N*-aryl final compounds **28**, **29** and **31** with good yields.

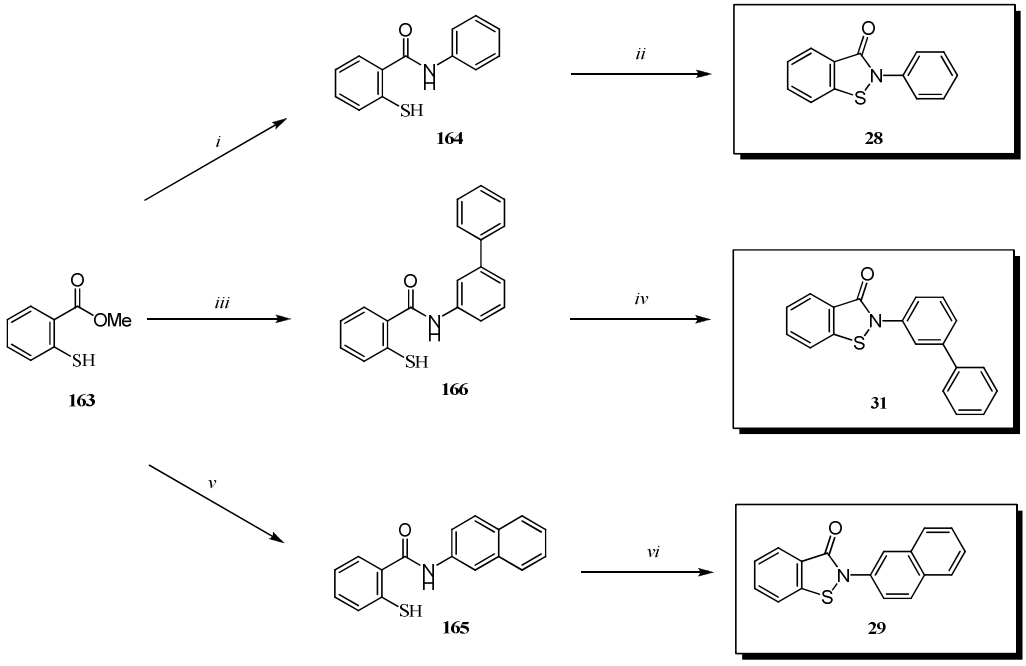

Scheme 3.7. Main synthetic scheme for compounds synthesized with method C. (i)Aniline, $Al(Me)_3$, dry CH_2Cl_2, 0°C to RT then compound **163**, reflux; (ii) PIFA, TFA, CH_2Cl_2, 0 °C; iii) *m*-phenylaniline, AlMe3, dry CH_2Cl_2, 0 °C to RT then compound **163**, reflux; (iv) PIFA, TFA, CH_2Cl_2, 0 °C; (v)β-naphylamine, $Al(Me)_3$, dry CH_2Cl_2, 0°C to RT then compound **163,** reflux; (vi) PIFA, TFA, CH_2Cl_2, 0 °C.

Despite the observed good yields, this approach wasn't completely satisfactory because of the intrinsic instability of commercial starting

material **163** as well as intermediates **164**, **165**, **166**. Indeed, they tend to form disulfides when exposed to air so to hamper their purification and characterization. Strategy D seems to overcome these troubles, providing a fast and effective way to access to the acid sensitive *N*-carbamoylmamino final compound **35** and to products like **22** and **23** (boxed in scheme 3.8).

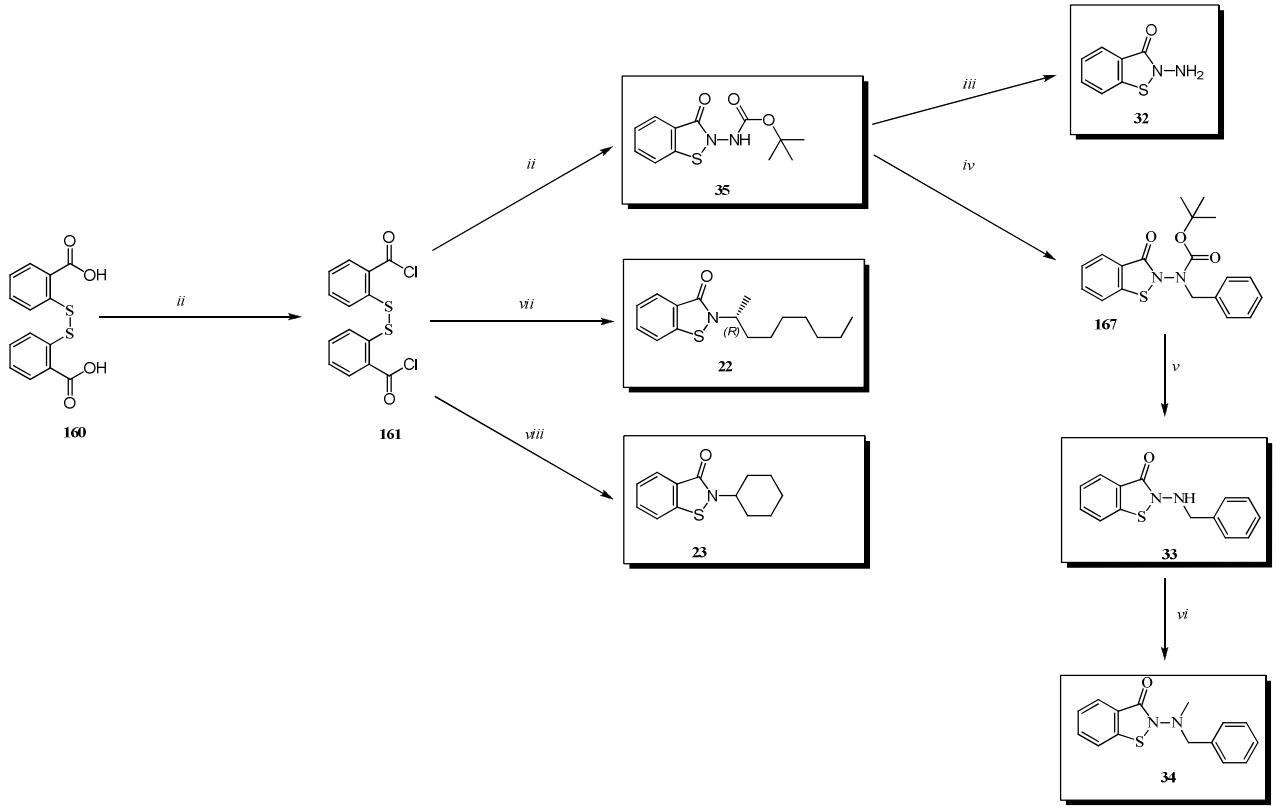

Scheme 3.8. Main synthetic scheme for compounds synthesized with method D. (i)$SOCl_2$, reflux; (ii) dry Et_3N, *t*-butylhydrazinecarboxylate, dry THF, 0°C to RT then I_2; (iii) TFA/H_2O 9/1, RT; (iv) Lithium hexamethyldisilazide (LiHMDS) 1.06M in dry THF, benzylbromide, dry THF, 0°C to RT; (v) trichloroacetic acid/H_2O 9/1, 0°C then RT; (vi) MeI, imidazole, RT; (vii) dry Et_3N, 2-aminononane, dry THF, 0°C to R.T then I_2; (viii) dry Et_3N, 2-aminocyclohexane, dry THF, 0°C to RT then I_2.

After the chlorinating conversion[110] of starting material **160** into the highly reactive acylchloride **161**, compounds **22**, **23** and **35** were obtained through an adaption of the procedure described by Kersting, B. and coworkers (1999).[184]

In this one-pot adaption, the obtained disulfide bis-amides (not shown in figure 3.8) were not isolated but directly cyclized in presence of Et_3N by addition of iodine as oxidizer. Despite the nearly complete conversion of bis-amides to desired products, accurate reaction yield estimations were done only for solid derivatives like **35** and **23**. Indeed, the purification of oily products like **22** was difficult and provided multiple fractions of desired product with different purity grades.

A simple *N*-Boc deprotection of compound **35** afforded the 2-amino final product **32** (boxed in scheme 3.8) whereas product **33** was obtained by benzylation[191] and subsequent *N*-Boc deprotection[43a] of carbamoylated nitrogen of compound **32**. Finally, final compound **34** (boxed in Scheme 3.8) was synthesized by a simple methylation of exocyclic nitrogen of product **33** in presence of non-nucleophilic weak bases like imidazole.

Despite the efficacy of strategy **D** to produce a large array of benzo[d]isothiazol-3(2*H*)-one derivatives, this approach was not applicable to the synthesis of isothiazol-3(2*H*)-one derivatives **38** and **39** (boxed in scheme 3.9). For this reason, all of them were synthesized following strategy **E**. The 3,3-dithiopropionic acid **168** was converted to the highly reactive acylchloride **162** by reflux in $SOCl_2$,[110] and coupled with the proper amine to give the bis-amide **170**. Alternatively, The 3,3-dithiopropionic acid **168** was directly converted in the bis-amide **172** using O-(benzotriazol-1-yl)-*N,N,N',N'*-tetramethyluronium hexafluorophosphate (HBTU) as coupling agent.[192] Then obtained bis-amides **170** and **172** were cyclized to final products **36** and **37** by addition of SO_2Cl_2, a chlorinating agent.[108]

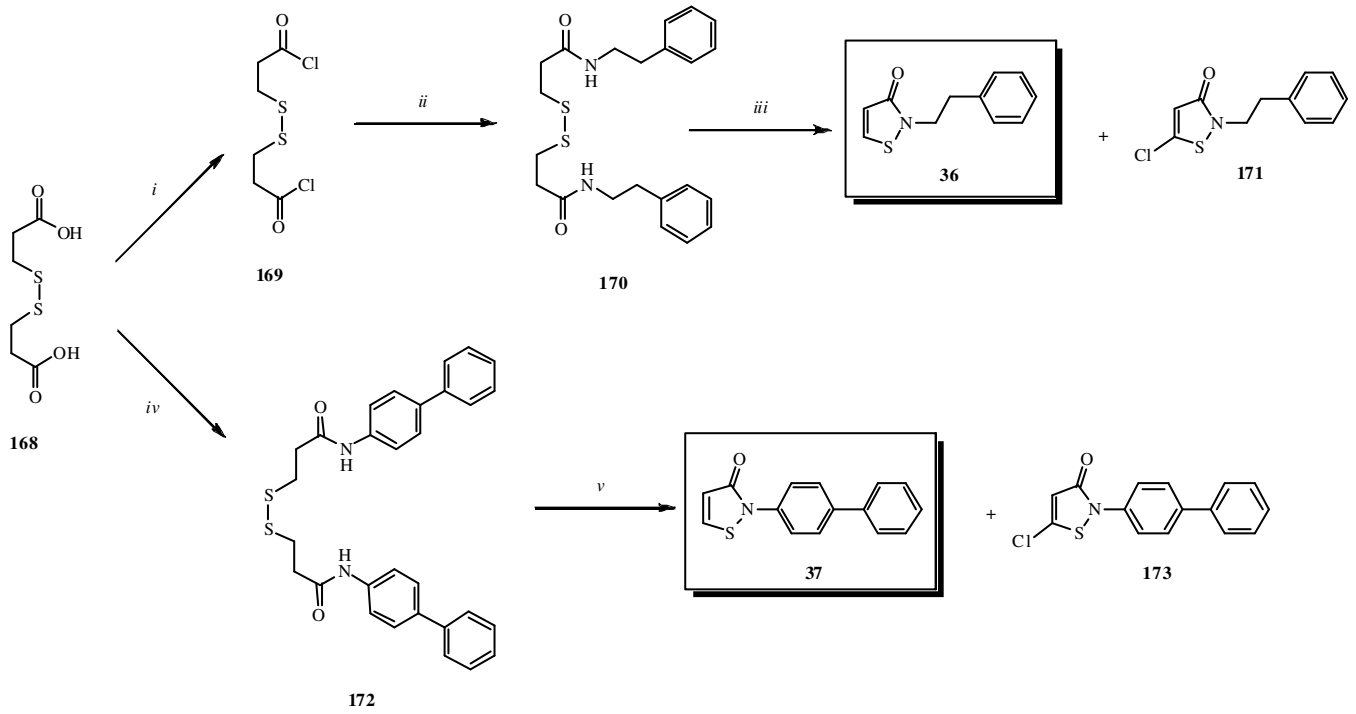

Scheme 3.9. Main synthetic scheme for compounds synthesized with method E. (i) $SOCl_2$, reflux, quantitative; (ii) 2-phenylethylamine, dry Et_3N, dry $ClCH_2CH_2Cl$, RT; (iii) SO_2Cl_2., dry $ClCH_2CH_2Cl$, 0°C; (i)HBTU, ET_3N, dry DMF RT then 4-phenylaniline; (ii) SO_2Cl_2., dry $ClCH_2CH_2Cl$, 0°C then RT

This approach differs from **D** strategy because the warhead portion cyclization[109] was not carried out by a simple oxidative process. Indeed, the isothiazol-3(2*H*)-one warhead was obtained from bis-amides like **170** and **172** by a complex sequence of reactions triggered by the slow addition of sulfuryl chloride (SO_2Cl_2) to the reaction medium. A possible reaction mechanism able to explain the formation of isothiazol-3(2*H*)-one warheads is here proposed. (Scheme 3.10)

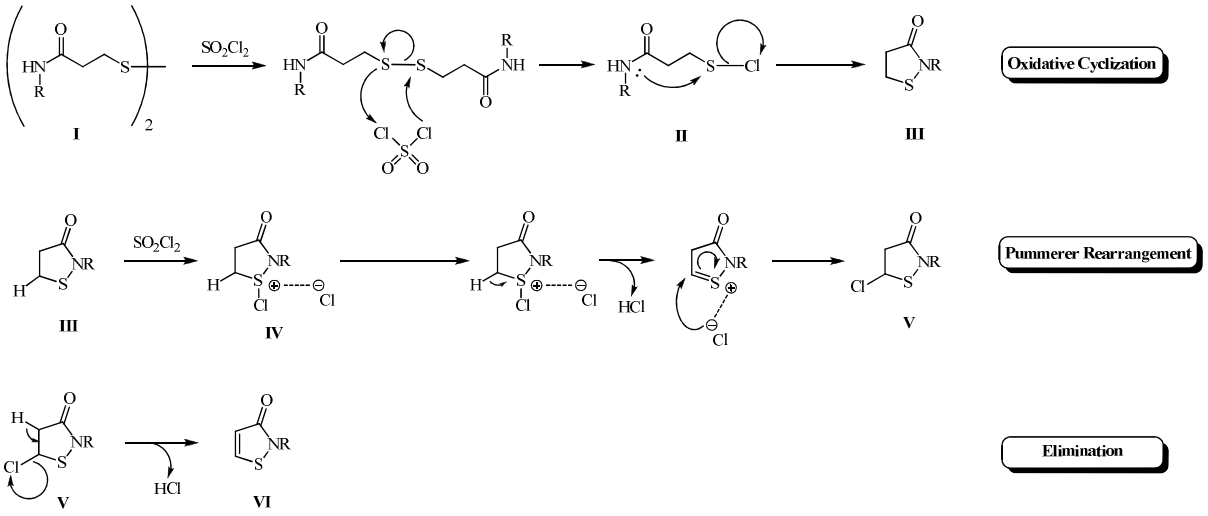

Scheme 3.10. Proposed reaction mechanism of SO_2Cl_2 to produce a *N*-substituted isothiazol-3(2*H*)-one warheads in presence of a general 3,3'-dithiopropionamide.

SO_2Cl_2 directly chlorinate sulfur atoms of bis-amide **I** inducing the breakage of disulfide bond and affording highly reactive sulfenyl chlorides **II**. These species undergo an intramolecular cyclization producing isothiazolidin-3(2H)-one **III** that are quickly further chlorinated on sulfur atom to form sulfonium-salt **IV**. At this time, the Pummerer rearrangement takes place transferring the chlorine atom to the neighboring α-carbon[16] with production of HCl. Finally, an elimination reaction provides the formation of an endocyclic carbon-carbon double bond leading to the isothiazol-3(2*H*)-one warhead **VI**.

It is reported that obtained isothiazol-3(*2H*)-one can be further chlorinated producing side product like 5-Chloroisothiazol-3(*2H*)-one when the reaction was carried out using an excess of SO_2Cl_2.[109] This reaction conditions can locally occurs when SO_2Cl_2 is added too quickly to the reaction mixture or when the solubility of starting material in the reaction medium is low. During the synthesis of isothiazol-3(*2H*)-ones **38** and **39**, despite a very slow addition of SO_2Cl_2 to the reaction mixture using high dilution conditions, 5-Chloroisothiazol-3(*2H*)-one by-products were always produced, lowering, in this way, the reaction yields.

3.3.3 Results and discussion

At the moment, only a first group of synthesized benzo[d]isothiazol-3(*2H*)-one-based compounds were tested toward purified rMAGL. The MAGL inhibition assay was carried out as described in the Experimental Section (Chapter 4.2.3) of this PhD thesis. Collected MAGL inhibition data provided by tested benzo[d]isothiazol-3(*2H*)-one-based inhibitors are reported in Table 3.10.

Compound	R	IC_{50} (nM)
19		59±5.7
21	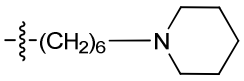	195±12
25	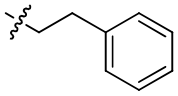	19±1.8
27	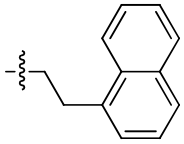	22±5.2
26	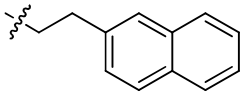	54±16
13	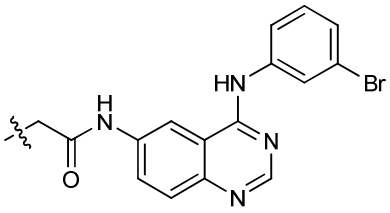	21±0.9
30	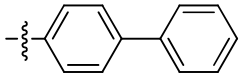	15±0.6

Table 3.10. Synthesized MAGL inhibitor already evaluated as MAGL inhibitor on rMAGL purified enzyme.

All tested compounds show potent inhibition of MAGL but no significant variation of IC_{50} value were observed within the series, despite the structural variability of the R substituents. In this way, IC_{50} changes observed for tested inhibitors could be addressed mainly to lipophilicity changes. This hypothesis is supported by comparison between IC_{50} value of already published compounds **147**[179] and IC_{50} values calculated for compounds **21**. Indeed, the increased polarity of compound **21** side chain, provided by the presence of the piperidinyl moiety, significantly increased its IC_{50} value with respect to those obtained for its structural homologues **147**

T

Compound	R	IC_{50} (nM)
147		59±7
21	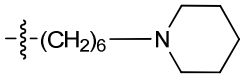	195±12

Table 3.11. Comparison of IC_{50} values measured for compound **147** and **21**. Despite the different source of these data, IC_{50} values can be compared because obtained using the same experimental methodology.

These results were in agreement with a previously published SAR study focused on a short panel of isothiazol-3(2*H*)-one based inhibitors (table 3.12).[179]

#	Warhead	R	IC_{50} (nM)
144	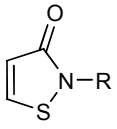	Methyl	239±68
145		*n*-Octyl	88±12
146		Oleoyl	43±8

Table 3.12. Comparison of IC^{50} value published for compound **144**-**145**.

Also in this case, indeed, a pivotal relationship between MAGL inhibition potency and lipophilicity of tested compounds has been observed. This study has been shown that an increased lipophilicity of the carbon side chain of isothiazol-3(2*H*)-one derivatives enhances their inhibitory potency toward MAGL. Indeed, substitution of their *n*-octyl group driver group (compounds **145**) with a more lipophilic oleoyl chain (compound **146**) increased their potency, while substitution with a methyl group (compound **144**) decreased it.

The constant magnitude of IC_{50} values shown by compounds synthesized during this PhD project could have two the different explanations:

1. an over-reactivity of the cysteine-trapping warhead could have overcome the structural diversity provided by the R substitution

2. there is a very large pharmacophoric space to explore around the target cysteine. In this case, the diversity of designed driver groups could not be broad enough to properly exploit the pharmacophoric space features located around the binding site.

The latter hypothesis is supported by the MAGL crystal structure (recently available) in which targeted Cys208 was accurately localized at the entrance of the lipophilic tunnel that allow to 2-AG to reach the enzyme active site.[149] It was reported that this fully solvent exposed cysteine residue does not point toward the main liphophilic tunnel entrance and this suggests the presence of a huge pharmacophoric space to explore around it.

3.3.4 Conclusions

Too few biological data were collected until now to allow the proposal of any meaningful conclusive considerations. The dependence of observed IC_{50} values from liphophilicity of tested products and their proposed covalent binding with Cys208 residue on MAGL surface only suggests some considerations about the binding mode of tested compounds. In a first time, these compounds could be recognized by a Cys208 neighboring liphophilic cleft so to establish non-covalent and non-polar interaction with it. Afterwards, they could react with Cys208 producing a covalent mixed disulfide bond, strengthening the compound-target binding. In this framework, the lipophilicity of

synthesized compound could enhance the non-covalent target binding so to favor the establishment of the covalent interaction with Cys208.

The position and the spatial orientation of Cys208 on MAGL surface suggests that synthesized benzo[d]isothiazol-3(2*H*)-one and isothiazol-3(2*H*)-one derivatives could act through an allosteric inhibition mechanism,[149] perhaps hampering the postulated "interfacial activation" of MAGL by induction of cap domain conformation changes. Despite this, an inhibition mechanism based on a non-competitive obstruction of the active site entrance cannot be ruled out.

The intrinsic reactivity evaluation of synthesized compounds and the biological activity data about compounds not yet tested will be probably helpful to verify these hypotheses and to set-up a properly refined SAR study focused on this new class of cysteine-trapping MAGL inhibitors. However, the high basal inhibition potency provided by tested cysteine trapping benzo[d]isothiazol-3(2*H*)-one derivatives can be considered a good starting point for further structural optimizations directed to achieve new MAGL partially irreversible inhibitors with improved selectivity and bioavailability.

Chapter 4

Experimental section

4.1 EGFR inhibitors

4.1.1 Chemistry

Reagents were obtained from commercial suppliers and used without further purification. Solvents were purified and stored according to standard procedures. Anhydrous reactions were conducted under a positive pressure of dry N_2. Reactions were monitored by TLC, on Kieselgel 60 F 254 (DC-Alufolien, Merck). Final compounds and intermediates were purified by flash chromatography (SiO_2 60, 40-63 μm). Microwave reactions were conducted using a CEM Discover synthesis unit (CEM Corp., Matthews, NC). Melting points were not corrected and were determined with Gallenkamp melting point apparatus. The ^{1}H NMR spectra were recorded on a Bruker 300 MHz spectrometer and on a Bruker 300 MHz Avance spectrometer. Chemical shifts (δ scale) are reported in parts per million (ppm) relative to the central peak of the solvent. ^{1}HNMR spectra are reported in the following order: multiplicity, approximate coupling constant (*J* value) in hertz (Hz), and number of protons; signals were characterized as s (singlet), d (doublet), dd (doublet of doublets), t (triplet), dt (doublet of triplets), q (quartet), m (multiplet), br s (broad signal). Mass spectra were recorded using an API 150 EX instrument (Applied Biosystems/MDS SCIEX, Foster City, CA). Liquid chromatography/mass spectrometry analysis was performed on an Agilent 1100 LC gradient system coupled with an Applied Biosystem 150-EX single quadrupole mass spectrometer equipped with a Turbolon-Spray ion source working in positive ion mode. Final compounds **1**,[193] **2**,[98] and **3**[99] were synthesized according to literature methods. The final compounds were analyzed on ThermoQuest (Italia) FlashEA1112 Elemental Analyzer for C,H, and N (analyses were within 0.4% of theoretical values). All tested compounds were >95% pure by elemental analysis.

4.1.2 Synthesis

A) Intermediate compounds:

Potassium (2*R*,3*S*)-3-(piperidin-1-ylmethyl)oxirane-2-carboxylate (94). To an ice cold stirring solution of (2*R*,3*S*)-ethyl 3-(piperidin-1-ylmethyl)oxirane-2-carboxylate **109** (170 mg, 0.80 mmol) in abs. EtOH (1 mL), a solution of KOH (45 mg, 0.8 mmol) in abs. EtOH (1.5 mL) was added dropwise. The resulting mixture was stirred for 2 h at 0 °C. The solvent was removed under reduced pressure and the residue was washed with petroleum ether. The product **19** was obtained as a pale brown solid (83%): mp > 230 °C; MS (APCI) *m*/z 184.2; ^{1}H NMR (300 MHz, $CDCl_3$) δ 1.49 (m, 2H), 1.63 (m, 4H), 2.32 (dd, *J* = 13.4, 6.7 Hz, 1H), 2.54 (m, 4H), 2.74 (dd, *J* = 13.4, 3.7 Hz, 1H), 3.02 (d, *J* = 2.16 Hz, 1H), 3.12 (m, 1H).

2-(3-Oxoisothiazolin-2-yl)acetic acid (100). A suspension of ethyl 2-(3-oxoisothiazolin-2-yl)acetate **112**[109] (200 mg, 1.07 mmol) in 1 M trifluoroacetic acid (TFA) (25 mL, 25 mmol) was refluxed for 12 h and then evaporated. The residue was dried at 50-55 °C in vacuo to yield **100** (98%) as a white solid: mp 171-172 °C; ^{1}H NMR (300 MHz, DMSO-*d*6) δ 4.41 (s, 2H), 6.19 (d, *J* = 6.2 Hz, 1H), 8.51 (d, *J* = 6.2 Hz, 1H).

(2R,3S)-Ethyl 3-(hydroxymethyl)oxirane-2-carboxylate (108).[106] To a stirred 0°C cooled solution of (2*R*,3*R*)-diethyl oxirane-2,3-dicarboxylate **107**[104] (1.2 g, 6.377 mmol) in *abs.* EtOH (10 ml), a solution of $NaBH_4$ (305 mg, 7.943 mmol) in *abs.* EtOH (13 ml) was dropwise added over 5 min under nitrogen atmosphere. The mixture was stirred for 2 h and then the reaction was quenched by addition of a pH=7.0 Phosphate buffer (40 ml). The crude was extracted with CH_2Cl_2 (4 X 10ml) and the combined organic layers were dried over anhydrous Na_2SO_4, filtered and evaporated under reduced pressure giving 742 mg of yellow oil. It was

purified by FC (SiO_2, EtOAc/Hexane 50/50) giving 572 mg of desired (2*R*(2R,3S)-ethyl 3-(hydroxymethyl)oxirane-2-carboxylate **108** as white crystals (62%). mp = 44-45°C (Lit. 43-44°C)[106]; H^1-NMR (300 MHz, $CDCl_3$): δ = 1.30 (t, *J*= 7.09 Hz, 3H), 3.39 (m, 1H), 3.53 (d, *J* = 2.00 Hz,1H), 3.76 (dd, J_1= 3.31 Hz, J_2= 13.05 Hz, 1H), 4.02 (dd, J_1= 2.16 Hz, J_2= 13.15 Hz, 1H), 4.24 (m, 2H)

(2*R*,3*S*)-Ethyl 3-(piperidin-1-ylmethyl)oxirane-2-carboxylate (109). A 0°C cooled solution of (2*R*,3*S*)-ethyl 3-(hydroxymethyl)oxirane-2-carboxylate **108** (405 mg, 2.77 mmol) and Et_3N (582 µL, 4.16 mmol) in anhydrous CH_2Cl_2 (12 mL) was stirred for 30 min before the dropwise addition of methanesulfonyl chloride (MsCl) (407 µL, 4.16 mmol). The mixture was then stirred for 10 min at 0 °C and for 2 h at RT, then the solvent was evaporated. The resulting yellow paste was dissolved in anhydrous DMF (12 mL) and KI (23 mg, 0.14 mmol) was added. The yellow solution was cooled to 0 °C and stirred for 5 min before the dropwise addition of anhydrous piperidine (830 µL, 8.31 mmol). The resulting suspension was slowly warmed to RT and stirred for 7 days, diluted with saturated aqueous $NaHCO_3$ (85 mL) and extracted with Et_2O. The combined organic layers were dried and evaporated to give a brown oil that was purified by FC (CH_2Cl_2:MeOH, 100:0 to 96:4) furnishing **109** as yellow oil (30%); ^1H NMR (300 MHz, $CDCl_3$) δ 1.25 (t, *J* = 7.1 Hz, 3H), 1.39 (m, 2H), 1.55 (m, 4H), 2.31 (dd, *J* = 13.6, 6.4 Hz, 1H), 2.36-2.55 (m, 4H), 2.71 (dd, *J* = 13.6, 3.4 Hz, 1H), 3.19 (d, *J* = 2.0 Hz, 1H), 3.29 (m, 1H), 4.18 (m, 2H).

***N*-(4-(3-bromoanilino)quinazolin-6-yl)-3-chloropropanamide (118).** A stirring suspension of 6-amino-4-(3-bromoanilino)quinazoline (**3**) (300 mg, 0.95 mmol) and 3-chloropropionyl chloride (3 mL, 31.28 mmol) was refluxed for 16 h, cooled to RT and filtered. The filtered solid was washed with Et_2O, dried under reduced pressure and purified by FC (SiO_2, eluent= CH_2Cl_2/CH_3OH from 98:2 to 95:5) furnishing the pure compound (36%) as

a pale yellow solid: mp >230; MS (APCI): *m/z* 407.4; ^{1}H NMR ($CDCl_3$, 300 MHz): δ 2.96 (t, *J* = 6.2 Hz, 2H), 3.95 (t, *J* = 6.2 Hz, 2H), 7.31-7.33 (m, 2H), 7.78 (m, 3H), 8.14 (s, 1H), 8.55 (s, 1H), 8.72 (s, 1H).

B) Final compounds:

***N*-(4-(3-Bromophenylamino)quinazolin-6-yl)acrylamide (2).** Anal.calc. for $C_{17}H_{13}BrN_4O$ (MW= 369,22) C, 55.30; H, 3.55; N, 15.17. Found: C, 54.96; H, 3.83; N, 14.98.

6-Amino-4-(3-bromoanilino)quinazoline (3). Anal.calc. for $C_{14}H_{11}BrN_4$ 1,5H_2O (MW= 342,19) C, 49.92; H, 3.65; N, 16.63. Found: C, 49.73; H, 3.92; N, 16.23.

(2*R*,3*R*) Ethyl 3-(4-(3-bromoanilino)quinazolin-6-ylcarbamoyl)oxirane-2-carboxylate (4). Method A. Dichloromethylene dimethyliminium chloride (356 mg, 2.19 mmol) was added to a stirred solution of (2*R*,3*R*)-2,3-epoxysuccinic acid monoethyl ester **92**[105] (350 mg, 2.19 mmol) in anhydrous CH_2Cl_2 (10 mL). After the reactants were stirred for 1 h with ice-cooling, 6-amino-4-(3-bromoanilino)quinazoline **3** (458 mg, 1.46 mmol) and $NaHCO_3$ (613 mg, 7.3 mmol) were added, and the suspension was stirred for 1 h at 0 °C. The mixture was washed with water, dried, and concentrated to obtain the crude compound. Crystallization from MeOH gave the pure product **4** as white crystals (60%): mp (MeOH) > 230 °C dec.; MS (APCI) *m/z* 458.3, 459.2; ^{1}H NMR (300 MHz, DMSO-*d6*) δ 1.26 (t, *J* = 7.1 Hz, 3H), 3.82 (d, *J* = 1.7 Hz, 1H), 3.93 (d, *J* = 1.7 Hz, 1H), 4.23 (q, *J* = 7.1 Hz, 2H), 7.29 (d, *J* = 8.1 Hz, 1H), 7.35 (t, *J* = 7.9 Hz, 1H), 7.82-7.92 (m, 3H), 8.16 (br s, 1H), 8.60 (s, 1H), 8.72 (d, *J* = 1.3 Hz, 1H), 9.93 (br s, 1H), 10.80 (br s, 1H). Anal.calc. for $C_{20}H_{17}BrN_4O_4$ (MW=457,28) C, 52,53; H, 3.75; N, 12.25. Found: C, 52.19; H, 3.76; N, 11.91.

(2*S*,3*S*) Ethyl 3-(4-(3-bromoanilino)quinazolin-6-ylcarbamoyl)oxirane-2-carboxylate (5). 6-Amino-4-(3-bromoanilino)quinazoline **3** was reacted with (2*S*,3*S*)-2,3-epoxysuccinic acid monoethyl ester **93**[107] according to the procedure described in method A. The crude product was purified by silica gel chromatography (CH_2Cl_2:MeOH, 99:1 to 97:3) to give **5** (66%) as white solid: mp (MeOH) > 230 °C; MS (APCI) *m/z* 457.9, 459.3; ^{1}H NMR (300 MHz, DMSO-*d6*) δ 1.26 (t, *J* = 7.2 Hz, 3H), 3.81 (d, *J* = 1.7 Hz, 1H), 3.92 (d, *J* = 1.7 Hz, 1H), 4.23 (q, *J* = 7.1 Hz, 2H), 7.29 (d, *J* = 8.1 Hz, 1H), 7.35 (t, *J* = 7.8 Hz, 1H), 7.80-7.87 (m, 2H), 7.89 (dd, *J* = 9.0, 2.2 Hz, 1H), 8.16 (s, 1H), 8.60 (s, 1H), 8.72 (s, 1H), 9.94 (br s, 1H), 10.80 (br s, 1H). Anal.calc. for $C_{20}H_{17}BrN_4O_4$ (MW=457,28) C, 52.53; H, 3.75; N, 12.25. Found: C, 52.62; H, 3.81; N, 11.89.

(2*R*,3*S*) *N*-(4-(3-Bromoanilino)quinazolin-6-yl)-3-(piperidin-1-ylmethyl)oxirane-2-carboxamide (6). Method B. To a suspension of potassium (2*R*,3*S*)-3-(piperidin-1-ylmethyl)oxirane-2-carboxylate **94** (58 mg, 0.26 mmol) in anhydrous DMF (2 mL), HBTU (205 mg, 0.54 mmol) was added at RT. The mixture was stirred for 40 min before the dropwise addition of 6-amino-4-(3-bromoanilino)quinazoline **3** (80 mg, 0.26 mmol) in DMF (2 mL). The reaction mixture was stirred for 16 h, the solvent was removed and the residue was dissolved in CH_2Cl_2 and washed with saturated aqueous Na_2CO_3. The organic phase was evaporated and the crude product purified by silica gel chromatography (CH_2Cl_2:MeOH, 99:1 to 97:3) to give **6** as a pale yellow solid (30%): mp > 230 °C; MS (APCI) *m/z* 482.2, 484.2; ^{1}H NMR (300 MHz, CD_3OD): δ 1.41-1.43 (m, 2H), 1.53-1.64 (m, 4H), 2.36 (dd, *J* = 13.6, 6.7 Hz, 1H), 2.48-2.56 (m, 4H), 2.80 (dd, *J* = 13.7, 3.4 Hz, 1H), 3.30-3.34 (m, 1H), 3.39 (d, *J* = 1.89 Hz, 1H), 7.21-7.22 (m, 2H), 7.64-7.69 (m, 2H), 7.77 (dd, *J* = 9.0, 2.2 Hz, 1H), 8.03 (s, 1H), 8.45 (s, 1H), 8.56 (d, *J* = 2.1 Hz, 1H). Anal.calc. for $C_{23}H_{24}BrN_5O_2$ (MW=482,37) C, 57.72; H, 5.01; N, 14.52. Found: C, 57.35; H, 5.20; N, 14.22.

***N*-(4-(3-Bromoanilino)quinazolin-6-yl)-2-phenoxyacetamide (7). Method C.** Phenoxyacetic acid **95** (361 mg, 2.37 mmol) was added to a stirred suspension of PCl_5 (490 mg, 2.37 mmol) in CH_2Cl_2 (15 mL) at RT. The reactants were refluxed for 30 min, then cooled to RT, and 6-amino-4-(3-bromoanilino)quinazoline **3** (500 mg, 1.59 mmol) was added in 10 min. After refluxing for 2 h, the mixture was cooled in an ice/water bath, 2.5 mL of water were added, the mixture stirred for 30 min and then Na_2CO_3 was added. The solid was filtered and purified by silica gel chromatography (CH_2Cl_2:MeOH, 99:1 to 97:3) to afford **7** as a white solid (77%): mp (EtOH/water) 212 °C; MS (APCI) *m/z* 449.0, 451.0; ^{1}H NMR (300 MHz, DMSO-*d6*) δ 4.79 (s, 2H), 6.99 (t, *J* = 7.4 Hz, 1H), 7.05 (d, *J* = 7.8 Hz, 2H), 7.27-7.36 (m, 4H), 7.80 (d, *J* = 8.9 Hz, 1H), 7.85 (d, *J* = 7.9 Hz, 1H), 7.95 (dd, *J* = 9.0, 2.1 Hz, 1H), 8.16 (s, 1H), 8.58 (s, 1H), 8.74 (d, *J* = 1.7 Hz, 1H), 9.93 (s, 1H), 10.44 (s, 1H). Anal.calc. for $C_{22}H_{17}BrN_4O_2$ (MW=449,30) C, 58.81; H, 3.81; N, 12.47. Found: C, 58.89; H, 4.03; N, 12.09.

***N*-(4-(3-Bromoanilino)quinazolin-6-yl)-2-(4-fluorophenoxy)acetamide (8).** 6-Amino-4-(3-bromoanilino)quinazoline **3** was reacted with 2-(4-fluorophenoxy)acetic acid **96** according to the procedure described in method C. The crude product was purified by silica gel chromatography (CH_2Cl_2:MeOH, 99:1 to 97:3) to give **8** (67%) as white solid: mp (EtOH/water) 224 °C; MS (APCI) *m/z* 467.3, 469.1; ^{1}H NMR (300 MHz, DMSO-*d6*) δ 4.78 (s, 2H), 7.07 (dd, *J* = 9.2, 4.3 Hz, 2H), 7.15-7.21 (m, 2H), 7.27-7.37 (m, 2H), 7.85 (m, 2H), 7.95 (dd, *J* = 8.2, 1.4 Hz, 1H), 8.16 (br s, 1H), 8.59 (s, 1H), 8.74 (br s, 1H), 9.93 (br s, 1H), 10.44 (br s, 1H). Anal.calc. for $C_{22}H_{16}BrN_4O_2$ (MW=448,29) C, 56.55; H, 3.45; N, 11.99. Found: C, 56.30; H, 3.51; N, 11.59.

***N*-(4-(3-Bromoanilino)quinazolin-6-yl)-2-(perfluorophenoxy)acetamide (9).** 6-Amino-4-(3-bromoanilino)quinazoline **3** was reacted with 2-(perfluorophenoxy)acetic acid **97** according to the procedure

described in method C. The crude product was purified by silica gel chromatography (CH_2Cl_2:MeOH, 99:1 to 97:3) to give **9** (50%) as white solid: mp 220-221 °C; MS (APCI): *m/z* 539.1, 541.1. ^{1}H NMR (300 MHz, DMSO-*d6*) δ 4.99 (s, 2H), 7.24-7.34 (m, 2H), 7.75-7.87 (m, 3H), 8.11 (s, 1H), 8.55 (s, 1H), 8.66 (s, 1H), 9.91 (br s, 1H), 10.50 (br s, 1H). Anal.calc. for $C_{22}H_{12}BrF_5N_4O_2$ (MW=539,25) C, 49.00; H, 2.24; N, 10.39. Found: C, 49.29; H, 2.76; N, 9.92.

***N*-[2-[(4-(3-Bromoanilino)quinazolin-6-yl)amino]-2-oxoethyl] phenylcarbamate (10). Method D.** 2-(Phenoxycarbonylamino)acetic acid **98** (375 mg, 1.92 mmol) and *N*,*N*'-dicyclohexylcarbodiimide (DCC) (416 mg, 1.04 mmol) were added to a solution of **3** (400 mg, 1.28 mmol) in anhydrous DMF (6 mL) at 0 °C. The mixture was stirred 16 h at RT, the solid was removed by filtration and the filtrate evaporated in vacuo to obtain the crude product, which was purified by silica gel chromatography (EtOAc). The pure product **10** (55%) appeared as a white solid: mp (EtOH/water) >250 °C dec.; MS (APCI) *m/z* 492.1; ^{1}H NMR (300 MHz, DMSO-*d6*) δ 4.20 (s, 2H), 6.73-6.78 (m, 3H), 7.15 (t, *J* = 8.6 Hz, 2H), 7.32 (dt, *J* = 8.1, 1.6 Hz, 1H), 7.37 (t, *J* = 7.9 Hz, 1H), 7.82-7.93 (m, 3H), 8.21 (s, 1H), 8.50 (s, 1H), 8.57 (d, *J* = 1.7 Hz, 1H), 8.70 (s, 1H), 9.32 (s, 1H), 9.98 (br s, 1H). Anal.calc. for $C_{25}H_{20}BrN_3O_3 \cdot 0.5H_20$ (MW=499,36) C, 53.75; H, 3.56; N, 13.63. Found: C, 53.65; H, 3.95; N, 13.29.

***N*-(4-(3-Bromoanilino)quinazolin-6-yl)-2-cyanoacetamide (11).** 6-Amino-4-(3-bromoanilino)quinazoline **3** was reacted with 2-cyanoacetic acid **99** according to the procedure described in method C. The crude product was purified by silica gel chromatography (EtOAc) to give **11** (55%) as white solid: mp (EtOH/water) 263 °C; MS (APCI) *m/z* 382.0, 384.1; ^{1}H NMR (300 MHz, DMSO-*d6*) δ 4.00 (s, 2H), 7.30-7.35 (m, 2H), 7.81-7.86 (m, 3H), 8.15 (t, *J* = 1.7 Hz, 1H), 8.59 (s, 1H), 8.70 (s, 1H), 9.95 (s, 1H), 10.64 (s, 1H). Anal.calc. for $C_{17}H_{12}BrN_5O \cdot 1.5H_2O$ (MW=409,24) C, 49.90; H, 2.96; N, 17.11. Found: C, 50.28; H, 2.99; N, 16.71.

***N*-(4-(3-Bromoanilino)quinazolin-6-yl)-2-(3-oxoisothiazolin-2-yl)acetamide (12).** 6-Amino-4-(3-bromoanilino)quinazoline **3** was reacted with 2-(3-oxoisothiazolin-2-yl)acetic acid **100** according to the procedure described in method D. The crude product was purified by silica gel chromatography (EtOAc:MeOH, 99:1 to 90:10) to give **12** (40%) as a white solid: mp (EtOH/water) > 230 °C; MS (APCI) *m/z* 456.1, 458.3; ^{1}H NMR (300 MHz, DMSO-*d6*) δ 4.65 (s, 2H), 6.24 (d, *J* = 6.2 Hz, 1H), 7.28 (d, *J* = 8.0 Hz, 1H), 7.33 (t, *J* = 7.9 Hz, 1H), 7.79-7.85 (m, 3H), 8.10 (s, 1H), 8.55 (d, *J* = 6.2 Hz, 1H), 8.55 (s, 1H), 8.71 (s, 1H), 9.94 (br s, 1H), 10.69 (br s, 1H). Anal.calc. for $C_{19}H_{14}BrN_5O_2S \cdot 1.5H_2O$ (MW=483,34) C, 47.21; H, 3.52; N, 14.48. Found: C, 47.70; H, 3.39; N, 13.98.

***N*-(4-(3-Bromoanilino)quinazolin-6-yl)-2-(3-oxobenzo[*d*]isothiazolin-2-yl)acetamide (13).** 6-Amino-4-(3-bromoanilino)quinazoline **3** was reacted with 2-(3-oxobenzo[*d*]isothiazolin-2-yl)acetic acid **101** according to the procedure described in method D. The crude product was purified by silica gel chromatography (EtOAc:*n*-hexane, 99:1) to afford **13** (50%) as a white solid; mp (MeOH) 238 °C; MS (APCI) *m/z* 506.1, 508.1; ^{1}H NMR (300 MHz, DMSO-*d6*) δ 4.75 (s, 2H), 7.25-7.31 (m, 2H), 7.43 (t, *J* = 7.5 Hz, 1H), 7.69 (t, *J* = 7.8 Hz, 1H), 7.76-7.83 (m, 3H), 7.88 (d, *J* = 7.9 Hz, 1H), 7.98 (d, *J* = 8.5 Hz, 1H), 8.09 (s, 1H), 8.54 (s, 1H), 8.72 (s, 1H), 9.89 (br s, 1H), 10.66 (br s, 1H). Anal.calc. for $C_{23}H_{16}BrN_5O_2S \cdot 0.5H_2O$ (MW=515,38) C, 52.32; H, 3.42; N, 13.25. Found: C, 52.30; H, 3.28; N, 12.91.

***N*-(4-(3-Bromoanilino)quinazolin-6-yl)-3-isopropyl-1,2,4-thiadiazole-5-carboxamide (14). Method E.** Potassium *tert*-butoxide (84 mg, 0.75 mmol) was added to a premixed mixture of ethyl 3-isopropyl-1,2,4-thiadiazole-5-carboxylate **102**[111] (150 mg, 0.75 mmol) and 6-amino-4-(3-bromoanilino)quinazoline **3** (235 mg, 0.75 mmol) in anhydrous DMF (1 mL). The reaction mixture was microwaved (150 W) to 100 °C for 8 min. The solution was diluted with water and extracted with EtOAc. The organic phase was evaporated to obtain the crude compound, that

was purified by silica gel chromatography (CH_2Cl_2:MeOH, 99:1 to 97:3) to give **14** (50%) as a pale yellow crystals: mp (CH_2Cl_2) 224 °C; MS (APCI) *m*/*z* 469.0, 471.0; ^{1}H NMR (300 MHz, DMSO-*d6*) δ 1.47 (d, *J* = 6.9 Hz, 6H), 3.43 (m, 1H), 7.34 (dt, *J* = 8.2, 1.5 Hz, 1H), 7.40 (t, *J* = 8.0 Hz, 1H), 7.90 (d, *J* = 8.9 Hz, 1H), 7.93 (d, *J* = 7.9 Hz, 1H), 8.20-8.23 (m, 2H), 8.68 (s, 1H), 8.93 (d, *J* = 1.8 Hz, 1H), 10.01 (s, 1H), 11.33 (br s, 1H). Anal.calc. for $C_{20}H_{17}BrN_6OS \cdot 0.5H_2O$ (MW=478,37) C, 50.22; H, 3.79; N, 17.57. Found: C, 50.17; H, 3.72; N, 17.29.

***N*-(4-(3-Bromoanilino)quinazolin-6-yl)-3-(dimethylamino)propanamide (15).** A 33% v/v solution of dimethylamine in abs EtOH (0.8 mL, 4.46 mmol) was added over 15 min to a stirring suspension of 3-chloropropionamide **118** (145 mg, 0.357 mmol) and NaI (37.50 mg, 0.25 mmol) in EtOH abs (10 ml). The resulting mixture was refluxed for 8h. After cooling to 0 °C, the mixture was basified with KOH (741 mg, 13.21 mmol) and stirred for 1 h at 0 °C. The solvent was evaporated under reduced pressure and the obtained solid residue was dissolved with EtOAc and diluted with brine. The organic layer was separated, dried over anhydrous Na_2SO_4, filtered, concentrated under reduced pressure, purified by FC (SiO_2, eluent CH_2Cl_2/CH_3OH from 100:0 to 70:30), and crystallized from EtOAc/Hexane. The pure product was isolated as a yellow solid (86%): mp 170-172°C; MS (APCI): *m*/*z* 414.4; ^{1}H NMR (DMSO-*d6*, 300 MHz) δ 2.35, (s, 6H), 2.65 (t, *J* = 6.5 Hz, 2H), 2.78 (t, *J* = 6.5 Hz, 2H), 7.29-7.31 (m, 2H), 7.74 (m, 3 H), 8.12 (b s, 1H), 8.53 (s, 1H), 8.66 (b s, 1H). Anal.calc. for $C_{19}H_{20}BrN_5O$ (MW=414.30) C, 55.08; H, 4.87; N, 16.90. Found: C, 54.64; H, 4.89; N, 16.63.

(2*R*,3*R*) Ethyl 3-(naphthalen-2-ylcarbamoyl)oxirane-2-carboxylate (16). Compound **16** was synthesized by coupling the carboxylic acid **92** and 2-naphthylamine **106** following the procedure described in method A. Purification by silica gel chromatography (*n*-hexane:EtOAc, 90:10 to 70:30) gave the pure compound (70%) as a white solid: mp (EtOH/water)

118-119 °C; MS (APCI) *m*/z 283.3; ^{1}H NMR (300 MHz, $CDCl_3$) δ 1.32 (t, *J* = 7.1 Hz, 3H), 3.66 (d, *J* = 1.9 Hz, 1H), 3.85 (d, *J* = 2.0 Hz, 1H), 4.29 (m, 2H), 7.39-7.49 (m, 3H), 7.77-7.83 (m, 4H), 8.18 (d, *J* = 2.0 Hz, 1H). Anal.calc. for $C_{16}H_{15}NO_4$ (MW=285,29) C, 67.36; H, 5.30; N, 4.91. Found: C, 67.25; H, 5.41; N, 4.75.

***N*-(Naphthalen-2-yl)-2-phenoxyacetamide (17).** Compound **17** was synthesized by coupling the carboxylic acid **95** and 2-naphtylamine **106** using the procedure described in method C. Purification by silica gel chromatography (*n*-hexane:EtOAc, 70:30) gave the pure compound (80%) as a pale yellow solid: mp (EtOH/water) 142-144 °C; MS (APCI) *m*/z 184.3; ^{1}H NMR (300 MHz, $CDCl_3$) δ 4.65 (s, 2H), 7.00-7.09 (m, 3H), 7.33-7.55 (m, 5H), 7.77-7.82 (m, 3H), 8,25 (d, *J* = 1.7 Hz, 1H), 8.43 (br s, 1H). Anal.calc. for $C_{16}H_{15}NO_4$ (MW=277,32) C, 77.96; H, 5.45; N, 5.05. Found: C, 77.56; H, 5.49; N, 4.92.

4.1.3 Biology

Collected biological data were from experimentations carried out by Prof. P.G. Petronini's research group of *(Dipartimento di Medicina Sperimentale – Università degli studi di Parma, Parma, Italy)*.

Kinase assay. Evaluation of the effects of compounds on the kinase activity of human EGFR was performed by measuring the phosphorylation of the substrate Ulight-CAGAGAIETDKEYYTVKD (JAK1) using a human recombinant enzyme expressed in insect cells[194] and the LANCE detection method,[195] employing the Cerep EGFR kinase assay.[196] Briefly, the test compound, reference compound or water (control), was mixed with the enzyme (0.0452 ng) in a buffer containing 40 mM Hepes/Tris (pH 7.4), 0.8 mM EGTA/Tris, 8 mM $MgCl_2$, 1.6 mM DTT, 0.008% Tween 20 and 100 nM poly-D-lysine. Thereafter, the reaction was initiated by the addition of 100 nM of the substrate and 10 μM ATP, and the

mixture was incubated for 15 min at room temperature. For control basal measurements, the enzyme was omitted from the reaction medium. Following incubation, the reaction was stopped by the addition of 13 mM EDTA. After 5 min, the anti-phopho-PT66 antibody labeled with europium chelate was added. After 60 min, the fluorescence transfer was measured at excitation wavelength 337 nm and emission wavelength 620 nm using a microplate reader (Envision, Perkin Elmer). The concentration of compound that inhibited receptor phosphorylation by 50% (IC_{50}) was calculated from inhibition curves.

Cell culture. The human A431 epidermoid cancer cell line was cultured in D-MEM 4.5 g/L glucose. NSCLC cell line H1975 and SW620 cell line were cultured in RPMI. All media were supplemented with 2 mmol/L glutamine, 10% FCS. A431 was from ATCC, H1975 was kindly provided by Dr E. Giovannetti (*Department of Medical Oncology, VU University Medical Center, Amsterdam, The Netherlands*) and were maintained under standard cell culture conditions at 37 °C in a water-saturated atmosphere of 5% CO_2 in air.

Antibodies and reagents. Media were from Euroclone, FBS was purchased from Gibco-BRL (Grand Island, NY, USA). Monoclonal anti-EGFR, polyclonal anti-phospho-EGFR (Tyr1068), monoclonal anti erbB2, monoclonal anti-phospho-erbB2 (Tyr 1221/1222), polyclonal Akt, polyclonal anti-phospho-Akt (Ser473), monoclonal anti-p44/42 MAPK, monoclonal anti-phospho-p44/42 MAPK (Thr202/Tyr204), polyclonal anti-caspase-3 antibodies were from Cell Signaling Technology (Beverly, MA, USA). Horseradish peroxidase-conjugated (HRP) secondary antibodies were from Pierce. The enhanced chemiluminescence system (ECL) was from Millipore (Millipore, MA, USA). Reagents for electrophoresis and blotting analysis were obtained from, respectively, BIO-RAD Laboratories and Millipore.

Western blot analysis. Procedures for protein extraction, solubilization, and protein analysis by 1-D PAGE are described elsewhere.[197] 50-100 µg proteins from lysates were resolved by 5-15% SDS-PAGE and transferred to PVDF membranes (Millipore). The membranes were then incubated with primary antibody, washed and then incubated with HRP-anti-mouse or HRP-anti-rabbit antibodies. Immunoreactive bands were visualized using an enhanced chemiluminescence system.

Autophosphorylation assay. Inhibition of EGFR autophosphorylation was determined as previously described using specific anti-phosphotyrosine and anti-total EGFR antibodies by Western blot analysis.[88]

Cell growth inhibition. Cell viability was assessed after 3 days of treatment by tetrazolium dye [3-(4,5-dimethylthiazol-2-yl)-2,5-diphenyltetrazolium bromide (MTT), Sigma, Dorset, UK] assay as previously described.[197] Representative results of at least three independent experiments were used for evaluation of dose-response curves, calculated from experimental points using Graph Pad Prism5 software. The concentration that inhibits 50% (IC_{50}) (e.g., the point at which viability is 50%) was extrapolated from the dose-response curves. The compounds were renewed every 24 h.

Cell death. Cell death was assessed by morphology on stained (Hoechst 33342, propidium iodide) or unstained cells using light, phase contrast, and fluorescence microscopy.[121] Activation of caspase-3 was evaluated by Western blotting procedure as previously described.[121]

4.1.4 Stability

Reactivity with reduced glutathione. The reactivity of compounds **4**, **16** and **7**, **17** with reduced glutathione (GSH) was evaluated in an

aqueous buffered solution (Phosphate Buffered Saline, PBS, pH 7.4), at 37 °C and compared to that of the acrylamide **2**. Briefly, 10 µL of the compound standard solution in DMSO (1 mM) was diluted with 890 µL of PBS pH 7.4. Then 100 µL of a freshly prepared GSH solution in PBS (20 mM) were added. Conversion of the compounds and formation of conjugates at 37 °C and at different time points were measured by LC-UV and LC-ESI-MS. The LC column used was a Phenomenex Synergi Fusion (2.0 × 100 mm, 4 µm) and the mobile phase was a gradient of 50-10% aqueous trifluoroacetic acid (0.05%) in methanol in 10 min at the flow rate of 250 µL/min.

4.2 MAGL inhibitors

4.2.1 Chemistry

Reagents were obtained from commercial suppliers and used without further purification. Solvents were purified and stored according to standard procedures. Anhydrous reactions were conducted under a positive pressure of dry N_2. Reactions were monitored by TLC, on Kieselgel 60 F 254 (DC-Alufolien, Merck). Final compounds and intermediates were purified by flash chromatography (SiO_2 60, 40-63 μm). Microwave reactions were conducted using a CEM Discover synthesis unit (CEM Corp., Matthews, NC). Melting points were not corrected and were determined with a Büchi instrument (Tottoli) and with a Gallenkamp melting point apparatus. The ^{1}H NMR spectra were recorded on a Bruker 300 MHz spectrometer and on a Bruker 300 MHz Avance spectrometer. Chemical shifts (δ scale) are reported in parts per million (ppm) relative to the central peak of the solvent. ^{1}HNMR spectra are reported in the following order: multiplicity, approximate coupling constant (*J* value) in hertz (Hz), and number of protons; signals were characterized as s (singlet), d (doublet), dd (doublet of doublets), t (triplet), dt (doublet of triplets), q (quartet), m (multiplet), br s (broad signal). Mass spectra were recorded using an API 150 EX instrument (Applied Biosystems/MDS SCIEX, Foster City, CA). Liquid chromatography/mass spectrometry analysis was performed on an Agilent 1100 LC gradient system coupled with an Applied Biosystem 150-EX single quadrupole mass spectrometer equipped with a TurboIon-Spray ion source working in positive ion mode. Final compound **18** was purchased from Sigma-Aldrich whereas compound **28** was synthesized according to literature methods.[190] Final compounds were analysed on ThermoQuest (Italia) FlashEA1112 Elemental Analyzer for C, H, and N (analyses were within 0.4% of

theoretical values). All tested compounds were >95% pure by elemental analysis.

4.2.2 Synthesis

A) Intermediate compounds:

2-(6-Chlorohexyl)benzo[d]isothiazol-3(2H)-one (153). To a RT stirring solution of benzo[d]isothiazol-3(2H)-one **18** (100 mg 0.66 mmol) in CH_3CN (2 ml) K_2CO_3 (91.41 mg, 0.66 mmol) was added and the resulting suspension was stirred for 10 min under nitrogen atmosphere. 1-chloro-6-iodohexane (1,0 ml, 6.6 mmol) was dropwise added over 5 min and the resulting mixture was stirred for 18 h and then refluxed for 1h. The solvent was removed by distillation under reduced pressure and the crude was purified by FC (SiO_2, EtOAc/Hx 50/50) to give 66 mg of the expected product **153** as colorless oil (37%). ^{1}H NMR (300 Mz, $CDCl_3$): δ 1.51 (m, 4H), 1.78 (m, 4H), 3.52 (t, *J*=6.63 Hz, 2H), 3.90 (t, *J*=7.1 Hz, 2H), 7.40 (td,J_1=7.95 Hz, J_2=1.32 Hz, 1H), 7.55 (d, *J* = 6.9 Hz, 1H), 7.60 (td, J_1=8.04 Hz, J_2=1.17 Hz, 1H), 8.03 (d, *J*= 7.86 Hz, 1H).

7-Octyn-ole (156).[198] To a stirring 0°C cooled 1,2-ethylendiamine (90 ml, 1346 mmol) under nitrogen atmosphere, NaH (4,8 g, 200,19 mmol) was added in one portion. The cooling bath was removed and the resulting yellow suspension was allowed to slowly warm up to R:T. During the worm up, the color of the suspension turn to a deep blue-violet and bubbling was observed. The reaction mixture was stirred for 1h at RT, 1h at 60°C and then was cooled to 45°C. 3-Octyn-1-ole **155** (7,4 ml, 50,047 mmol) was dropwise added and the resulting mixture was stirred at 60-65°C for 1h. The resulting blue-black solution was cooled to 0°C and H_2O (90 ml) and HCl 1.0M (90 ml) were slowly added. The solution was diluted with further HCl 1.0M (180 ml) and extracted with Et_2O (2 times). The combined organic layers were dried over anhydrous Na_2SO_4, filtered and evaporated under reduced pressure to give 4,7 g of yellow oil that was

purified by FC (SiO_2, EtOAc/Hexane 30/70) furnishing 3.350 g of pure product **156** as pale yellow oil (53%); H^1-NMR (300 MHz, $CDCl_3$): δ = 1.17-1.45 (m, 8H), 1.79 (t, *J*=2.64 Hz, 1H), 2.03 (td, J_1=6.51 Hz, J_2=2.61 Hz, 2H), 2.18 (s, 1H), 3,46 (t, *J*=6.6 Hz, 2H).

Oct-7-ynyl methanesulfonate (157). [199] Methanesulfonyl chloride MsCl (795,59 μl, 8,146 mmol) was dropwise added over 5 min to a 0°C cooled stirring solution of 7-Octyn-ole **156** (514 mg, 4,073 mmol) and Et_3N (1,142 ml, 8,146 mmol) in dry CH_2Cl_2 (5ml) under nitrogen atmosphere. The resulting mixture was slowly warmed up to R.T, stirred for 16h and then washed with H_2O. The organic phase was dried over anhydrous Na_2SO_4, filtered and evaporated under reduced pressure to give 1.106 g of red oil that was purified by FC (SiO_2, CH_2Cl_2 100%) furnishing 703 mg of pure product **157** as pale yellow oil (quantitative); H^1-NMR (300 MHz, $CDCl_3$): δ = 1.46-1.55 (m, 8H), 1.92 (t, *J*=2.91 Hz, 1H), 2.16 (td, J_1=6.85 Hz, J_2=2.60 Hz, 2H), 2.97 (s, 3H), 4,19 (t, *J*=6.53 Hz, 2H).

4-Ethylbenzyl methanesulfonate (159). Methansulfonyl chloride MsCl (732 μl, 7.473 mmol) was dropwise added over 5 min to a 0°C cooled stirring solution of 4-Ethylbenzylalcool **158** (500 μl, 3.736 mmol) and Et_3N (1,053 ml, 7.473 mmol) in dry CH_2Cl_2 (5ml) under nitrogen atmosphere. The resulting mixture was slowly warmed up to R.T, stirred for 16h and then washed with H_2O. The organic phase was dried over anhydrous Na_2SO_4, filtered and evaporated under reduced pressure furnishing 864 mg of dark-red oil that was purified by FC (SiO_2, petroleum ether 100%) furnishing 325 mg of pure product **159** as pale yellow oil (40%).

2,2'-Disulfanediyldibenzoyl chloride (161).[,200] A RT stirring suspension of 2,2'-Dithiosalicylic acid **160** (600 mg 1.959 mmol) in $SOCl_2$ (19.6 ml, 268.4 mmol) was refluxed until it became a solution and then for further 3h. The solution was cooled to RT and exceeding $SOCl_2$ was distilled away under reduced pressure. The obtained dark-red residue was stripped with anhydrous toluol (twice) and used, without any further

purification, to synthesize compound **22**, **23**, **35** and **162**. ^{1}H NMR (300 MHz, $CDCl_3$): δ 7.40 (bt, *J*=8.13 Hz, 2H), 7.57 (td, J_1=7.35 Hz, J_2=1.41 Hz, 2H), 7.78 (dd, J_1=8.16 Hz, J_2=0.84 Hz, 2H), 8.40 (dd, J_1=7.95 Hz, J_2=1.29 Hz, 2H)

2-(Chlorocarbonyl)phenyl hypochlorothioite (162). The crude 2,2'-disulfanediyldibenzoyl chloride was suspended in dry CCl_4 at RT and an anhydrous[3] flux of Cl_2 was bubbled through the suspension until the suspended solid residue was completely dissolved. The reaction vessel was tightly closed and the bubbling was stopped so to leave the reaction mixture under a Cl_2 saturated atmosphere for an additional 1 h. The reaction mixture was rapidly filtered and the solvent was distilled away under reduced pressure giving a yellow oil which was used, without any further purification, to synthesize compounds **25**-**27** and **30**.

2-Mercapto-*N*-phenylbenzamide (164). [190] To a 0°C stirring solution of aniline (232μl, 2.377mmol) in dry CH_2Cl_2 (3 ml), a 2.0 solution of $Al(Me)_3$ in dry toluol (1.19 ml, 2.377mmol) was dropwise added under nitrogen atmosphere. When the addition was complete, the reaction mixture was allowed to warm to RT and the stirring was continued until the gas evolution ceased (30 min). Then, a 1.44M solution of methyl thiosalycilate **163** in dry CH_2Cl_2 (1.651 ml, 2.377 mmol) was dropwise added and the resulting mixture was refluxed overnight. The mixture was cooled to RT and carefully added of 5 % aq HCl (5 mL) HCl 5% v/v aqueous solution (tree times) and the solvent was distilled away under reduced pressure. The resulting crude residue (874 mg) was purified by FC (SiO_2, EtOAc/Hx 20/80 to 40/60) giving 315 mg of desired product **164** (23%). mp = 116-118°C [Lit. 117-118°C (Et_2O)];[190] H^1-NMR (300 MHz, $CDCl_3$): δ = 4.55 (s, 1H), 7.14-7.22 (m, 2H), 7.27-7.39 (m, 4H), 7.56-7.62 (m, 3H), 7.82 (br s, 1H).

[3] Dried by bubbling in concentrated H_2SO_4

2-Mercapto-*N*-(naphtalen-2-yl)benzamide (165).[190] To a 0°C stirring solution of β-naphtylamine (286 mg, 2.0 mmol) in dry CH_2Cl_2 (5 ml), a 2.0M solution of $Al(Me)_3$ in dry toluol (1.00 ml, 2.0 mmol) was dropwise added under argon atmosphere. The resulting reaction mixture was allowed to warm up to RT and the stirring was continued until the gas evolution ceased (30 min). A 1.44M solution of methyl thiosalycilate **163** in dry CH_2Cl_2 (1.39 ml, 2.0 mmol) was dropwise added and the resulting mixture was refluxed overnight. The mixture was cooled to RT and carefully added of 5 % aq HCl (5 mL)with HCl 5% v/v aqueous solution (tree times) and the solvent was distilled away under reduced pressure. The resulting crude residue was purified by FC (SiO_2, EtOAc/Hx 50/50) giving 520 mg of desired product **165** as white solid (yield = 93%). mp (Et_2O)= 168-169°C [Lit. 167-168°C (Nitrobenzene)]; MS (APCI): *m*/z 278.2; H^1-NMR (300 MHz, $CDCl_3$): δ = 4.57 (s, 1H), 7.23 (m, 1H), 7.33 (td, J_1=5.92 Hz, J_2=1.26 Hz,1H), 7.38-756 (m, 4H), 7.64 (dd, J_1=7.60 Hz, J_2=1.29 Hz, 1H), 7.77-7.85 (m, 3H), 7.94 (br s, 1H), 8.33 (d, *J*=0.96 Hz, 1H).

***N*-(Biphenyl-3-yl)-2-mercaptobenzamide (166).** A solution of $AlMe_3$ (1.43 mL of 2.0 M sol. in toluene, 2.86 mmol) was added dropwise to a cooled (O °C) suspension of 3-biphenylamine (487 mg, 2.86 mmol) in anhydrous CH_2Cl_2. When the addition was complete, the reaction mixture was allowed to warm to RT and stirring was continued until the gas evolution ceased (30 min). Then, a solution of methyl thiosalicylate **163** (241 mg, 1.43 mmol) was added and the mixture was refluxed overnight. The mixture was cooled to RT and carefully added of 5 % aq HCl (5 mL). The organic layer was separated and the aqueous layer was extracted with CH_2Cl_2 (3x). The combined organic extracts were further washed with 1N HCl (2x), saturated $NaHCO_3$ and brine. Then, the organic layer was dried over anhydrous Na_2SO_4, filtered and the solvent was evaporated under reduced pressure. The residue was crystallized from CH_2Cl_2/petroleum ether furnishing 309 mg of desired product **166** as pale

yellow solid (71 %). mp (CH_2Cl_2/petroleum ether) 131-132 °C. MS (APCI): *m/z* 304.2. ^{1}H NMR ($CDCl_3$, 300 MHz): δ 4.60 (s, 1H), 7.26 (t, *J* = 7.4 Hz, 1H), 7.33-7.49 (m, 7H), 7.63-7.65 (m, 4H), 7.82 (bs, 1H), 7.89 (br s, 1H).

***tert*-Butyl benzyl(3-oxobenzo[d]isothiazol-2(3H)-yl)carbamate (167).**

Lithium hexamethyldisilazide (LiHMDS) 1.06M in dry THF (3.542 ml, 3.755 mmol) was dropwise added to a 0°C stirring solution of 2-(butoxycarbonylamino)-benzo[d]isothiazol-3(2H)-one **35** (1,0 g 3.755 mmol) in dry THF (5 ml). After 30 min, benzylbromide (547 μl, 4.506 mmol) was dropwise added and the resulting solution was stirred at RT for 20h. The reaction mixture was cooled back to 0°C and further LiHMDS 1.06M in dry THF (708 μl, 0.751 mmol) and benzylbromide (92 μl, 0.751 mmol) wad dropwise added. The resulting solution was allowed to reach RT. After 2h, the solvent was removed under reduced pressure and the obtained orange residue was taken up with Et_2O. The organic phase was washed with pH=7.0 phosphate buffer (2 times) and brine giving 2.3 g of pale yellow oil. The crude was purified by FC (SiO_2, EtOAc/Hx, 10/90 then 20/80) furnishing 467 mg of the desired compound as white solid (59%). mp 110-111°C; MS (ACPI): *m/z* 357.2; ^{1}H NMR (300 MHz, $CDCl_3$): δ 1.43 (br s, 9H), 1.63 (d, *J*=3.99 Hz, 2H), 4.47 (d, *J*=14.8 Hz, 1H), 5.28 (d, *J*=14.5 Hz, 1H), 7.32-7.37 (m, 7H), 7.58 (t, *J*=7.26 Hz,1H), 8.03 (s, *J*=8.11 Hz,1H).

3,3'-Dithiopropionyl chloride (169). A stirring suspension of 3,3'-Dithiopropionic acid **168** (1200 mg 5.7 mmol) in $SOCl_2$ (6 ml) was refluxed until complete dissolution of the solid starting material (30 min). The solvent was evaporated under reduced pressure giving a brown oil that was used for the synthesis of compound **170** without any further purifications (Quantitative) ^{1}H NMR (300 MHz, $CDCl_3$): δ 3.33 (t, *J*=6.9 Hz 4H), 2.96 (t, *J*=6.9 , 4H).

3,3'-Disulfanediylbis(*N*-phenethylpropanamide) (170).[109] To a 0°C stirring solution of 2-phenylethanamine (1370 μl, 10.88 mmol) and Et_3N (987 μl, 7.04 mmol) in dry 1,2-dichloroethane (17 ml) a 1.18 M solution (2.7

ml, 3.2 mmol) of 2,2'-dithiopropionyl chloride **169** in dry CH_2Cl_2 was dropwise added over 2 min maintaining the temperature of reaction mixture below 15°C. The resulting suspension was allowed to reach RT and was stirred for 2 h. The crude was diluted with CH_2Cl_2 (30 ml), washed with pH=4.75 acetate buffer (10 ml, 2 times) and water (10 ml, 1 time). The organic layer was dried over anhydrous Na_2SO_4, filtered and the solvent was evaporated under reduced pressure giving 2.020 g of pale yellow solid. The obtained solid was washed with Et_2O giving 1.389 g of desired product **170** as a white solid (85%). mp 134-135°C [Lit. 131-134];[109] MS (APCI): 417.4; ^{1}H NMR (300 MHz, $CDCl_3$): δ 2.53 (t, *J*=6.99 Hz, 4H), 2.84 (t, *J*=7.02 Hz, 4H), 3,55 (q, *J*=6.87 Hz, 4H), 5.93 (br s, 2H), 7.20-7.35 (m, 10H)

3,3'-Disulfanediylbis(N-(biphenyl-4-yl)propanamide) (172). To a 0°C cooled stirring solution of 3,3'-dithiopropionic acid **168** (200 mg, 0.95 mmol) in dry DMF (6.8 ml), Et_3N (202 μl, 2.079 mmol) and HBTU (765 mg, 1.98 mmol) were added. The resulting solution was allowed to reach RT and it was stirred under N_2 for 45 min. 4-phenylaniline (321 mg, 1.9 mmol) was added in one portion and suddenly the crude solution became a white suspension. After DMF removal by vacuum distillation, the crude was diluted with CH_2Cl_2 and filtered giving 392 mg of desired product **172** as white solid. mp >230°C; MS(APCI): 256.3; ^{1}H NMR (300 MHz, $CDCl_3$): δ 2.77 (t, *J*=6.84 Hz, 4H), 3.04 (t, *J*=7.05 Hz, 4H), 7.31 (t, *J*=6.72 Hz, 2H), 7.42 (t, *J*=7.77 Hz, 4H), 7.58-7.68 (m, 12H), 10.15 (br s, 2H).

B) Final compounds:

2-Methylbenzo[d]isothiazol-3(2H)-one (19).[190, 201] To a RT stirring solution of benzo[d]isothiazol-3(2H)-one **18** (61 mg, 0.393 mmol) in CH_3CN (2 ml) anhydrous K_2CO_3 (54 mg, 0.393 mmol) and KI (88 mg, 166.00) was added. The resulting white suspension was refluxed for 30 min and then

cooled back to RT. Iodomethane (25 μl, 0.393 mmol) was added and the reaction mixture was stirred at RT for 20h under nitrogen atmosphere. The solvent was evaporated under reduced pressure and the crude was purified by FC(SiO_2, CH_2Cl_2 100% then CH_2Cl_2/Et_2O 95/5) furnishing 287 mg of pure 2-methylbenzo[d]isothiazol-3(2H)-one **19** as white waxy solid (65%); mp = 54°C (Lit. 54°C);[201] MS (APCI): *m/z* 165.8; ^{1}H NMR (300 MHz, $CDCl_3$): δ 3.46 (s, 3H) , 7.41 (td, J_1= 7.98 Hz, J_2= 1.23 Hz, 1H), 7,55 (d, *J*=7.86 Hz, 1H), 7.62 (d, J_1= 8.1 Hz, J_2= 7.05 Hz, 1H), 8.05 (d, *J*= 7.98 Hz, 1H). Anal.calc. for C_8H_7NOS (MW=165.21) C, 58.15; H, 4.27; N, 8.48. Found: C, 58.43; H, 4.35; N, 8.19.

2-(Oct-7-ynyl)benzo[d]isothiazol-3(2H)-one (20). A stirring suspension of benzo[d]isothiazol-3(2H)-one **18** (486 mg, 3.213 mmol), K_2CO_3 (555 mg, 4,06 mmol) and KI (89 mg, 0,536 mmol) CH_3CN (24 ml) was refluxed for 30 min under nitrogen atmosphere and cooled back to RT. Then, a solution 13.38M of oct-7-ynyl methanesulfonate **157** (200 μl, 2,68 mmol) in dry CH_2Cl_2 was dropwise added and the resulting mixture was refluxed for 1h. The solvent was evaporated under reduced pressure, EtOAc was added and the obtained suspension was washed (twice) with H_2O. The organic phase was dried over anhydrous Na_2SO_4, filtered and evaporated under reduced pressure furnishing 536 mg of yellow oil that was purified by FC (SiO_2, CH_2Cl_2/Et_2O 95/5) furnishing 156 mg of pure product **20** as pale yellow powder (23%); mp = 46-48°C; MS (APCI) *m/z* 259.8; H^1-NMR (300 MHz, $CDCl_3$): δ = 1.32-1.50 (m, 6H), 1.73 (quint, *J*=7.38 Hz, 2H), 1.89 (t, *J*=2.61 Hz, 1H), 2.13 (td, J_1=6.75 Hz, J_2=2.55 Hz, 2H), 3.85 (t, *J*=7.08 Hz, 2H), 7.34 (t, *J*=6.76 Hz, 1H), 7.57-7.4881 (m, 2H), 7.97 (br d, *J*=7.92 Hz, 1H) Anal.calc. for $C_{15}H_{17}NOS$ (MW=259,37) C, 69.46; H, 6.61; N, 5.40. Found: C, 69.55; H, 6.65; N, 5.31.

2-(6-(Piperidin-1-yl)hexyl)benzo[d]isothiazol-3(2H)-one (21). Piperidine (29 μl, 0.29 mmol) was dropwise added to a RT stirring solution of K_2CO_3 (169.03 mg, 1.223 mmol), KI (8.13 mg, 0.049 mmol) and 2-(6-

chlorohexyl)benzo[d]isothiazol-3(2H)-one **153** (66 mg, 0.245 mmol) in dry DMF (1 ml). The resulting suspension was heated to 60°C and stirred under nitrogen atmosphere. After 18 h the reaction wasn't complete so further piperidine (29 μl, 0.29 mmol) and DMF (1 ml) was added and the reaction was carried out by microwave irradiation (Power=200 W, Temperature=110°C, Pressure=100 psi, Time=5 min). DMF was removed by distillation under reduced pressure and EtOAc was added. After filtration, the crude was purified by FC (SiO_2, CH_2Cl_2/MeOH 95/5 then CH_2Cl_2/$MeOH_{(NH3)}$ from 99/1 to 97/3) giving 33 mg of expected product **21** as colorless oil (Yield=41%); MS (APCI): *m/z* 319.5; ^{1}H NMR (300 MHz, $CDCl_3$): δ 1.32-1.61 (m, 12H) , 1.75 (q, *J*= 7.08 Hz, 2H), 2.27 (t, *J*=7.77 Hz, 2H), 2.35 (br s, 4H), 3.87 (t, *J*=7.29 Hz, 2H), 7.38(t, *J*=6.72 Hz, 1H), 7.53 (d, *J*=7.41 Hz, 1H), 7.58 (t, *J*=5.88 Hz, 1H), 8.00 (d, *J*=7.89 Hz, 1H); Anal.calc. for $C_{18}H_{26}N_2OS$ x ½ H_2O (MW=327.48) C, 66.01; H, 8.31; N, 8.55. Found: C, 66.33; H, 8.15; N, 8.42.

Nonan-2-ylbenzo[d]isothiazol-3(2H)-one (22). To a 0°C stirring solution of Et_3N (2207 μl, 15.732 mmol) and 2-aminononane (1007 μl, 5.496 mmol) in dry THF (13.77 ml), a 0.21 M solution of 2,2'-disulfanediyldibenzoyl chloride **161** in dry THF (12.30 ml, 2.583 mmol) was dropwise added over 15 min under nitrogen atmosphere. The obtained white suspension was gradually warmed to RT and stirred for 16h. A 0.08M solution of I_2 in dry THF (52 ml, 4.16 mmol) was dropwise added and the resulting pale brown suspension was stirred overnight. The solvent was distilled away under reduced pressure. Then, a pH=7.00 phosphate buffer was added and the resulting mixture was extracted with CH_2Cl_2 (3 times). The combined organic layers were dried over anhydrous Na_2SO_4, filtered and concentrated under reduced pressure to give 591 mg of yellow residue that was purified by FC (SiO_2, EtOAc/Hx 10/90 then 55/45) and distilled (rectified using a distillation apparatus equipped with Vigreux column) furnishing 170 mg of pure product **22** as colourless oil (44%) and 103 mg

of slightly dirty desired product as pale yellow oil. MS (APCI): *m*/z 277.8; H^1-NMR (300 MHz, CDCl3): δ = 0.87 (t, *J*=6.45 Hz, 3H), 1.31-1.25 (m, 10H), 1.39 (d, *J*=6.66 Hz, 3H), 1.71 (m, 2H), 4.93-4.82 (m, 1H), 7.41 (ddd, J_1=7.95 Hz, J_2=6.33 Hz, J_3=1.86 Hz, 1H), 7.64-7.57 (m, 2H), 8.06 (d, *J*=7.86 Hz, 1H). Anal.calc. for $C_{16}H_{23}NOS$ (MW=277,42) C, 69.27; H, 8.36; N, 5.05. Found: C, 69.57; H, 8.32; N, 5.05

Cyclohexylbenzo[d]isothiazol-3(2H)-one (23).[42a] To a 0°C stirring solution of Et_3N (2.200 ml, 15.72 mmol) and aminocyclohexane (635 μl, 5.5 mmol) in dry THF (10.7 ml), a 0.22 M solution of 2,2'-disulfanediyldibenzoyl chloride **161** in dry THF (11.90 ml , 2.62 mmol) was dropwise added over 15 min under nitrogen atmosphere. The obtained white suspension was gradually warmed to RT and stirred for 16h. A 1.6 M solution of I_2 in dry THF (3.62 ml, 5.8 mmol) was dropwise added and the resulting pale brown suspension was stirred overnight. The solvent was distilled away under reduced pressure. Then, a pH=4.55 acetate buffer was added and the resulting mixture was extracted with CH_2Cl_2 (3 times). The combined organic layers were washed with brine, dried over anhydrous Na_2SO_4, filtered and purified by FC (SiO_2, Hx/Et_2O 64/46) and vacuum distillation furnishing 312 mg of white solid (30%). mp = 84-85°C [Lit. 85-87];[42a] MS (APCI): *m*/z 234.0; H^1-NMR (300 MHz, $CDCl_3$): δ = 1.20-1.30 (m, 1H), 1.42-1.60 (m, 4H), 1.74 (br d, *J*=13.08 Hz, 1H), 1.89 (d, *J*=11.97 Hz, 2H), 2.06 (d, *J*=10.32 Hz, 2H), 4.58-4.65 (m, 1H), 7.39 (ddd, J_1=7.95 Hz, J_2=6.15 Hz, J_3=1.95 Hz, 1H), 7.62-7.55 (m, 2H), 8.04 (d, *J*=7.89 Hz, 1H). Anal.calc. for $C_{15}H_{17}NOS$ (MW=233,33) C, 66.92; H, 6.48; N, 6.00. Found: C, 66.68; H, 6.58; N, 5.82.

2-(4-Ethylbenzyl)benzo[d]isothiazol-3(2H)-one (24). A stirring suspension of benzo[d]isothiazol-3(2H)-one **18** (238 mg, 1.568 mmol), K_2CO_3 (271 mg, 1.96 mmol) and KI (44 mg, 0,26 mmol) CH_3CN (12 ml) was refluxed for 30 min under nitrogen atmosphere and cooled back to RT Then, a solution 6.53M of 4-Ethylbenzyl methanesulfonate **159** (200 μl,

1.307 mmol) in dry CH_2Cl_2 was dropwise added and the resulting mixture was refluxed for 30 min. The reaction mixture was filtered and the solvent was evaporated under reduced pressure. The resulting residue (395 mg) was purified by FC (SiO_2, CH_2Cl_2 100% then CH_2Cl_2/MeOH 98/2) giving 195 mg of desired product **24**.(55%); mp (Hexane) = 84-86°C ; MS (APCI): *m/z* 270.4; H^1-NMR (300 MHz, $CDCl_3$): δ = 1.22 (t, *J*=7.5 Hz, 3H), 2.63 (quart, *J*=7.8 Hz, 2H), 5.02 (s, 1H), 7.19 (d, *J*=8.1 Hz, 2H), 7.27 (d, *J*=8.1 Hz, 2H), 7.40 (ddd,J_1=7.8 Hz, J_2=7.2 Hz, J_3=1.2 Hz, 1H), 7.40 (dt, J_1=8.1 Hz, J_2=0.9 Hz, 1H), 7.59 (ddd, J_1=8.1 Hz, J_2=7.2 Hz, J_3=1.5 Hz, 1H) 8.06 (br d, *J*=7.8 Hz, 1H). Anal.calc. for $C_{15}H_{17}NOS$ * 1/3 H_2O (MW=275,31) C, 69.80; H, 5.73; N, 5.09. Found: C, 70.00; H, 5.65; N, 5.11.

2-(Phenylethyl)benzo[d]isothiazol-3(2H)-one (25).[42a] To a 0°C stirring suspension of 2-phenylethanamine (74 μl, 0.587 mmol) and Et_3N (400 μl, 2.853 mmol) in dry CH_2Cl_2 (1 ml) a 0.392M solution (1.0 ml, 0.39 mmol) of 2-(chlorocarbonyl)phenyl hypochlorothioite **162** in dry CH_2Cl_2 was dropwise added over 2 min. The reaction mixture was stirred at RT under N_2 overnight (18 h). The solvent was distilled away under reduced pressure from the reaction mixture obtaining a dark-yellow residue. It was taken up with EtOAc and the resulting mixture was washed with Na_2CO_3 saturated aqueous solution (10 ml), 0.1M HCl aqueous solution (3*10 ml) and brine. The organic layer was concentrated under reduced pressure and purified by FC (SiO_2, EtOAc/Hx 30/70) giving 16 mg of expected product **25** as pale yellow powder (11%). mp (Hexane) 90-92°C [Lit. 93-95] [42a] MS (APCI): *m/z* = 256.2;^{1}H NMR (300 MHz, $CDCl_3$): δ 3.09 (d, *J*=7.68 Hz, 2H) , 4.15 (d, *J*= 7.35 Hz, 2H), 7.24-7.35 (m, 5H), 7.40 (td, J_1=7.95 Hz, J_2=1.02 Hz, 1H), 7.52 (br d, *J*=8.1 Hz, 1H), 7.60 (td, J_1=8.16 Hz, J_2=1.2 Hz, 1H), 7.53 (d, *J*=7.41 Hz, 1H), 7.58 (t, *J*=5.88 Hz, 1H), 8.04 (dd, J_1=7.86 Hz, J_2=0.66 Hz, 1H). Anal.calc. for $C_{15}H_{13}NOS$ (MW=255,33) C, 70.56; H, 5.13; N, 5.49. Found: C, 70.58; H, 5.10; N, 5.39.

2-(2-(Naphthalen-2-yl)ethyl)benzo[d]isothiazol-3(2H)-one (26). To a 0°C stirring suspension of 2-(naphthalen-2-yl)ethanamine hydrochloride (129.2 mg, 0.5909 mmol) and Et_3N (500 μl, 3.587 mmol) in dry CH_2Cl_2 (1 ml) a 0.392M solution (2.60ml, 1.0187 mmol) of 2-(chlorocarbonyl)phenyl hypochlorothioite (**162**) in dry CH_2Cl_2 was dropwise added over 2 min. The reaction mixture was stirred at RT under N_2 overnight (18 h). The solvent was distilled away under reduced pressure from the reaction mixture obtaining a dark-yellow residue. It was taken up with EtOAc and the resulting mixture was washed with Na_2CO_3 saturated aqueous solution (10 ml), 0.1M HCl aqueous solution (3*10 ml) and brine. The organic layer was concentrated under reduced pressure and purified by FC (SiO_2, CH_2Cl_2 100%) giving 28 mg of expected product **26** as pale yellow powder (15%). mp (Hexane) 114-115°C; MS (APCI): *m/z* = 306.3; ^{1}H NMR (300 MHz, $CDCl_3$): δ 3.24 (t, *J*= 7.5Hz Hz, 2H) , 4.23 (t, *J*= 7.2 Hz, 2H), 7.36-7.50 (m, 5H), 7.581 (td, J_1= 8.16 Hz, J_2= 1.17 Hz, 1H), 7.71 (s, 1H), 7.76-7.83 (m, 3H), 8.04 (d, *J*=7.8 Hz, 1H). Anal.calc. for $C_{19}H_{15}NOS$ * 1/10 H_2O (MW=307.17) C, 74.28; H, 4.99; N, 4.56. Found: C, 74.21; H, 4.97; N, 4.58.

2-(2-(Naphthalen-1-yl)ethyl)benzo[d]isothiazol-3(2H)-one (27). To a 0°C stirring suspension of 2-(naphthalen-1-yl)ethanamine hydrochloride (129.2 mg, 0.5909 mmol) and Et_3N (500 μl, 3.587 mmol) in dry CH_2Cl_2 (1 ml) a 0.392M solution (2.60ml, 1.0187 mmol) of 2-(chlorocarbonyl)phenyl hypochlorothioite (**162**) in dry CH_2Cl_2 was dropwise added over 2 min. The reaction mixture was stirred at RT under N_2 overnight (18 h). The solvent was distilled away under reduced pressure from the reaction mixture obtaining a dark-yellow residue. It was taken up with EtOAc and the resulting mixture was washed with Na_2CO_3 saturated aqueous solution (10 ml), 0.1M HCl aqueous solution (3*10 ml) and brine. The organic layer was concentrated under reduced pressure and purified by FC (SiO_2, CH_2Cl_2 100%) giving 25 mg of expected product **27** as pale yellow powder (14%). mp (Hexane) 101-102°C; MS (APCI): *m/z* = 306.2; ^{1}H

NMR (300 MHz, $CDCl_3$): δ 3.54 (t, *J*=7.8 Hz, 2H) , 4.218 (t, *J*=7.8 Hz, 2H), 7.63-7.388 (m, 7H), 7.777 (t, *J* = 4,5 Hz, 1H), 7.881 (d, *J*=7.8 Hz, 1H), 8.078 (d, *J*=7.8 Hz, 1H), 8.25 (d, *J*=8.4 Hz, 1H). Anal.calc. for $C_{19}H_{15}NOS$ (MW=305,39) C, 74.72; H, 4.95; N, 4.59. Found: C, 74.66; H, 4.98; N, 4.61.

2-Phenylbenzo[d]isothiazol-3(2H)-one (28).[190] To a 0°C stirring solution of 2-mercapto-N-phenylbenzamide **164** (315 mg, 1.373 mmol) and TFA (312.45 μl, 4.08 mmol) in dry CH_2Cl_2 (16.6 ml), a solution of PIFA ([bis(trifluoroacetoxy)iodo]benzene) (877.3 mg, 2.04 mmol) in dry CH_2Cl_2 (27.4 ml) was dropwise added under nitrogen atmosphere and the resulting mixture was stirred for 1h. The solvent was removed under reduced pressure and the crude was purified by FC (SiO_2, EtOAc/Hx 30/70) giving 311 mg of pure product **28** as brown solid (99%); mp (Hexane) = 135-137°C [Lit. 139-140 (EtOH)] [190]; H^1-NMR (300 MHz, $CDCl_3$): δ = 7.34 (tt, J_1=7.5 Hz, J_2=1.0 Hz, 1H), 7.488 (dt, J_1=8.13 Hz, J_2= 7.35 Hz, 3H), 7.61 (br d, *J*=8.01 Hz, 1H), 7.67-7.75 (m, 3H), 8.13 (br d, *J*=7.92 Hz, 1H). MS (APCI): *m/z* 228.0. Anal.calc. for $C_{13}H_9NOS$ (MW=227,28) C, 68.70; H, 3.99; N, 6.16. Found: C, 68.88; H, 4.13; N, 6.01.

2-Naphtyllbenzo[d]isothiazol-3(2H)-one (29). [190] To a 0°C stirring solution of 2-mercapto-N-(naphtalen-2-yl)benzamide **2** (140 mg, 0.5 mmol) and TFA (114 μl, 4.08 mmol) in dry CH_2Cl_2 (16.6 ml), a solution of PIFA ([bis(trifluoroacetoxy)iodo]benzene) (877.3 mg, 1.49 mmol) in dry CH_2Cl_2 (8 ml) was dropwise added under nitrogen atmosphere and the resulting mixture was stirred for 1h. The solvent was removed under reduced pressure and the crude was purified by FC (SiO_2, CH_2Cl_2/Hx 80/20) giving 85 mg of desired product **29** as brown solid (61%). mp (petroleum ether)= 164-166°C [Lit. 165 (EtOH)];[202] MS (APCI): *m/z* 278.1; H^1-NMR (300 MHz, $CDCl_3$): δ = 7.48 (d, *J*=7.2 Hz, 1H), 7.52-7.58 (m, 2H), 7.63 (d, *J*=7.95 Hz, 1H), 7.72 (t, *J*=7.15 Hz), 7.89-7.98 (m, 4H), 8.16 (m, 2H). Anal.calc. for $C_{17}H_{11}NOS$ (MW=277,34) C, 73.62; H, 4.00; N, 5.03. Found: C, 73.39; H, 4.04; N, 5.00.

2-(Biphenyl-4-yl)benzo[d]isothiazol-3(2H)-one (30). To a 0°C stirring suspension of *p*-phenylaniline (100 mg, 0.5909 mmol) and Et_3N (500 µl, 3.587 mmol) in dry CH_2Cl_2 (1 ml) a 0.392M solution (2.30ml, 0.90 mmol) of 2-(chlorocarbonyl)phenyl hypochlorothioite (**162**) in dry CH_2Cl_2 was dropwise added over 2 min. The reaction mixture was stirred at RT under N_2 overnight (18 h). The solvent was distilled away under reduced pressure from the reaction mixture obtaining a dark-yellow residue. It was taken up with EtOAc and the resulting mixture was washed with Na_2CO_3 saturated aqueous solution (10 ml), 0.1M HCl aqueous solution (3*10 ml) and brine. The solvent was distilled away from organic layer under reduced pressure giving a crude that was purified by FC (SiO_2, CH_2Cl_2 100%) giving 21 mg of expected product **30** as pale yellow powder (12%); mp (Hexane) 175-176°C; MS (APCI): *m/z* = 304.5; ^{1}H NMR (300 MHz, $CDCl_3$): δ 7.37 (t, *J*=7.2 Hz, 1H) , 7.46 (t, *J*= 7.5 Hz, 3H), 7.59-7.705 (m, 6H), 7.79 (d, *J*=8.4 Hz, 4H), 8.13 (d, *J*=7.8 Hz, 1H). Anal.calc. for $C_{19}H_{13}NOS$ * 1/2 H_2O (MW=312,39) C, 73.05; H, 4.52; N, 4.48. Found: C, 72.75; H, 4.31; N, 4.36.

2-(Biphenyl-3-yl)benzo[d]isothiazol-3(2H)-one (31) A solution of PIFA ([bis(trifluoroacetoxy)iodo]benzene), 598 mg, 1.39 mmol) in 20 mL of anhydrous CH_2Cl_2 was added at 0 °C to a solution of **166** (284 mg, 0.930 mmol) and TFA (0.216 mL, 2.79 mmol) in 15 mL of anhydrous CH_2Cl_2, and the solution was stirred for 1 h. Then, the solvent was removed under reduced pressure and the resulting residue was purified by FC (SiO_2, n-hexane/EtOAc, 5:1) furnishing 200 mg of desired product **31** as white solid (71 %). mp (EtOH/ H_2O) 104-105 °C; MS (APCI): *m/z* 304.4. ^{1}H NMR ($CDCl_3$, 300 MHz) δ 7.38 (t, *J* = 7.0 Hz, 1H), 7.44-7.49 (m, 3H), 7.54-7.55 (m, 2H), 7.59-7.71 (m, 5H), 7.95 (t, *J* = 1.0 Hz), 8.12 (d, *J* = 8.5 Hz, 1H). Anal.calc. for $C_{19}H_{13}NOS$ (MW=303.38) C, 75.22; H, 4.32; N, 4.62. Found: C, 75.32; H, 4.11; N, 4.57.

2-Amino-benzo[d]isothiazol-3(2H)-one (32)[43a] A mixture of trifluoroacetic acid (8.9 ml, 116 mmol), water (1 ml) and 2-(butoxycarbonylamino)-benzo[d]isothiazol-3(2H)-one **35** (510 mg, 1.91 mmol) was stirred for 150 min at RT. Then, $NaHCO_3$ 10% aqueous solution (123.2 ml) was added and the resulting solution was extracted with CH_2Cl_2 (three times). The combined organic layers were dried over anhydrous Na_2SO_4, filtered, concentrated under reduced pressure and purified by FC (SiO2, EtOAc/Hx 60/40) giving 180 mg desired product **32** as pale yellow solid (yield = 57%). mp (H_2O)= 128-129°C[Lit. 138-141 (H_2O)];[43a] MS (APCI): *m*/z 167.2; H^1-NMR (300 MHz, CDCl3): δ = 4.65 (br s, 2H), 7.39 (br t, *J*=7.72 Hz, 1H), 7.50 (d, *J*=8.2 Hz, 1H), 7.62 (ddd, J_1=8.23 Hz, J_2= 5.42 Hz, J_3=1.125 Hz, 1H), 8.02 (br d, *J*=7.86 Hz, 1H). Anal.calc. for $C_7H_6N_2OS$ * 1/10 H_2O (MW=168,00) C, 50.04; H, 3.72; N, 16.67. Found: C, 50.39; H, 3.59; N, 16.28

2-(Benzylamino)benzo[d]isothiazol-3(2H)-one (33). A 0°C cooled suspension of *tert*-butyl benzyl(3-oxobenzo[d]isothiazol-2(3H)-yl)carbamate (**167**) (400 mg, 1.1216 mmol) in Cl_3CCOOH/H_2O 9:1 w/w mixture (4.447 mg) was stirred for 2h and then for further 2h at RT. To the resulting solution, a $NaHCO_3$ saturated aqueous solution was dropwise added until the gas evolution ceased. The crude was saturated with Na_2CO_3 and extracted with EtOAc (4 times). Mixed organic layers was evaporated to dryness and purified by FC (SiO_2, CH_2Cl_2 100% then CH_2Cl_2/Et_2O 90/10) giving 282 mg of desired final product **33** as a pale yellow residue (98%). mp (Hexane) 121.1-121.5°C; MS (ACPI): *m*/z 257.2; ^{1}H NMR (300 MHz, $CDCl_3$): δ 3.66 (bs, 1H), 4.34 (s, 2H), 7.47-7.33 (m, 8H), 7.62 (td, J_1=7.08 Hz, J_2=0.99 Hz, 1H), 8.0 (d, *J*=7.86 Hz ,1H). Anal.calc. for $C_{14}H_{12}N_2OS$ (MW=256,32) C, 65.60; H, 4.72; N, 10.93. Found: C, 65.60; H, 4.72; N, 10.93.

2-(Benzyl(methyl)amino)benzo[d]isothiazol-3(2H)-one (34). To a RT stirring solution of 2-(benzylamino)benzo[d]isothiazol-3(2H)-one **33** (58

mg, 0.226 mmol) in MeI (700 μl, 11.18 mmol) imidazole (16 mg, 0.235 mmol) was added in one portion. The stirring was maintained for 16 h under nitrogen atmosphere. The solvent was evaporated under reduced pressure. The crude was purified by FC (SiO_2, CH_2Cl_2/MeOH 99/1) and by vacuum distillation giving 39 mg of desired product **34** as a pale yellow waxy solid (64%). mp 136-139°C (darkening) then 142-143°C (melting); MS (APCI): 271.3; ^{1}H NMR (300 MHz, $CDCl_3$): δ 2.95 (s, 3H), 4.24 (s, 2H), 7,25-7.35 (m, 4H), 7.44 (d, *J*= 8.01 Hz,1H), 7.58 (td, J_1= 7.98 Hz, J_2= 1.23 Hz,1H), 8.00 (d, *J*=7.86 Hz,1H). Anal.calc. for $C_{15}H_{14}N_2OS$ (MW=270,35) C, 66.64; H, 5.22; N, 10.36. Found: C, 66.87; H, 5.46; N, 9.84.

2-(Butoxycarbonylamino)-benzo[d]isothiazol-3(2H)-one (35).[43a] To a 0°C stirring solution of Et_3N (1.520 ml, 10.84 mmol) and *tert*-butyl hydrazinecarboxylate (501 mg, 3.78 mmol) in dry THF (7.4 ml), a 0.209 M solution of 2,2'-disulfanediyldibenzoyl chloride **161** (620 mg, 1.8 mmol) in dry THF (8.6 ml) was dropwise added over 15 min under nitrogen atmosphere. The obtained white suspension was gradually warmed to RT and stirred for 16h. A 0.263M solution of I_2 (15 ml) in dry THF was dropwise added and the resulting pale brown suspension was stirred for 4h. The solvent was distilled away under reduced pressure, a pH=7.00 phosphate buffer was added and the resulting mixture was extracted with CH_2Cl_2 (3 times). The combined organic layers were dried over anhydrous Na_2SO_4, filtered and concentrated under reduced pressure furnishing 1.6 g of brown residue that was purified by FC (SiO_2, EtOAc/Hx 40/60) giving 865 mg of desired product **35** as a pale yellow wax (90%). m.p. (CH_2Cl_2/Et_2O) = 170-171°C [Lit. 170-171 (EtOAc)] [43a] MS (APCI): *m*/z 267.2; H^1-NMR (300 MHz, $CDCl_3$): δ = 1.51 (s, 9H), 7.06 (bs, 1H), 7.41 (t, *J*=7.26 Hz, 1H), 7.51 (d, *J*=8.07 Hz, 1H), 7.67 (t, *J*=8.22 Hz, 1H), 8.07 (d, *J*=7.89 Hz, 1H). Anal.calc. for $C_{12}H_{14}N_2O_3S$ (MW=266,32) C, 54.12; H, 5.30; N, 10.52. Found: C, 54.08; H, 5.14; N, 10.52.

2-Phenethylisothiazol-3(2H)-one (36). [109] A 0.75M solution of SO_2Cl_2 in dry 1,2-dichloroethane (4,8 ml, 3.6 mmol) was dropwise added to a 0°C stirring suspension of 3,3'-disulfanediylbis(*N*-phenethylpropanamide) **170** (500 mg, 1.2 mmol) in dry 1,2-dichloroethane (7 ml) over 2h. The solvent was evaporated under reduced pressure and the yellow oily residue was taken up with CH_2Cl_2. The resulting mixture was washed with H_2O (10 ml, 2 times), dried over anhydrous Na_2SO_4, filtered and concentrated under reduced pressure giving 697 mg of yellow oil. The crude was purified by FC (SiO_2, CH_2Cl_2/Et_2O 98/2 then 90/10) giving 194 mg of desired product **36** as a pale yellow powder (39%). mp (Hexane) 78-79°C [Lit. 76-78 (benzene/hezane)]; [109] MS (APCI): 206.2; ^{1}H NMR (300 MHz, $CDCl_3$): δ 3.04 (t, *J*=7.44 Hz, 2H), 4.051 (t, *J*=7.14 Hz, 2H), 6.27 (q, *J*=6.24 Hz, 1H), 7.22-7.35 (bs, 5H), 8.00 (d, *J*=6.24 Hz, 1H).

2-(Biphenyl-4-yl)isothiazol-3(2H)-one (37) A 0.75M solution of SO_2Cl_2 in dry 1,2-dichloroethane (2,37 ml, 1.78 mmol) was dropwise added to a 0°C stirring suspension of 3,3'-disulfanediylbis(*N*-(biphenyl-4-yl)propanamide) **172** (300 mg, 0.58 mmol) in dry 1,2-dichloroethane (3 ml) over 2h. The resulting white suspension was allowed to reach RT and stirred for 1h. The solvent was evaporated under reduced pressure and the solid residue was taken up with CH_2Cl_2. The obtained suspension was filtered, concentrated to reduced pressure and purified by FC((SiO_2, EtOAc/Hx 30/70 then 50/50) giving 80 mg of pale yellow solid. Two consecutive crystallization from toluene gave 40 mg of desired product **39** as white crystals (54%). mp (toluol) 196-197°C; MS (APCI): 254.1; ^{1}H NMR (300 MHz, $CDCl_3$): δ 6.38 (d, *J*=6.33 Hz, 1H), 7.39 (t, *J*=7.29 Hz, 1H), 7.48 (t, *J*=7.17 Hz, 2H), 7.61 (d, *J*=7.44 Hz, 2H), 7.69 (s, 4H), 8.20 (d, *J*=6.36 Hz, 1H).

3-(Oct-7-ynyloxy)benzo[d]isothiazole (38). It was co-synthesized with compounds **20**. The crude product (300 mg of yellow oil) was purified by FC (SiO_2, EtOAc/Hx 4/96) furnishing 218 mg of pure product as

a pale yellow oil (31%); MS (APCI): *m*/z 260.2; H^1-NMR (300 MHz, $CDCl_3$): δ = 1.61 (m, 6H), 1.90 (m, 3H), 2.23 (td, J_1=6.57 Hz, J_2=2.52 Hz, 2H), 4.56 (t, *J*=6.57 Hz, 2H), 7.39 (t, *J*=7.83 Hz, 1H), 7.53 (t, *J*=8.01 Hz, 1H), 7.78 (d, *J*=8.1 Hz, 1H), 7.93 (d, *J*=7.98 Hz, 1H). Anal.calc. for $C_{15}H_{17}NOS$ (MW=259,37) C, 69.46; H, 6.61; N, 5.40. Found: C, 69.62; H, 6.60; N, 5.37.

3-(4-Ethylbenzyl)benzo[d]isothiazol-3(2H)-one (39). It was co-synthesized with compounds **24**. The crude residue (395 mg) was purified by FC (SiO_2, EtOAc/Hx 4/96) giving 169 mg of desired product **39** as a pale yellow oil (48%); MS (APCI): *m*/z 270.4; H^1-NMR (300 MHz, $CDCl_3$): δ = 1.259 (t, *J*=7.8 Hz, 3H), 2.68 (q, *J*=7.8 Hz, 2H), 5.56 (s, 2H), 7.24 (d, *J*=7.8 Hz, 2H), 7.37 (t, *J*=7.8 Hz, 1H), 7.45 (d, *J*=8.1 Hz, 2H), 7.51 (t, *J*=6.9 Hz, 2H), 7.77 (d, *J*=7.5 Hz, 1H), 7.93 (d, *J*=7.8 Hz, 1H). Anal.calc. for $C_{15}H_{17}NOS$ (MW=269,36) C, 71.34; H, 5.61; N, 5.20. Found: C, 71.46; H, 5.61; N, 5.30.

4.2.3 Biology

Collected biological data were from experimentations carried out by Prof. D. Piomelli's research group *(Department of Pharmacology, University of California Irvine, Irvine, CA, USA)*.

MAGL inhibition assay. Monoacylglycerol lipase activity was measured as previously described (King *et al.*, 2007). Briefly, either 10 ng of purified MAGL or 2.5–50 μg of protein from MAGL-transfected HeLa cell lysates were pre-incubated with inhibitors for 10 min at 37°C in assay buffer (50 mM Tris-HCL, pH 8.0, 0.5 mg/ml bovine serum albumin, fatty acid-free). Following pre-incubation, 2-oleoylglycerol (2-OG) substrate (10 μM final) was added, and samples were incubated for an additional 10 min at 37°C. Reactions were stopped with chloroform/methanol (2:1, v/v), containing heptadecanoic acid (5 nmol) as an internal standard. In some experiments with cell lysates, 1-heptadecanoylglycerol (1-HG) and

heptadecenoic acid were used as substrate and internal standard respectively. Samples were subjected to centrifugation at 2000 x *g* at 4°C for 10 min, and the organic layers were collected and dried under a stream of N_2. The residues were suspended in chloroform/methanol (1:3, v/v) and analyzed by liquid chromatography/mass spectrometry (LC/MS).

LC/MS analysis. A reversed-phase Eclipse C18 column (30 x 2.1 mm i.d., 1.8 μM, Agilent Technologies, Wilmington, DE, USA) was used. It was eluted with 95% of solvent A and 5% solvent B for 0.6 min at a flow rate of 0.6 mL/min^{-1} with column temperature set at 50°C. Solvent A consisted of methanol containing 0.25% acetic acid and 5 mM ammonium acetate. Solvent B consisted of water containing 0.25% acetic acid and 5 mM ammonium acetate. Under these conditions, analytes eluted from the column at the following retention times: oleic acid, 0.34 min; heptadecanoic acid, 0.37 min; heptadecenoic acid, 0.29 min. Electrospray ionization was in the negative mode, capillary voltage was set at 4 Kv, and fragmentor voltage was 100 V. N_2 was used as drying gas at a flow rate of 13 L/min^{-1} and a temperature of 350°C. Nebulizer pressure was set at 60 psi. For quantification purposes, we monitored the $[M-H]^-$ ions of *m/z* = 281.3 for oleic acid, *m/z* = 269 for heptadecanoic acid, and *m/z* = 267 for heptadecenoic acid.

Chapter 5

References

1. (a) Evans, D. C. *et al*.; *Chem. Res. Toxocol*. **2004**, *17*, 3–16. (b) Kalgutkar, A. S. *et al*.; *Curr. Drug Metab*. **2005**, 6, 161–225. (c) Liebler, D. C. *et al*.; *Nat. Rev. Drug Discovery* **2005**, *4*, 410–420. (d) Wiliams, *D. P. Toxicology* **2006**, *226*, 1–11. (e) Park, B., K. *et al*.; *R. Chem. Res. Toxicol*. **1998**, *11*,969–988.
2. Potashman, Michele H. *et al*.; *J. Med. Chem*. **2009**, *52*(5), 1231-1246.
3. Giron P. *et al.*; *Mass Spectrom. Rev.* **2010**, DOI 10.1002/mas.
4. Power J.C. *et al*; *Chem. Rev*. **2002**, *102*(12), 4639-4750.
5. Viaud J. *et al.*; *Mol. Cancer. Ther.* **2009,** *8*(9), 2559-2565.
6. Picone, R.P. *et al*.; *Mol. Pharmacol.* **2005**, *68*, 1623–1635.
7. Copeland, R. A. *Irreversible Enzyme Inactivators in Evaluation of Enzyme Inhibitors in Drug Discovery*. A Guide for Medicinal Chemists and Pharmacologists; John Wiley & Sons: New York; *Chapter 8*, pp 214-248.
8. Alvarez-Sàncez, R. *et al*.; *Chem. Res. Toxicol*. **2003**, *16* (5), 627-636.
9. Morley, J.O. *et al*.; *Int. J. Chem. Kinet.* **2007**, *39*(5), 254-260.
10. Collier P.J. *et al.*; *J. Appl. Bacteriol.* **1990**, *69*, 578-584.
11. Collier P.J. *et al.*; *J. Appl. Bacteriol.* **I990**, *69*, 569-577.
12. Tipper, D. J. *et al*.; *Proc. Natl. Acad. Sci. U.S.A*. **1965**, *54*, 1133-1141.
13. Boid D.B. *et al.*; *J. Am. Chem. Soc*. **1980**, *102*(6), 1812-1814.
14. De Biase, D. *et al.*; *J. Biol. Chem*. **1991**, *266*(30), 20056-20061.
15. Ho, T.; *Chem. Rev.*, **1975**, *75*(1), 1-20.

16. Clayden, J. *et al.;* in "*Organic Chemistry*", Oxford University Press inc., *Chap. 46*, **2001**.
17. David, A.W., *Drug metabolism in Foye's principles of medicinal chemistry*, **2008**, Foye W.O. *et al*, Ed. Lippincott Williams and Wilkins; *Chapter 10*, p. 253-326.
18. Kato, D. *et al*.; *Nat. Chem. Biol.* **2005**, *1*(1), 33-38.
19. Jeffery, A.D. *et al*.; *Curr. Opin. Biotechnol.* **2003**, *14*, 87-95.
20. A. Tiss *et al*.; *J. Mol. Catal. B: Enzym.* **2009**, *58*, 41–47.
21. Leung-Toung, R. *et al*.; *Curr. Med. Chem*. **2006**, *13*(5), 547-581.
22. Rasnick D.; *Anal. Biochem.* **1985**, *149*, 461-465.
23. Green, G.D.J. *et al*.; *J. Biol. Chem.* **1981**, *256*(4), 1923-1928.
24. Kirk, K. L. *et al*.; *Recent Advances in the Biomedicinal Chemistry of Fluorine-Containing Compounds in In Biomedical Frontiers of Fluorine Chemistry* **1996**, ACS Symposium Series; American Chemical Society: Washington, DC.
25. Singh, N. *et al*.; *Exp. Parasitol.* **2006**; *112*, 187–192.
26. Mahieu, J.P. *et al*.; *Int. J. Biomol. Macromol*., **1993**, *15*, 233-240.
27. Kraine, L. *et al*.; M.; *Chem. Rev*. **1989**, *89*(4), 689-712.
28. Shen M.L. *et al*.; *Biochem. Pharmacol.* **2000**, *60*, 947-953.
29. Shen M.L. *et al*.; *Biochem. Pharmacol.* **2001**, *61*, 537-545.
30. Casini A. *et al.*; *Environmental health perspective* **2002**, *110 (suppl. 5)*, 801-806.
31. Antonello A. *et al*.; *J. Med. Chem*.; **2006**, *49* (23), 6642-6645.
32. Labar, G. *et al*.; *ChemBioChem* **2007**, *8*, 1293-1297.
33. Kapanda, C. N. *et al*.; *J. Med. Chem*. **2009**, *52*, 7310-7314.
34. Trevillyan, J.M. *et al*.; *Arch. Bioch and Biophysics*. **1999**, *364*(1), 19-29.
35. Leung-Toung, R. *et al*.; *Bioorg. Med. Chem*. **2003**, *11*, 5529-5537.
36. Shin, J.M. *et al*.; *J. Am. Chem. Soc*. **2004**, *126*, 7800-7811.

37. a) Stimson, L. *et al*.; *Mol. Canc. Ther*. **2005**, *4*(10), 1521-1532. b) Dekker, F.J. *et al*.; *Bioorg. Med. Chem*. **2009**, *17*, 460-466. c) Dekker, F.J. *et al*.; *Bioorg. Med. Chem*. **2009**, *17*(2), 467-474.
38. Hayakawa, N. *et al*.; *Biochemistry* **1999**, *38*, 11501-11507.
39. Zani, F.; *Il Farmaco* **1992**, *47*(2), 219-228.
40. a) Domagala, J.M. *et al*.; *Bioorg. Med. Chem*. **1997**, *5*(3), 569-579. b) Domagala J.M. *et al*.; *Drug Des. Discov*. **1997**, *15*, 49-61.
41. Leung-Toung, R. *et al*.; *J. Med. Chem*. **2003**, *48*, 2266-2269.
42. a) Fischer, R. *et al*; *Arzneim.-Forsch*. **1964**, *14*, 1301-1306. b) Hurni, H. *et al*; *Arzneim.-Forsch*. **1964**, *14*, 1306-1309. c) Gialdi, F. *et al*.; *Il Farmaco Ed. Sci*. **1961**, *16*(7), 509-526. d) Ponci, R. *et al*.; *Il Farmaco Ed. Sci*. **1964**, *19*(3), 254-268.
43. a) Vicini, P. *et al*.; *Arzneim.-Forsch*. **1997**, *47(II)* Nr. 11, 1218-1221. b) Vicini P. *et al*.; *Bioorg. Med. Chem*. **2000**, *8*, 2355-2358. c) Ballabeni, V. *et al*.; *Pharm. Res*. **2002**, *46*(5), 389-393. d) Vicini, P. *et al*.; *Arzneim.-Forsch*. **1999**, *49(I)* Nr. 11, 896-899.
44. a) Wright, S.W. *et al*.; *Bioorg. Med. Chem. Lett*. **1993**, *3*(12), 2875-2878. b) Wright, S.W. *et al*.; *J. Med. Chem*. **1994**, *37*, 3071-3078. c) Wright, S.W. *et al*.; *Bioorg. Med. Chem*. **1995**, *3*(3), 227-234.
45. Schanuch. A. *et al*.; *Br. J. Dermatol*. **1998**, *138*, 467-476.
46. Weiss, G.A. *et al*.; *Proc. Natl. Acad. Sci. USA*, **1996**, 93, 10945–10948.
47. Peters, J.U.; *Curr. Top. Med. Chem*. **2007**, *7*, 579-595.
48. J. Y., Gauthier *et al*.; *Bioorg. Med. Chem. Lett*. **2008**, *18*, 923–928.
49. Smith, M.E.B. *et al*.; *J. Am. Chem. Soc*. **2010**, *132*, 1960–1965.
50. Patick, A. K.; *Antiviral Res*. **2006**, *71*, 391–396.
51. Olayioye, M. A. *et al*.; *EMBO J*. **2000**, *19*, 3159-3167.
52. Aaronson, *S. A. Science* **1991**, *254*, 1146.
53. Yarden, Y. *et al*.; *Nat. Rev. Mol. Cell. Biol*. **2001**, *2*, 127-137.
54. Kobayashi, S. *et al*.; *Engl. J. Med*. **2005**, *352*, 786–792.

55. Carter, T. A. *et al*.; *Proc. Natl. Acad. Sci.* **2005**, *102*, 11011-11016.
56. Guy PM *et al.*; *Proc. Natl. Acad. Sci. U S A* **1994**, *91*, 8132–8136.
57. Rowinsky, E.K.; *Annu. Rev. Med*. **2004**. *55*, 433–457.
58. Wells, A.; *Int. J. Biochem. Cell. Biol*. **1999**; *31*; 637-643.
59. Alroy, I. *et al.*; *FEBS Lett*. **1997**, *410*, 83-86.
60. Yarden, Y.; *Eur. J. Cancer* **2001**; *37* (Suppl. 4), 3-8.
61. Marmor, M.D. *et al.*; *Oncogene* **2004**, *23*, 2057-2070.
62. Klapper, L. N. *et al*.; *Adv. Cancer Res*. **2000**, *77*, 25-79.
63. Engebraaten, O. *et al*.; *Int. J. Cancer* **1993**, *53*, 209-214.
64. Petit, A. M. *et al*.; *Am. J. Pathol*. **1997**, *151*, 1523-1530.
65. Goldman, C. K. *et al*.; *Mol. Biol. Cell*. **1993**, *4*, 121-133.
66. Ekstrand, A. J. *et al*.; *Oncogene* **1994**, *9*, 2313-2320.
67. Moscatello, D. K. *et al*.; *J. Biol. Chem*. **1998**, *273*, 200-206.
68. Erschbamer, M. *et al*.; *J. Neurosci.* **2007**, *27*(24), 6428-6435.
69. Lynch,T.J. *et al*.; *Engl. J. Med*. **2004**, *350*, 2129–2139.
70. Yun, C.H. *et al.*; *Proc. Natl. Acad. Sci. USA*; **2008**, *105*, 2070-2075.
71. Ross J.S. *et al*.; *Stem Cells*; **1998**, *16*, 413-428.
72. Akiyama, T. *et al.; J. Biol. Chem*. **1987**, *262*, 5592.
73. Thompson, A. M. *et al*.; *J. Med. Chem*. **1995**, *38*, 3780–3788.
74. Gibson, K. H. *et al*.; *Bioorg. Med. Chem. Lett*. **1997**, *7*, 2723–2728.
75. Rewcastle, G. W. *et al*.; *J. Med. Chem*. **1997**, *40*, 1820–1826.
76. Wissner, A. *et al*.; *J. Med. Chem*. **2000**, *43*, 3244–3256.
77. Nuijen, B. *et al*.; *Int. J. Pharmac*. **2000**, *194*, 261-267.
78. Traxler, P.M. *et al*.; *J. Med. Chem*. **1996**, *39*, 2285–2292.
79. Traxler, P.M *et al*.; *J. Med. Chem*. **1997**, *40*, 3601–3616.
80. Rewcastle, G. W. *et al*.; *J. Med. Chem*. **1996**, *39*, 918–928.
81. Palmer, B. D. *et al*.; *J. Med. Chem*. **1997**, *40*, 1519–1529.
82. Stamos, J. *et al*.; *J. Biol. Chem*. **2002**, *277*, 46265–46272.
83. Traxler, P. *et al*.; *Pharmacol. Ther*. **1999**, *82*, 195-206.
84. Mishani, E.; *et al*.; *J. Med. Chem*.; **2005**, *48*(16), 5337-5348.

85. Smaill, J.B. *et al.*; *J. Med. Chem*. **2001**, *44*, 429-440.
86. Klutchko, S.R. *et al.*; *J. Med. Chem*. **2006**, *49*(4), 1475-1485.
87. Wood, E. R. *et al.*; *Cancer Res.* **2004**, *64*, 6652-6659.
88. Fry, D. W. *et al.*; *Proc. Natl. Acad. Sci. USA* **1998**, *95*, 12022–12027.
89. Blair, J. A. *et al.*; *Nature Chem. Biol.* **2007**, *3*, 229-238.
90. Hur, W *et al.*; *Bioorg. Med. Chem. Lett.* **2008**, *18*, 5916–5919.
91. Menard, S. *et al.*; *Annals of Oncology* 12 (Suppl. I): S15-S19, **2001**.
92. O'Donovan, N. *et al.*; *Invest. New Drugs*, **2010** (DOI 10.1007/s10637-010-9415-5).
93. O'Shaughnessy, J. *et al.*; *J. Clin. Oncol*. **2008**, *26 (15S)*: abstract 1015.
94. Ocana, A. *et al.*; *Cancer. Treat. Rev.* **2009**, *35*, 685–691.
95. Bianco, R. *et al.*; *Int. J. Biochem. Cell Biol.* **2007**, *39*, 1416–1431.
96. Rabindran, S.K. *et al.*; *Cancer Res.* **2004**, *64*, 3958–3965.
97. Zhou, W. *et al.*; *Nature Letters* **2009**, *462*, 1070-1074.
98. Smaill, J. B. *et al.*; *J. Med. Chem*. **1999**, *42*, 1803–1815.
99. Rewcastle, G. W. *et al.*; *J. Med. Chem*. **1995**, *38*, 3482–3487.
100. E. Davioud-Charvet, M.J. *et al.; Biochemistry* **2003**, *42*, 13319-13330.
101. Kooechel D.A. *et al.*; *J. Med. Chem.* **1978**, *21*(8), 764-769.
102. Estébanez-Perpiñá, E. *et al.*; *Molecular Endocrinology* **2007**, *21*(12), 2919-2928.
103. Roth, G. A. *et al.*; *J. Heterocycl. Chem*. **1996**, *33*, 2051–2053.
104. Saito, S. *et al.*; *Org. Synth*. **1995**, *73*, 184–200.
105. Korn, A. *et al.*; *Tetrahedron* **1994**, *50*, 8381–8392
106. Hayashi, Y. *et al.*; *J. Org. Chem*. **2005**, *70*, 5643–5654.
107. Tamai, M. *et al.*; *Chem. Pharm. Bull*. **1987**, *35*, 1098–1104.
108. Clerici, F. *et al.*; *Tetrahedron* **2003**, *59*, 9399–9408.
109. Lewis, S. N. *et al.*; *J. Heterocycl. Chem*. **1971**, *8*(4), 571–580.
110. Bordi, F. *et al.*; *Il Farmaco* **1989**, *44*, 795–807.

111. Buck, W. *Herbicidal [1,2,4] thiadiazoles.* U.S. Patent 5,583,092, **1996**.
112. Domarkas, J. *et al.*; *J. Med. Chem*. **2006**, *49*, 3544–3552.
113. Tsou, H.-R. *et al.*; *J. Med. Chem*. **2005**, *48*, 1107–1131.
114. Fry, D. W.; *Exp. Cell Res*. **2003**, *284*, 131–139.
115. Wissner, A. *et al*.; *J. Med. Chem*. **2003**, *46*, 49–63.
116. Tsou, H.-R. *et al*.; *J. Med. Chem*. **2001**, *44*, 2719–2734.
117. Carmi, C. *et al*.; *J. Med. Chem* **2010**, *53*, 2038-2050.
118. Rachid, Z. *et al*.; *J. Med. Chem*. **2007**, *50*, 2605–2608.
119. Smaill, J. B. *et al*.; *J. Med. Chem*. **2000**, *43*, 1380–1397.
120. Matheson, S. L. *et al*.; *J. Pharmacol. Exp. Ther*. **2001**, *296*, 832–840.
121. Cavazzoni, A. *et al*.; *Mol. Cancer Ther*. **2008**, *7*, 361–370.
122. Mor, M. *et al*.; *Composti inibitori irreversibili di EGFR con attività antiproliferativa*. Italian Patent Application MI2008A002336, **2008**.
123. Yates, L.M. *et al*.; *Mol. Pharmacol*. **2009**, *76* (1), 1–17.
124. Kano, M. *et al*.; *Physiol. Rev*. **2009**, *89*, 309-380.
125. Saito, M.V. *et al.*; *Psychology & Neuroscience* **2010**, *3*(1), 39 – 42.
126. Maejima, T. *et al.*; *J. Neurosci. Res.* **2001**, *40*, 205–210.
127. Dinh, T.P.; *Proc. Natl. Acad. Sci.* **2002**, 99(16), 10819-10824.
128. Fernández-Ruiz, J.; *Br. J. Pharmacol.* **2009**, *156*, 1029–1040.
129. Mackie, K; *HEP* **2005**, *168*, 299–325.
130. Rea, K. et al.; *Br. J. Pharmacol.* **2007**, 152, 633–648.
131. Long, J.Z. *et al*.; *Proc Natl Acad Sci* **2009**, *106*(48), 20270-20275.
132. Bosier, B. *et al.*; *Biochem. Pharmacol.* **2010**, 80, 1–12.
133. Starowicz, K. et al.; *Pharmacol. Ther.* **2007**, 114, 13–33.
134. Cui, M. *et al*.; *J. Neurosci.* **2006**, *26*(37), 9385−9393.
135. Hu, G. *et al.*; *Oncogene (advance online publication)* **2010** ; doi: 10.1038/onc.2010.502.
136. Kim, J. *et al*.; *Nat. Neurosci.* **2010** ,*13*(5), 592-600.
137. Sugiura, T. *et al*.; *Prog. Lipid Res.* **2006**, *45*, 405–446.

138. Siugiura, T.; in "*Cannabinoids and the brain*" (Eds. A. Köfalvi), Springer, **2008**, Chap. 2, 15-30.
139. Deutsch, DG *et al*.; *J. Biol. Chem*. **2001**, *276*, 6967–6973.
140. Dinh, T.P.; *Chem. Phys. Lipids* **2002**, *121*, 149–158.
141. Long, J.Z.; *Nat. Chem. Biol*. **2009**, *5*, 37-44.
142. Gulyas, A. I.; *Eur. J. Neurosci.* **2004**, *20*, 441–458.
143. Di Marzo, V. in *Rev. Physiol. Biochem. Pharmacol*. **2006**, *160*, 1 –24.
144. Karlsson, M. *et al*.; *J. Biol. Chem*. **1997**, *272*, 27218-27223.
145. Saario, S.M. *et al*.; *Chem. Biol.* **2005**, *12*, 649–656.
146. Saario, S.M. *et al*.; *Chem. Biodivers*. **2007**, *4*(8), 1903-1913.
147. Labar, G. *et al*.; *ChemBioChem* **2010**, *11*, 218-227.
148. Blankman J. L. *et al.*; *Chem. Biol*. **2007**, *14*, 1347-1356.
149. Bertrand, T. *et al.*; *J. Mol. Biol*. **2010**, *396*, 663–673.
150. a) Tornqvist, H. *et al*; *J. Biol. Chem*. **1976**, *251*, 813–819. b) Sakurada T. *et al*; *J. Biochem*. **1981**, *90*, 1413–1419.
151. King, A.R. *et al*.; *Chem. Biol*. **2007**, *14*, 1357-1365.
152. Zimmer, A. *et al*.; *Proc. Natl. Acad. Sci.* **1999**, *96*, 5780–5785.
153. Ledent, C. *et al*.; *Science* **1999**, *283*, 401–404.
154. Martin, B.R. *et al*.; *Pharmacol. Biochem. Behav*. **1991**, *40*, 471-478.
155. Darmani, N.A., *Neuropsychopharmacol.* **2001**, *24* (2), 198-203.
156. Koch J.E.; *Pharmacol. Biochem. Behav*. **2001**, *68*, 539-543.
157. Ràck, I. et al.; *Eur. J. Pharmacol.* **2008**, *596*, 98–101.
158. Costa, B. *et al.*; *Behav. Pharmacol*. **1999**, *10*(3), 327-331.
159. Jamshidi, N. *et al.*; *Br J Pharmacol* **2001**, *134*, 1151-1154.
160. Calignano, A. *et al.*; *Nature* **1998**, *394*, 277-281.
161. Seierstad M. *et al*.; *J. Med. Chem.* **2008**, *51*, 7327–7343.
162. Nomura, D.K.; *Cell* **2010**, *140*, 49-61.
163. Stalder, H. *et al*.; *Helv. Chem. Act*. **1992**, *75*, 1593-1603.
164. a) Bisogno, T. *et al.*; *Biochim. Biophys. Acta* **2009**, *1791*, 53-60; b) Ortar, G. et al.; *J. Med Chem.* **2008**, *51(21)*, 6970–6979.

165. Goparaju. S.K. *et al.*; *Biochem. Pharmacol.* **1999**, *57*, 417-423
166. Quistad, G.B.; *Toxicol. Appl. Pharmacol.* **2006**, 211, 78–83.
167. Segall, Y.; *Toxicol. Sci.* **2003**, *76*, 131–137.
168. Martin, B.R. *et al.*; *JPET* **2000**, *294*, 1209–1218.
169. Segall, Y. *et al*.; *Syn. Comm*. **2003**, *33*, 2151–2159.
170. Quistad, G.B. et al.; *Toxicol. Appl. Pharmacol.* **2002**, 179, 57–63.
171. Segall, Y. *et al*.; *Bioorg. Med. Chem. Lett*. **2003**, *13*, 3301–3303.
172. Karageorgos, I.; *Mol. BioSyst*., **2010**, 6, 1381–1388.
173. Alexander J.P.; *J. Am. Chem. Soc*. **2006**, *128*, 9699-9704.
174. Long J. Z. *et al*.; *J. Med. Chem*. **2010**, *53*, 1830–1842.
175. King A.R. *et al*.; *Chem. Biol.* **2009**, *16*, 1045-1052.
176. Zvonok, N. *et al*.; *Chem. Biol*. **2008**, *15*, 854-862.
177. Burston J. J. *et al.*; *JPET* **2008**, *327*, 546–553.
178. Cleland, W.W.; *Biochemistry*, **1964**, *3*(4), 480–482.
179. King, A.R. *et al*.; *Br. J. Pharmacol*. **2009**, *157*, 974-983.
180. Copeland R.A.; *In Evaluation of Enzyme Inhibitors in Drug Discovery*. (Eds. Copeland R.A.), John Wiley and Sons Inc.: Hoboken, NJ, *Chap. 5*, **2005**.
181. Capozzi G. *et al*.; in *The chemistry of sulphenic acids and their derivatives*, (Eds. Saul Patai), Wiley Interscience, Chap. 10, **1990**.
182. Wright, S.W. *et al*.; *Bioorg. Med. Chem*. **1995**, *3*(3), 227-234.
183. Katritzky, A.R. *et al.*; in "*Advance in Heterocyclic Chemistry*" - supplement 1: "*The tautomerism of Heterocycles*", (Eds. Katritzky A.R and Boulton A.J.), Academic Press, **1976**, Sec. 2E, 312-313.
184. Kersting, B. *et al*.; *Z. Naturforsch., B: Chem. Sci.* **1999**, *54*(8), 1042-1047.
185. Zlotin, S.G. *et al*.; *J. Org. Chem*. **2000**, *65*, 8439-8443.
186. Boruwa J. *et al.*; *Org. Biomol. Chem*. **2006**, *4*, 3521-3525.
187. Brown, C.A. and Yamashita, A.; *J. Am. Chem. Soc*., **1975**, *97* (4), 891–892.

188. Sing, K. R. *et al*.; *Tetrahedron* **2006**, *62*(17), 4011-4017.

189. Caliendo, G. *et al.*; *Eur. J. Pharm. Sci.* **2002**, 16, 15-28.

190. Correa, A. *et al.*; *Org. Lett*. **2006**, *8*(21), 4811-4813.

191. Masuya, K. *et al.*; *3,4,(5)-substituted tetrahydropyridines*, WO/2006/074924, Appl. PCT/EP2006/000216, **2006**.

192. Okram, B. *et al*.; *Chem. Biol.* **2006**, *13*, 779-786.

193. Gilday, J. P.; David, M. *Process for the preparation of 4- (3'-chloro-4'-fluoroanilino) -7-methoxy-6- (3-morpholinopropoxy) quinazoline.* PCT Int. Appl.WO2004/024703, **2004**.

194. Weber, W.; et al. *J. Biol. Chem.* **1984**, *259*, 14631–14636.

195. Olive, D. M.; *Expert Rev. Proteomics* **2004**, *1*, 327–341.

196. www.cerep.fr

197. Cavazzoni, A. et al.; *Oncogene* **2004**, *23*, 8439–8446.

198. Denmark S. E. *et al*.; *Tetrahedron* **2004**, *60*, 9695-9708.

199. Patwardhan A. P. *et al*; *Langmuir* **2000**, *16*(26), 10340-10350.

200. Neamati N. *et al.*; *J. Med. Chem.* **2002**, *45*, 5661-5670.

201. *Boshagen, H.; Chem. Ber.* ***1966****, 99, 2566-2571.*

202. Gialdi F. *et al.*; *Il Farmaco Ed. Sci.* **1961**, *16*, 509-526.